Titre: Title:	Heterogeneous Catalytic Conversion of Lactose to Lactic Acid to Valorize Residual Whey Permeate
Auteur: Author:	Maoline Divina Houndedoke
Date:	2026
Type:	Mémoire ou thèse / Dissertation or Thesis
Référence: Citation:	Houndedoke, M. D. (2026). Heterogeneous Catalytic Conversion of Lactose to Lactic Acid to Valorize Residual Whey Permeate [Thèse de doctorat, Polytechnique Montréal]. PolyPublie. https://publications.polymtl.ca/76612/

POLYTECHNIQUE MONTRÉAL
affiliée à l'Université de Montréal

Heterogeneous Catalytic Conversion of Lactose to Lactic Acid to Valorize Residual Whey Permeate

MAOLINE DIVINA HOUNDEDOKE
Département de génie chimique

Thèse présentée en vue de l'obtention du diplôme de *Philosophiæ Doctor*
Génie chimique

Mai 2026

POLYTECHNIQUE MONTRÉAL
affiliée à l'Université de Montréal

Cette thèse intitulée :

Heterogeneous Catalytic Conversion of Lactose to Lactic Acid to Valorize Residual Whey Permeate

présentée par **Maoline Divina HOUNDEDOKE**
en vue de l'obtention du diplôme de *Philosophiæ Doctor*
a été dûment acceptée par le jury d'examen constitué de :

Olivier HENRY, président
Gregory PATIENCE, membre et directeur de recherche
Daria Camilla BOFFITO, membre et codirectrice de recherche
Michel PERRIER, membre
Nicolas ABATZOGLOU, membre externe

DEDICATION

Pour Jésus Christ,
Pour Olga Zokia Ablavi,
Pour Kane...

ACKNOWLEDGEMENTS

Voilà. Le moment tant attendu. Merci Seigneur Jésus, de m'avoir permise de m'embarquer sur ce chemin sans jamais m'abandonner. Toute la gloire te revient, j'ai eu raison de mettre ma confiance en toi.

Thank you Gregory, for your support, your kindness and your enthusiasm. Your passion for research is inspiring and contagious. You always pushed me to do better and you took the time to sit with me to review my articles and explain how I could improve. I am very grateful to have been under your supervision. Thank you Daria, for your patience and taking the time to sit with me and look into my results when Gregory went on sabbaticals. Your wise advices helped me going forward. I want to thank all the group of Polytechnique past, and present : Mina, Mahdi, Jildimara, Jacopo, Paula Andrea, Nooshin, Dat, Yanfa, Tugce, Lucciana, Mario, Dalma, Debbie. It was a privilege to learn, laugh, and work alongside you. Thank you Gino and Martine for being available anytime when I needed lab supplies. Thank you Sameer for your hard work in helping me set up my installation.

Merci à Nathalie de la bibliothèque, qui m'a toujours accueillie avec le sourire et me souhaitait bon courage quand je venais passer mes journées à la bibliothèque. Merci à tous ceux que je n'ai pas cités mais qui, de près ou de loin, ont rendu cette aventure unique.

Romane, Gaby, Véro, mes colocs qui sont devenues des soeurs. Merci pour vos encouragements, votre patience envers mes absences répétées aux sorties, pour vos attentions remplies d'amour. Quelle grâce que celle de vous connaître.

Maman, tu sais tout. Tu es là depuis le début. Tu n'as jamais cessé de croire en moi, de prier pour moi, de me soutenir autant moralement, que financièrement et spirituellement. Ce doctorat est aussi pour toi. C'est l'accomplissement de tous nos efforts. Tu es pour moi un modèle et je suis tellement reconnaissante que Dieu m'ait donné une mère comme toi. Merci de m'avoir toujours soutenue, merci pour nos fous rires, nos appels quotidiens. Merci pour ton amour et ta présence dans ma vie. Merci Mathi pour ton soutien, tes prières et tes appels pour t'assurer que j'allais bien.

Kane, pendant que j'écris ces mots tu es tranquillement assis sur le canapé, attendant que je rende enfin ma thèse. J'ai tellement de mercis à te dire que je ne sais pas par où commencer. Cette thèse est notre thèse. Merci pour ton amour, ton soutien, ta présence. Merci pour tes encouragements quand tout allait mal au labo, merci d'être venu me chercher à des heures tardives toujours avec le sourire, une parole réconfortante et un repas. Dieu savait que j'allais

avoir besoin de toi comme allié pour aller jusqu'au bout. J'ai hâte de devenir bientôt ton alliée pour la vie, N'klowô.

RÉSUMÉ

Avec l'objectif du gouvernement canadien d'atteindre la neutralité carbone d'ici 2050 et dans un contexte où les préoccupations concernant l'épuisement des combustibles fossiles sont croissantes, il est devenu essentiel de développer des matériaux alternatifs provenant de ressources renouvelables.

Les eaux usées des fermes laitières représentent une source potentielle de matière première durable pour la fabrication de matériaux biosourcés. En 2023, la production fromagère du Canada a atteint 540 kt: 1 kt de fromage génère 9 kt de perméat de lactosérum, un sous-produit peu valorisé, qui est généralement rejeté ou séché pour l'alimentation animale. Le perméat de lactosérum contient 4.4 à 5 % de lactose en masse. Par hydrolyse, le lactose se scinde en glucose et galactose, qui peuvent alors être convertis en produits verts, à valeur ajoutée tels que l'acide lactique (LA) ou le 5-hydroxyméthylfurfural (HMF).

Le LA figure parmi la liste des molécules clés pour l'avenir en raison de sa large gamme d'applications, que cela soit dans le secteur pharmaceutique, des cosmétiques ou encore dans celui du bioplastique. C'est le monomère de départ pour la production d'acide polylactique (PLA), un polymère biodégradable représentant 19 % du marché des bioplastiques. Les fabricants industriels produisent du LA par fermentation de sucres, mais ce processus présente des défis tels qu'un long temps de réaction (2 à 4 d) et de multiples étapes de séparation et de purification. La conversion hétérogène du lactose et du perméat de lactosérum de fromage en LA pourrait simplifier la synthèse tout en réduisant les coûts de fabrication. Cependant, un tel processus est rarement mentionné dans la littérature.

Dans le cadre de cette recherche doctorale, nous avons conçu un catalyseur acide solide composé d'erbium (0.15 g g^{-1} Er) sur un support de γ-Al_2O_3, capable de convertir complètement le lactose à 170 °C en moins de 30 min, avec un rendement en acide lactique atteignant 23 %. Nous avons tout d'abord émis l'hypothèse qu'un catalyseur bimétallique à base d'étain et d'erbium augmenterait le rendement en LA, mais la caractérisation du catalyseur par SEM-EDS et BET, a révélé que l'étain se trouvait principalement à la surface du support, tandis que l'erbium se trouvait au cœur de la structure, couvert par l'étain. L'erbium était plus sélectif que l'étain pour le LA : le catalyseur monométallique Er_2O_3/γ-Al_2O_3 a donc donné le rendement le plus élevé. Sur la base de ces résultats, nous avons développé un modèle permettant de prédire le rendement en acide lactique en fonction du temps de réaction, de la température et de la charge métallique.

Ensuite, nous avons évalué l'impact de plusieurs paramètres sur les performances de la réac-

tion : les résultats indiquent que le rendement en LA ne varie pas en fonction de l'agitation du milieu réactionnel, de la pression, ou du gaz atmosphérique, que ce soit de l'air, de l'hélium, du N_2 ou du H_2. Lorsque la température et le temps de réaction ont tous deux étés augmentés, le rendement en acide lactique a étonnamment atteint un quasi-équilibre pour toutes les conditions testées. En partant de l'hypothèse que le catalyseur Er_2O_3/γ-Al_2O_3 réagirait de la même manière que le lactose, nous avons supposé que le rendement du perméat de lactosérum serait équivalent à celui du lactose. Cependant, celui-ci était inférieur au lactose de 7 %, potentiellement en raison de la présence de cendres dans le perméat. Les réactions complémentaires du catalyseur usagé avec le lactose ont révélé que 6 % de l'erbium s'est lixivié dans la phase aqueuse après la première réaction, mais seulement 0.8 % après le deuxième test.

Ce travail doctoral contribue à l'avancement de la recherche sur la valorisation du perméat de lactosérum en fournissant des outils utiles pour développer des procédés efficaces sur le plan économique, qui permettront de convertir le lactose résiduel en acide lactique. Les travaux futurs devraient inclure une analyse technico-économique et des recherches supplémentaires sur la conception des catalyseurs afin de permettre une synergie entre plusieurs phases actives, d'éviter leur lixiviation et de réduire la barrière énergétique d'activation de l'isomerisation du glucose vers le fructose.

ABSTRACT

With rising concerns regarding fossil fuel depletion, and the Canadian objective of reaching net zero emissions by 2050, it became necessary to look for alternative materials that would originate from renewable resources.

In this context, wastewater from dairy farms represents a potential source of sustainable feed for bioderived materials. In 2023, Canada produced up to 540 kt of cheese: 1 kt of cheese generates 9 kt of cheese whey permeate, a by-product which is poorly valorized and usually discarded or dried for animal feed. Whey permeate contains 4.4 to 5 % of lactose by mass. Through hydrolysis, lactose splits to glucose and galactose, which can convert to green added value products such as lactic acid (LA) or 5-hydroxymethylfurfural (HMF).

LA is listed among the building block molecules for the future due to its large range of application in pharmaceuticals, cosmetics, and the bioplastic industry. It's the starting monomer for the production of polylactic acid (PLA), a biodegradable polymer which represents 19 % of the bioplastic market. Industrial manufacturers produce LA through the fermentation of sugars however this process presents challenges such as long reaction time (2 to 4 d) and multiple separation and purification steps. The heterogeneous conversion of lactose and cheese whey permeate to LA, could simplify the synthesis, while decreasing manufacturing cost, but such process is seldom reported in the literature.

Through this doctoral research, we designed a solid acidic catalyst made of Er ($0.15\,\mathrm{g\,g^{-1}}$ Er) supported on γ-Al_2O_3 that could completely convert lactose at 170 °C, within 30 min, and with an LA yield of 23 %. We first hypothesized that a bimetallic catalyst of tin and erbium would increase LA yields, but the characterization of the catalyst, through SEM-EDS and BET revealed that tin was mainly at the surface of the support, while erbium was in the core hindered by tin species. Erbium was more selective than tin to LA: the monometallic catalyst of Er_2O_3/γ-Al_2O_3 thus achieved the highest yield. Based on these results, we developed a model that could predict LA yield as a function of reaction time, temperature and metal loading.

In a subsequent study, we assessed the impact of different parameters on the reaction performance: the results indicate that LA yield was invariant with respect to mixing and pressure, with either air, He, N_2, or H_2. When the temperature and reaction time both increased, LA yield surprisingly reached a quasi-equilibrium for all the tested conditions. Assuming that the catalyst Er_2O_3/γ-Al_2O_3 would react in the same way as with lactose, we hypothesized that the yield of LA from whey permeate would be equivalent to the one of lactose. However,

it was lower than lactose by 7 %, potentially owing to the presence of ashes. Complimentary reactions of spent catalyst with lactose revealed that 6 % of erbium leached into the aqueous phase, after the first reaction, but only 0.8 % after the second test.

Finally, we developed a kinetic model to identify which step of the synthesis presented the main activation energy barrier to the conversion of lactose to LA. It appeared that glucose isomerization to fructose had the highest activation energy, and therefore limited LA yield. Galactose produced more LA than glucose, and with fructose, LA yield reached 28 % at 150 °C, within 5 minutes. The kinetic model, we developed could predict lactose, glucose, galactose, fructose, LA, HMF and humins as a function of temperature and time, with an $R^2 = 0.99$.

This doctoral work contributes to the advancement of the research on whey permeate valorization by providing useful tools, to develop cost-effective processes that will convert residual lactose to LA. Future work should include a technico-economical analysis and further investigations on catalyst design to promote active phases synergy, avoid leaching, and lower the activation energy barrier of glucose to fructose isomerization.

TABLE OF CONTENTS

LIST OF TABLES

LIST OF FIGURES

LIST OF SYMBOLS AND ACRONYMS

ANOVA	Analysis of Variance
BOD	Biological Oxygen Demand
BET	Brunauer-Emmett-Teller
BJH	Barret-Joyner-Halenda
COD	Chemical Oxygen Demand
CRIBIQ	Consortium in Research and Innovation for Industrial Bio processes in Quebec
CW	Cheese Whey
CWP	Cheese Whey Permeate
C_x	Concentration of a substrate x
DHA	Dihydroxyacetone
D_{eff}	Effective diffusion coefficient
D_{m}	Diffusion coefficient
DMSO	Dimethylsulfoxyde
Ea	Activation energy
EDS/X	Energy Dispersive X-ray Spectroscopy
Glu-TsOH	Glucose/p-toluenesulfonic acid
GLY	Glyceraldehyde
HMF	5-hydroxymethylfurfural
IF	Impact Factor
IL	Ionic liquid
k	Rate constant
k_{c}	Mass transfer coefficient
k_0	Pre-exponential Arrhenius factor
LA	Lactic Acid
LAB	Lactic Acid Bacteria
MLA	Methyl lactate
m_{catalyst}	Mass of catalyst
n_{lactose}	Number of moles of lactose
$n_{\text{i,lactose}}$	Initial number of moles of lactose
$n_{\text{f,lactose}}$	Final number of moles of lactose
n_{p}	Number of moles of the product
n_{r}	Number of moles of the reactant

nC_{p}	Number of carbon atoms in the product
nC_{r}	Number of carbon atoms in the reactant
NHSG	Non-hydrolytic sol-gel
N_{Re}	Reynolds number
N_{Sc}	Schmidt number
N_{Sh}	Sherwood number
PLA	Polylactic acid
PNb	Niobium phosphate
PVA	Pyruvaldehyde
R	Universal gas constant
RI	Refractive index
$r_{i,lactose}$	Initial rate of lactose conversion
R_{p}	Particle mean radius
R_x	Reactor of volume x
R^2	Coefficient of determination
SEM	Scanning Electron Microscopy
t	Time
t_0	Heating time
T	Temperature
TGA	Thermogravimetric analysis
TSA	Tungstosilicic acid
UHPLC	Ultra High Performance Liquid Chromatography
US	United States
USD	US Dollars
UV	Ultraviolet
WoS	Web of Science
X	Conversion
x_{C}	Mass fraction of carbon
XPS	X-ray Spectroscopy
XRD	X-ray Diffraction
XRF	X-Ray Fluorescence
Y_x	Yield of a substrate x

Greek letters

β	Crystalline phase of zeolite

β_0 Temperature impact factor on t_0
γ Crystalline phase of Al_2O_3
ω Mears number
ϕ_p Particle porosity
ρ_p Particle density
σ_c Constriction factor
τ Tortuosity
2θ Angle of diffraction

LIST OF APPENDICES

CHAPTER 1 INTRODUCTION

1.1 Background and motivations

For 2030, Canada aspires to reduce its greenhouse gas emissions by 40 % compared to the level in 2005, with a final objective of reaching carbon neutrality by 2050 [7]. Thus, finding alternative sources to fossil-fuels motivated the research on waste valorization and bio-based materials. The Canadian Dairy Information Centre registered a production of 540 kt of cheese in 2023 [8]. Each kg of cheese produced, generates 9 to 10 L of whey, a byproduct with a high biochemical oxygen demand, and therefore, harmful for the environment if discarded without treatment in water sources [9]. The ultra-filtration process separates whey proteins from the lactose fraction, and produces whey permeate with mainly water, up to 5 % lactose, and some proteins and lipids [10]. The explored value chains for whey valorization include conversion to biofuels, animal feed or drying to recover the lactose content. However, these processes involve extra manufacturing costs, hindering their expansion in small and medium size dairy industries [9–11].

Lactose is a disaccharide, with twelve carbon atoms, which can convert to lactic acid (LA), one of the potential building blocks for the future, listed by the US Department of Energy in 2010 [12]. LA has a wide range of applications: in cosmetics, due to its antimicrobial and rejuvenating properties, in pharmaceuticals as a supplement for dermatological drugs, and most importantly in the polymer market, for the manufacturing of the polylactic acid (PLA) biodegradable plastic [13–15]. PLA is the most abundant polymer in the bioplastic market, with a production poised to reach 4.5 billion USD by 2030 [16]. PLA is a successful candidate as a substitute for traditional plastic due to its versatility: PLA potential applications encompass biodegradable packaging such as films and food containers, textiles for clothing and fabrics or medical items with sutures and drug delivery systems [17].

Lactose conversion to LA starts with the hydrolysis of lactose to glucose and galactose. Glucose isomerizes to fructose, which either dehydrates to 5-hydroxymethylfurfural (HMF), another platform molecule known as a precursor for biofuel applications or, it converts to C3 intermediates (glyceraldehyde and dihydroxyacetone) through a retro aldol condensation, to finally yield LA.

Current industrial processes rely on enzymatic fermentation to produce LA from corn derived glucose. Luongo and al. performed the reaction of whey with an anaerobic digestate from a treatment plant to produce LA: it resulted in a productivity of $0.37\,\mathrm{g\,g^{-1}}$, with a residence

time of 2 days [18]. Several challenges as enzymes sensitivity to pH and temperature, microbial contamination, costly separation and purification steps, and long reaction time (2 to 4 days) are the bottlenecks of the process. For 1 t of LA manufactured, it's 1 t of gypsum generated to assure the media buffering and avoid acid inhibition. It results in separations cost accounting for half of the price of LA production [19, 20]. Therefore, researchers are exploring alternative routes with chemocatalysis.

Heterogeneous catalysis offers an interesting pathway due to a facilitated catalyst recovering compared to homogeneous catalysis. There's a lack in the literature regarding lactose and whey permeate heterogeneous conversion to LA in water. For the few reports who mention it, the reaction solvent is usually methanol, yielding methyl lactate with low productivities (up to 19 %) [21–23]. For those in aqueous media, the process involves heavy catalyst preparation, as dealumination with nitric acid and multiple washing steps, or reaction temperatures up to 325 °C [6, 24]. Moreover, brown particles formation, called humins and catalyst deactivation decrease the profitability of the reaction.

The design of novel catalytic systems to enhance LA yields, while operating at low energy-intensive conditions is a prerequisite for industrial scale valorization of whey permeate with solid catalysts. This work was part of a collaboration with Novalait, a research organization gathering producers and transformers from dairy industry, CRIBIQ, the consortium in research and innovation for industrial bio processes in Quebec and Patience Enterprises Group, specialized in wasted natural gas to green fuels. The project was subdivided in two research subjects: one student operating the reaction in gas phase while I was operating in liquid phase.

The idea was to come up with a proof of concept and pursue investigations on conditions that will optimize LA yield. I set out to design solid catalysts, simple to prepare and efficient for lactose hydrolysis, and its subsequent conversion to LA. Different conditions (temperature, pressure, agitation) were tested to assess the impact on LA yields from lactose, and industrial whey permeate. At the same time, I conducted kinetic studies to identify the critical barriers in the synthesis route and to give insights on energy requirements for galactose conversion to LA. This research will provide new tools to researchers in catalyst synthesis and reactor design, for the valorization of whey permeate.

1.2 Problem statement and research objectives

1.2.1 Research question

How to develop a one pot process which generates LA through the heterogeneous catalysis of residual lactose from cheese whey permeate?

1.2.2 Objectives

The **main objective** is to develop a one pot process to valorize cheese whey permeate, through the heterogeneous conversion of its lactose content to LA. In order to fulfill the principal objective, we divided the problem into 3 sub-objectives:

1. **To identify a solid acidic catalyst that converts lactose completely and is selective towards LA production.** Chapter 3 describes the outcomes of this research objective and the resulting article was accepted in Catalysis Today (IF= 5.3).
   Hypothesis: Sn promotes the isomerization of glucose to fructose in Sn-Er/γ-Al_2O_3 while erbium directs the selectivity to LA production

2. **To assess the effect of mixing, temperature and pressure on LA yield for different scale reactors and compare results from lactose with the ones from whey permeate.** Chapter 4 describes the outcomes of this research objective and the resulting article was submitted to Industrial & Engineering Chemistry Research (IF= 3.9).
   Hypothesis: LA yield increases with improved mass transfer, temperature, pressure and time, and Er catalyst exhibits the same performance for lactose and cheese whey permeate.

3. **To develop a kinetic model, which predicts products concentration and derive activation energy for each step of the heterogeneous synthesis of LA from lactose.** Chapter 5 describes the outcomes of this research objective and the resulting article was submitted to Chemical Engineering Journal (IF= 13.2).
   Hypothesis:

   - Lactose hydrolysis and subsequent conversion to LA and HMF follows a pseudo homogeneous first-order approach (equations 5.2 to 5.8) [25].
   - The reverse reaction of fructose to glucose is non-negligible (equations 5.3 and 5.4) [26]. Lactose hydrolysis, fructose and galactose conversion to LA and HMF, glucose, galactose conversion, and degradation routes are all irreversible reactions.

- Humins are either solids or soluble oligomers. Here, we explore the kinetics of the formation of solid humins, whose concentration corresponds to the carbon content of species deposited on the catalyst surface [27]. The model assumes that they originate from HMF, fructose, and galactose [28–31].
- LA, HMF, and solid humins are the main products of dissacharides and monosaccharides conversion. All other by-products are negligible.

1.3 Thesis structure and contributions

This thesis contributes to the research on the valorization of residual lactose as followed:

1. Chapter 1: the first chapter introduces the challenges related to whey permeate valorization and gives an overview of the research undertaken in this work to respond to these problems. It also presents the main objective, specific objectives, and related hypothesis.

2. Chapter 2: it covers the literature review on the subject, with the origin, composition, and usage of lactose, whey permeate and LA.

3. Chapter 3: it describes the one pot synthesis process to hydrolyze lactose and convert it to LA with monometallic and bimetallic catalysts, supported on γ-Al_2O_3. Results reveal that erbium is more effective than tin for lactose hydrolysis, while it selectively converts it to LA. An optimized amount of $0.15\,g\,g^{-1}$ Er produces up to 23 % yield of LA at 170 °C, and a short reaction time of 30 min. The catalyst characterization reveals the presence of a SnO_2 layer for tin based catalysts, which may decrease LA, due to mild Brønsted acidity: Sn-OH bonds from water reacting with Sn on the surface induce a low Brønsted acidity, which decreases the overall Lewis acidity of the catalyst compared to γ-Al_2O_3 This research article also contributed to building a model, which predicts LA concentration with time, temperature and metal ratio. This article was accepted in *Catalysis Today* journal.

4. Chapter 4: this chapter focuses on the effect of operations conditions on LA yield for multi-scale volume reactors, from 10 to 100 mL. Results reveal that LA yield reaches a quasi-equilibrium with time, independently of mixing, pressure, gas atmosphere and temperature, from 150 to 190 °C. The yield is limited by the formation of humins and LA degradation. The reaction with whey permeate reveal a slower hydrolysis, most probably due to cheese whey permeate ash content. However, this research gives valuable insights to researchers as the process generates all together 29 % of value added products (14 % of lactic acid and 15 % of HMF). The outcome of this research was submitted to *Industrial & Engineering Chemistry Research* journal.

5. Chapter 5: this chapter adresses the kinetics of the reaction and dives into the critical energy barriers responsible of the previously mentioned quasi-equilibrium state for LA production. While glucose to fructose isomerization remains the critical activation energy barrier, the tested catalytic system promotes humins formation, for increased

reaction temperature. A model based on aforementioned, predicts all the products concentration (lactose, glucose, galactose, LA, and HMF) with an $R^2 = 0.99$. The results of this study, are submitted to *Chemical Engineering Journal*.

6. Chapter 6: An overview of the main results of this doctoral project, with an emphasis on its contributions, limitations and future research.

7. Annexe A: Supplementary information related to the chapter 3

8. Annexe B: Supplementary information related to the chapter 5

CHAPTER 2 LITERATURE REVIEW

2.1 Lactic acid

2.1.1 Structure, applications and production forecast

In 1780, C.W. Scheele discovered in acid milk, the 2-Hydroxy-propanoic acid, commonly known as lactic acid. It is an hydroxiacid with 3 carbons, with two chiral forms: the L(+)-lactic acid, serves as a metabolic intermediate in biological processes, while plants, bacteria and specific algae produce the D(-)-lactic acid [1]. LA is involved in the production of food acidulant, mosturizers, and formulations for oral hygiene. It is also a precursor for the synthesis of monomers such as, propylene glycol or acrylic polymers [13,32]. Despite its wide range of applications, the most interesting product of LA transformation is into its polymer, the PLA.

PLA is a biodegradable plastic whose production accounted for 19 % of the bioplastic market in 2020 [16]. While LA can polymerize to dimers and trimers when concentrated, the synthesis to commercial PLA involves two condensations steps in which LA first turns to lactide, its cyclic dimer, then converts to PLA through a ring-opening polymerization [32]. The market value of LA is poised to reach 2.8 billions by 2028, with an annual growth rate of 12.4 % [33, 34]. It was listed among the potential building blocks for the future, by the US Department of Energy in 2010, which makes its production from residual biomass of high interest [12].

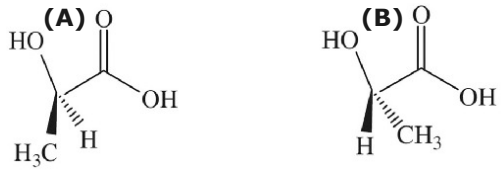

Figure 2.1 LA enantiomers: (A) LA L(+), (B) LA D(-), reproduced from Jánovová and al. [1]

2.1.2 LA acid synthesis

Currently, leaders of LA production, such as Corbion Purac (Netherlands), Henan Jindan (China), and NatureWorks LLC (joint venture between Cargill(USA) and PTT Global Chemical (Thailand), rely on fermentation techniques to convert carbohydrates to LA [35]. Another alternative consists in producing LA synthetically: HCN reacts with acetaldehyde and a base

catalyst to produce lactonitrile, followed by a distillation. Then, HCl or H_2SO_4 hydrolyses lactonitrile to LA. However, as the process depended on costly petroleum raw materials, Natureworks LLC modified its synthesis process to switch to fermentation [36, 37].

For producing large volumes of LA, food grade sugars, also known as first-generation feedstocks are preferred, as they avoid the risk of having contaminants and simplifies the process. However, their use contradicts sustainable development goals, as world's food needs have priority over these resources. Therefore, research efforts focus on second-generation feedstocks, i.e. biodegradable waste from organic matter, as corn residue, cassava bagasse, orange peel or even municipal waste.

We can separate them in 4 categories: food waste, lignocellulosic waste, starchy materials, and dairy waste [17]. Morales and al. achieved up to 83 % of LA yield, when reacting *Lactobacillus delbrueckii* microorganism with biopulp made of food residues from restaurants and canteens, municipal and supermarket organic waste. However, the process required a pretreatment to release biodegradable organics, a reaction time of 14 h to reach LA maximum yield, and pH control with sodium hydroxide: low pH negatively affects the hydrolysis rate by causing intracellular acidification of LA bacteria and inhibiting microbial activity (LAB) [38].

When reacting delignified, cellulose pulps with the same microbial strain, Karnaouri and al, reported a yield of $0.57\,\mathrm{g\,g^{-1}}$ of LA, after 72 h of fermentation and a pretreatment of 2 h at 160 °C [39]. This discrepancy, with the same strain suggests that cellulose gets less easily converted to LA than the monosaccharides of the previous example with biopulp, i.e. glucose and xylose.

The conversion of potato sillage to LA was also investigated, with immobilized *Lactobacillus paracasei* on sugar beet pulp, brewers' spent grain and sunflower seed hull. The best yield was with sugar beet pulp support, with LA reaching 97 % after 54 h. Researchers also mentioned the performance of up to 5 repeated batch of the immobilized strain, with yields ranging from 0.96 to $0.99\,\mathrm{g\,g^{-1}}$ [40]. Results demonstrate that starchy substrates represent great candidates for LA production, however they are food resources, which raises ethical considerations.

Luongo et al. reacted cheese whey with mixed cultures and achieved a maximum LA yield of $0.37\,\mathrm{g\,g^{-1}}$ in two days, without pH control. Dairy industry generates substantial amounts of waste as a result of a steady increase in demand for milk products. However, dairy waste composition is a hindrance to its valorization: proteins like casein resist to enzymatic degradation while lactose decomposition products can cause a partial inhibition of the transformation process [41].

Overall, fermentation processes suffer from several challenges such as multiple purification

steps, pretreatment, and costly separation: downstream separation represents 20–50 % of the total cost [38]. While starchy substrates display high yield of LA, they compete with food's need, which is unethical.

The development of new systems that will efficiently convert lignocellulosic waste and require minor to zero pretreatment, will have a leveraging effect on the industrial valorization of dairy waste. Therefore, researchers are exploring chemocatalysis, with homogeneous and heterogeneous catalysts, as potential alternative to fermentation for LA production.

2.2 Cheese whey permeate: composition, applications and conversion to LA

The manufacturing of cheese generates cheese whey, a green-yellowish liquid byproduct, formed through the removal of milk casein. Depending on factors such as breed, seasonal cycles or feed, whey generated is either qualified as sweet or acid: sweet whey has a pH in the range of 6 to 7, while acid whey has a pH between 4.5 to 5.8. They also differ in their composition in proteins, fat, lactose and minerals. Sweet whey exhibits the highest content of proteins and up to $52\,\mathrm{g\,L^{-1}}$ of lactose, and acid whey, contains more minerals, with up to $46\,\mathrm{g\,L^{-1}}$ of lactose [9, 41].

Cheese whey permeate (CWP) is the liquid remaining after the separation of proteins from cheese whey, through ultrafiltration [42]. The disposal of CWP without treatment causes a negative environmental impact, as it possesses a high biological and chemical oxygen demand (BOD and COD) due to its lactose content, in the range of 30 to $50\,\mathrm{g\,L^{-1}}$ and 60 to $80\,\mathrm{g\,L^{-1}}$ respectively. Typically, 70 % of sweet whey turns into whey protein and pure lactose while acid whey gets wasted and can either be sent to water treatment facilities or to farmers for spreading it on fields and animal feed [43]. Therefore, research efforts have been directed to finding new solutions to valorize CWP, that are cost-effective and environmentally friendly.

The baking sector holds 18 % of the total products with permeate in 2021 [44]. As an alternative to sucrose, whey permeate can reduce up to 22 % of total sugars and 70 % of sodium content in baked goods [42]. Other applications include ethanol and hydrogen production. Domingues and al. investigated the conversion of CWP to ethanol with *Saccharomyces cerevisiae* at 30 °C: the yield reached 0.43 kgof ethanol per kg of lactose, after 30 h.

Ethanol manufacturing from CWP is challenging due to an uneconomical low concentration (between 2 to $20\,\mathrm{kg\,m^{-3}}$), compared to other sources such as sugarcane or lignocellulosic biomass [41]. Yang and al. assessed the continuous production of biohydrogen and biogas from cheese whey permeate, with mixed strains of *Lactobacillus* and *Clostridia*, at an hydraulic retention time of 24 h: the system, was very sensitive to pH fluctuations, with biogas

ranging from 3 to 5 $L\,d^{-1}$ in 4 d, and decreasing until 1 $L\,d^{-1}$ over 22 d. The highest H_2 yield was 2 $mmol\,g^{-1}$ of COD after 6 d, then it decreased to lower than 0.5 $mmol\,g^{-1}$ of COD over 24 d(Yang and al., Figure 5 [45]).

Vasala and al. studied the conversion of CWP to LA with various strains and supplementation: results without pretreatments show that, with L. casei, after 48 h, LA could produce more than 20 $g\,L^{-1}$ with a lactose content of 50 $g\,L^{-1}$, which corresponds to an LA yield of 40 % [46]. Similarly, Delmoitié and al. fermented CWP with *Lactobacillus delbrueckii*, at 45 °C, and a controled pH of 6.5. They obtained up to 27 $g\,L^{-1}\,h^{-1}$ of LA and an LA yield of 70 % [47]. While fermentation of CWP to LA exhibits high yields, they require supplementation through yeast extract to support strains growth, pH control, and long residence time. A process that could achieve similar yields, through chemocatalysis is therefore desired.

LA production from the chemocatalysis conversion of cheese whey permeate is nearly absent of the literature: the majority of the reports mention lactose fermentation to LA. However, reviewing studies about disaccharides such as cellulose and sucrose to LA, give good insights on the potential catalytic systems that would be efficient with lactose. Similarly to lactose, cellulose is made of pairs of glucose, attached together while lactose is made of one unit of galactose and one of fructose. Both possess 1,4-glycosidic bonds. They are more stable than the 1,2-glycosidic bonds of sucrose, requiring more energy to break, and therefore, to produce LA.

The subsequent sections present an overview of the main reports for the homogeneous and heterogeneous catalysis of raw biomass and disaccharides to LA.

2.2.1 Disaccharides to LA: homogeneous catalysis

Multiple studies addressed the conversion of glucose to LA but few mention raw biomass as a feed. Kong et al. reported the hydrothermal conversion of maize straw, rice husk, wheat bran, and microcrystalline cellulose to LA with transition metal ions.

Althought the maximum LA yield from microcrystalline cellulose was 7 %, the presence of Ni(II) increased the yield by 4 %, compared to a non-catalytic process: at 300 °C, subcritical water tends to ionize and acts as a Bronsted acid catalyst while the metallic ions exhibit Lewis acidity [48]. Bicker and al. performed the conversion of sucrose to LA in subcritical water, with $ZnSO_4$ at 300 °C and 25 MPa.

Selectivity with dihydroxyacetone (3 carbon molecule) was 55 % (Figures 8-10 in their article). In the case of fructose, the presence of Lewis acidic Zn (II) slightly impacted the degradation rate but it catalyzed the selectivity towards LA and HMF [49].

Yan and al. investigated the hydrothermal conversion of glucose, cellulose and starch to LA with calcium and sodium hydroxide. Calcium hydroxide presented the best performances for LA production: calcium ions being divalent, with a radius larger than sodium ions, they tend to form complexes with oxygen and promote trioses production, leading to LA. LA yield from cellulose reached 19 % at 300 % within 90 s. At 350 °C LA degraded when increasing reaction time [50]. Some studies also explored the conversion of cellulose at temperatures lower than 200 °C: Wang and al. reacted cellulose with lead (II) ions at 190 °C. LA yield reached 68 % after 4 h. Lead ions not only catalyzed the isomerization of glucose to fructose but also increased the selectivity to LA.

The report mention the autocatalytic role of LA, which shortened the reaction time to hydrolyze cellulose, when added to the system [51]. Other studies with YCl_3, $YbCl_3$ and $ErCl_3$ revealed that the Lewis acidity of the catalyst collaborates with the Brønsted acidity to produce LA selectively. The former favors the conversion of monosaccharides to LA while the latter promotes the hydrolysis of polysaccharides [15, 52].

With rice straw made of 43 % of cellulose, LA yield reached 66 %, at 240 °C, and after 90 min, without any pretreatment [15]. The reaction of raw sugarcane bagasse with $ErCl_3$ achieved an LA yield of 95 % at 200 °C and 90 min, while $YbCl_3$ reached a yield of 92 % at 220 °C, after 15 min [52]. Hydrated lanthanides (III) ions tend to have a high affinity toward oxygen functional groups and can form a lanthanide-sugar complex that promote cellulose scission in coordination with the hydroxonium ions released by the autoprotolysis of water [53].

2.2.2 Disaccharides to LA: heterogeneous catalysis

Heterogenous catalysts have the advantage of simplifying the separation steps of a process, while being recyclable. Metal oxides exhibit both Brønsted and Lewis acidity sites. As previously mentioned, the former promote disaccharides hydrolysis, while the latter directs the selectivity of hexoses to LA. Through Lewis acidity properties, active metallic ions can coordinate with the carbonyl group of glucose, promoting its isomerization to fructose. Lewis acidity also promote retro aldol reactions and benzilic rearrangement for LA production [54].

The catalytic conversion of zirconium oxides with cellulose achieved up to 21 % of LA, at 200 °C, within 6 h. The synergetic association between acid and bases sites of the catalyst promoted the retro aldol conversion of fructose to C3 intermediates (glyceraldehyde and dihydroxyacetone), and their subsequent conversion to LA [55]. The proposed mechanism involved a coordination of the carbonyl group of fructose with zirconium as a Lewis acidic site and the adsorption of the hydroxide group on the oxygen site of ZrO_2.

Marianou et al investigated the performance of tungstosilicic acid (TSA) on a $SiO_2-Al_2O_3$ support. It appeared that the TSA/$SiO_2-Al_2O_3$ with the highest Lewis to Bronsted acidity ratio converted 61 % of the cellulose and directed the selectivity towards LA: LA yield of 24 %, at 175 °C, after 24 h [56]. Li and al. investigated the conversion of cellulose to LA with Er_2O_3 supported on γ-Al_2O_3: alumina make an excellent support, with a high surface area, multiple Lewis acidic sites, and an open porosity [57]. Cellulose conversion was complete in 3 h, at 240 °C, and under 2 MPa of N_2, for an erbium loading of 14 %. LA yield reached 46 % in the same conditions, with 0.2 g of cellulose. When cellulose amount increased, LA yield decreased, potentially due to a reduced depolymerization of the substrate.

Another study with erbium supported on dealuminated β-zeolite, reported an LA yield of 58 % from cellulose, within 30 min at 240 °C [58]. However, the catalyst preparation involved harsch conditions: a dealumination with nitric acid at 100 °C during 6 h and multiple washing with deionized water. Similarly to erbium, tin also exhibits good performances when converting sugars to LA: Holm and al. reported up to 64 % of methyl lactate yield from sucrose reaction in methanol with Sn/β-zeolite, at 160 °C, and over 20 h [59]. Dong and al. achieved an LA yield of 53 % in 2 h, at 190 °C from sucrose, with a bimetallic zinc and tin catalyst, supported on β-zeolite: the incorporation of Zn in the Sn/β-zeolite framework increased both Lewis acid and base sites, while decreasing fructose dehydration rate to HMF through the base sites [24].

These results are valuable insights for identifying solid catalysts, that would selectively convert sugars, and in the scope of this project, lactose to LA, at mild conditions. For this purpose, erbium and tin appear to be good candidates as they exhibit high yield for reduced reaction time (<3 h), when starting from cellulose.

2.2.3 Lactose heterogeneous conversion to polymer grade LA

Lactose is a disaccharide made of one glucose linked to a galactose unit and a melting point ranging from 200 to 250 °C, depending of it's structural form (α or β-lactose) [60]. At the equilibrium of the two forms, the total solubility is about 180 g L^{-1}, at 20 °C [61]. Its hydrolysis is of great interest as it generates two monosaccharides, which are feedstocks for multiple applications as sweetening syrups in dairy products and, in the framework of this project, for LA production [2, 60].

The mechanism of heterogeneous lactose conversion to LA is yet to uncover. However, starting the synthesis from monosaccharides is well documented: glucose isomerizes to fructose, which converts to C3 intermediates (glyceraldehyde, dihydroxyacetone, and pyruvaldehyde) through a retro aldol condensation. Finally, pyruvaldehyde isomerizes to LA [2, 49, 62–64].

For the few reports mentioning lactose as a feedstock, methanol is the solvent, for half of the reports, as it reduces the deposition of carbon species on the catalyst surface. However, LA yields range from 17 to 19 %, with a reaction time of up to 12 h [21–23]. One study from Dong and al. reported a yield of 35 % in an aqueous media. However the synthesis requires harsh conditions with a dealumination with nitric acid, of 20 h and multiple washing steps [24]. Quintero and al. achieved 23 % of LA, within 2 h, at 325 °C [65].

The reports points out that research on the heterogeneous conversion of lactose to LA, lacks of solutions that are easy-to-scale and would efficiently convert lactose, while reducing reaction time and energy requirements.

2.3 State of the art and forecast

A query in Web of Science (WoS) databae generated 154 articles, with the following algorithm: ALL=((("lactic acid" OR "2-hydroxypropanoic acid" OR lactate*) AND (glucose OR fructose OR galactose OR cellulose OR xylose OR lactose OR biomass OR whey permeate) AND (catalyst*) AND (fermentation OR enzyme* OR microorganism*))NOT (Patient OR human* OR mammal* OR metabol*)). The NOT exclusion parameter was necessary to exclude articles related to metabolic LA production, through the terms "Patient", "human", and "mammal". I also excluded research related to sensors through the terms "Sensor*" and "biosensor". As some studies still mentioned metabolites with the terms "glucose" and lactate", the query was furtber refined to exclude the additional term "metabol*", which gave the final set of 154 articles. Based on the result I generated a bibliographic map with VOSviewer(Figure 2.2). Most of the research on LA synthesis from residual waste focuses on fermentation through engineered micro organisms and enzymes (Figure 2.2, top). The red cluster shows that efforts are made to understand which parameters impact the carbohydrates catalytic conversion of polysaccharides such as cellulose and hemicellulose. The green cluster confirms the need of developed cost effective processes to valorize lignocellulosic feedstocks. From 2016 to 2020, we observed a shift from LA being produced by lactate dehydrogenase to studies directed to the development of industrial PLA production, through the catalytic conversion of more complex sugars, such as cellulose (Figure 2.2, bottom). As preciously mentioned, there's a need for new chemical systems that would reduce production cost, while relying on sustainable feedstock (Figure 2.2, top).

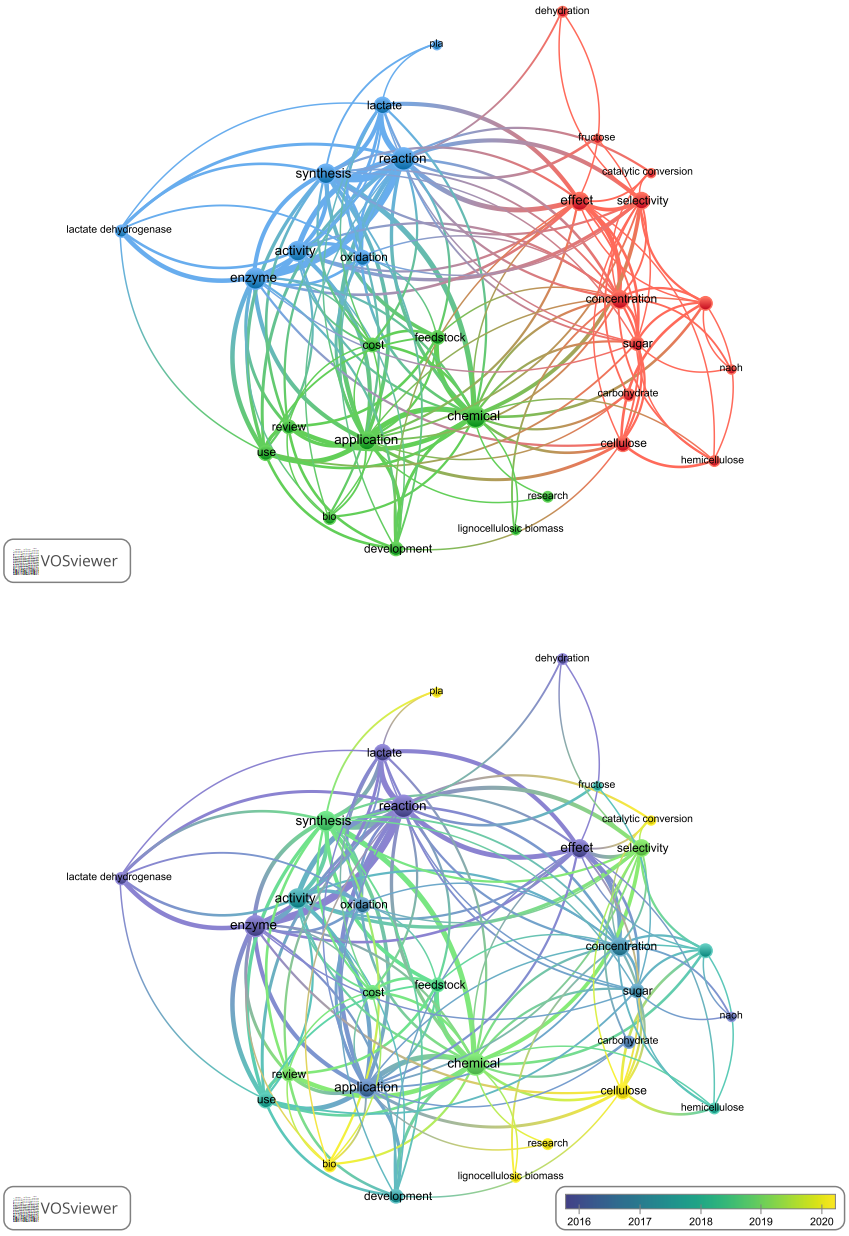

Figure 2.2 Bibliographic map with network visualization. Terms gathered in clusters of color(left). Overlay visualization with coloration based on average year publication (right).

CHAPTER 3 ARTICLE 1 - UNRAVELING ONE POT LACTOSE CONVERSION TO LACTIC ACID AND HMF OVER Sn-Er/γ-Al_2O_3

The state of the art regarding lactic acid production from biowaste, reveals that the majority of the research focuses on long fermentation processes, which rely on costly pretreatment, and multiple separation/purification steps. While starchy substrates exhibits high yields, they also compete with food needs which contradicts sustainable development goals. In this chapter, with an heterogeneous catalyst, we propose to convert lactose, a substrate present in cheese by-product, to value added green products: lactic acid and HMF. Multiple studies discussed the conversion of monosaccharides to LA but lactose was seldom reported as feedstock in aqueous media. Here, we identified potential metallic acid sites for converting lactose to LA and HMF, and we synthesized novel mono and bimetallic catalysts of erbium and tin, supported on γ-Al_2O_3. We compared the reaction performances between the synthesized catalysts and all were characterized (XRF, XRD and XPS, BET and SEM-EDS), to analyze the effect of catalyst composition and structure on lactose conversion and product's yield distribution. Then, we reacted the best-performing catalyst with the reaction intermediates, to provide a preliminary mechanism of the multiples steps involved. Finally, we built a model which predicts lactic acid production as a function of metal loading, temperature and time.

Maoline D. Houndedoke, Francesco Fabiani, Daria C. Boffito and Gregory S. Patience

Submitted in : Catalysis Today, 115658, July 4, 2025

Abstract

Residual whey permeate from cheese making contains 5 % lactose, and so is a potential feedstock for platform chemicals like lactic acid (LA), and hydroxymethylfurfural (HMF). Lactose hydrolyzes to glucose, and galactose monosaccharides as the first step followed by isomerization to fructose. Fructose either dehydrates to yield HMF or converts to C3 intermediates (glyceraldehyde, dihydroxyacetone) through a retro-aldol condensation. Those intermediates dehydrate to form α, β-unsaturated species, which convert to pyruvaldehyde (PVA) through keto-enol tautomerization. Adding one molecule of water leads to the formation of a diol, which tautomerizes to form LA. Heterogeneous catalysts come as a potential economic alternative to enzymes and homogeneous catalysts, with lower capital requirements (smaller reactors), and fewer separation steps. Here, an erbium catalyst ($0.15\,g\,g^{-1}$ Er) on a γ-Al_2O_3 support we synthesized, converted all the lactose at 170 °C, and lactic acid reached a maximum yield of 23 % after 30 min, at 70 rpm. XRF, XRD and XPS confirmed that metallic

active sites (Sn and Er) successfully incorporated the γ-Al_2O_3 in their oxide form. SEM-EDS and BET revealed that Sn is mainly at the surface of the support, while Er is embedded in the core, below Al, and O. Monometallic Er catalyst was more active than bimetallic Sn-Er catalyst, due to a hindering of Er species by Sn oxide at the surface. Experimental data matched with a model, which captures the reaction dependency on time, temperature, and metal loading, to form lactic acid. This study highlights the role of tin, erbium and operation parameters in the complex mechanism of lactose to lactic acid, and hydroxymethylfurfural.

Keywords: Lactose, Lactic acid, Hydroxymethylfurfural, Alumina, Heterogeneous catalysis

3.1 Introduction

In 2020, 88 % of chemicals, and derived materials were fossil based [66]. With rising concerns about CO_2 emissions, and depletion of fossil fuels, bio-based materials, from waste valorization, comes as a potential source of raw materials. In 2023, Canada produced 540 kt of cheese [8], and nearly 5 Mt of cheese whey (CW), a by-product of cheese manufacturing. Dairy processors recover the proteins from the CW, leaving whey permeate. The lactose from the whey becomes a low value animal feed or a feedstock for biomethanization. When lactose demand is high, the economics of drying the whey permeate are favourable. But, producers lose money when the demand is low.

Galactose, and glucose are the two monosaccharides of lactose, and are a source of high value-added green products. One of them is lactic acid (LA), a platform molecule with applications in the food industry, pharmaceutical, and chemical industries. It is also a monomer for poly-lactic acid, a biodegradable polymer [67]. The mechanism of glucose to LA requires first the isomerization of glucose to fructose. Through a retro aldol condensation, fructose converts to C3 intermediates (glyceraldehyde, dihydroxyacetone). While dehydrating, both intermediates form 2-hydroxypropenal, which tautomerizes to pyruvaldehyde. It subsequently isomerizes to lactic acid. [2, 22, 49, 62–64].

Another green product of interest is 5-hydroxymethylfurfural (HMF), a bio-based intermediate for high quality biofuel (e,g levulinic acid, 2,5-dimethylfuran, 2,5-diformylfuran) [68, 69]. HMF derives from C5, and C6 sugars, such as xylose, glucose, and fructose [70]. Glucose isomerizes to fructose, followed by its dehydration to HMF [71,72]. Fermentation processes, and homogeneous catalysis are currently the primary route to convert lactose to LA, and HMF but they require large reactors, long residence times, and costly distillation trains [73, 74].

Heterogenous catalysts are recyclable, and involve lower capital, higher space time yield, and potentially lower separation costs [75, 76]. Solid acid catalysts such as zeolites, mesoporous

silica, alumina, functionalized carbons, and metal oxides have both Brønsted, and Lewis acidity sites. The former is essential to hydrolyze biomass disaccharides, and their subsequent dehydration to HMF. The latter promotes the selectivity of hexoses to lactic acid [73, 77]. Sun et al. [78] reported up to 58 % yield of lactic acid from glucose, with Sn as a Lewis acid active phase, and up to 67 % from xylose. Marianou et al. [54] boosted the yield of HMF, reaching 27 % with Sn/γ-Al_2O_3 at 100 % glucose conversion. Xiao et al. achieved 72 % yield of LA with erbium supported on dealuminated ZSM-5 catalyst, at 200 °C, and 2 MPa [4]. However, constraints such as high temperature, and pressure, catalyst deactivation, and low reaction yield due to side products impede commercialization of the process.

Table 3.1 Highest yields for the heterogeneous catalysis of lactose to lactic acid or methyl lactate (MLA) in different studies

Catalyst	Steps	Conditions	X (%)	Y_P (%)
Zn-Sn-Beta zeolite [24]	Dealumination with HNO_3 (20 h at 80 °C), washing, drying, calcination (6 h, 550 °C)	190 °C, 2 h, cat./lac.: 0.7, in water, product: LA	>99	35
γ-NiOOH [21, 22]	Homogeneous precipitation, mixing (2h at 100 °C), washing and drying	200 °C, 12 h, cat./lac.: 0.5, in methanol, product: MLA	100	17
Mg-MOF-74 [23]	Mixed-matrix membranes, mixing (2 h at 25 °C), centrifugation and calcination (250 °C in N_2, 6 h)	220 °C, 6 h, cat./lac.: 0.33, in methanol, product: MLA	74	19
Sn-SiO_2 [65]	Wet impregnation, mixing (0.5 h at 90 °C), drying and calcination (500 °C, 4 h)	325 °C, 2 h, in water, product: LA	100	23
Er_{15}/Al_2O_3	Wet impregnation at 25 °C No dealumination nor washing, drying and calcination (550 °C, 4 h)	170 °C, 0.5 h, cat./lac.: 0.8, in water, product: LA	100	23

Lactose is seldom mentioned as a primary feedstock for specialty chemicals while other saccharide systems - hexose, pentose, triose (glycerol, dihydroxyacetone) sucrose, cellulose, and maltose- are more frequently mentioned in the open literature [3, 56]. For the articles who mention it, the solvent in most cases is methanol to minimize forming of carbon species, which is somewhat toxic [79, 80]. In these studies, the product of interest has been methyl lactate. However, the reaction require up to 12 h [21–23]. Dong et al. [24] reacted lactose with water as a solvent but the article doesn't mention any details about the mechanism of the reaction and the catalyst synthesis took 20 h, with multiple washing steps, and a dealuminatin step. Quintero et al. achieved a 23 % yield of LA in gas phase, for a reaction time

of 2 h at high temperature (325 °C) (Table 3.1).

Here, we identify a catalyst, and composition, to selectively react lactose to lactic acid directly. Based on an experimental design in a batch reactor (hydrothermal autoclave), we developed a mathematical expression to capture the relationship between the main factors (temperature, time, catalyst, loading, composition) and LA yield. The open literature has yet to identify a commercial heterogeneous catalyst system with high yield to lactic acid. Together with testing lactose, we reacted Er_{15}/Al_2O_3 with the potential intermediates of the reaction (glucose, galactose, and fructose) to propose a mechanism for lactose to LA heterogeneous catalysis.

3.2 Experimental

3.2.1 Catalyst preparation

To synthesize the bimetallic catalysts, we mixed γ-Al_2O_3 (Puralox SCCa-5/200, Sasol Chemicals USA) with the metal precursors following incipient wet impregnation [73, 81]. Distilled water dissolved the $ErCl_3$ (99 %, Sigma Aldrich), and $SnCl_2$ (99 %, Sigma Aldrich). The solution impregnated 2 g of Al_2O_3 support, drop by drop at room temperature to obtain the catalysts denoted as Sn_mEr_n/Al_2O_3, where m is the tin content (m= 0 %, 10 %, 15 %), and n is the erbium content (n=0 %, 10 %, 15 %). The impregnated powder dried in an oven at 60 °C overnight, followed by calcination at 550 °C for 4 h at a ramp of 5 °C min^{-1} (Table 3.1, final row).

3.2.2 Characterization of the catalysts

An Autosorb 1 BET, from Quantachrome Instruments, measured the porosity of the powders by N_2 physisorption. The catalysts degassed at 250 °C during 12-24 h, prior to the measurement. The Brunauer-Emmett-Teller equation (BET) derived the specific surface area of the samples, and the Barret-Joyner-Halenda method (BJH), the pore size distribution [82]. An X-ray fluorescence spectrophotometer (Malvern PANalytical Epsilon 4, with a silicon drift detector at 135 eV) confirmed the metal loading for each catalyst [83]. X-ray diffraction (XRD) characterized the crystalline structure of the support [84] and, the Sn_mEr_n/Al_2O_3 catalysts, with a Bruker D8 Advance Plus at a 2θ range of 5 to 90°. Scanning Electron Microscopy (SEM) revealed the morphology of the samples, with a JEOL JSM-7600F SEM (resolution of 1 nm at 15 kV) coupled with EDX to map the surface element composition of the powders. Gold sputtering coated the samples, prior to the analysis. A Thermo Scientific ESCALAB 250Xi analyzer measured the X-ray spectroscopy (XPS) of the catalysts, with an

Al Kα monochromatic source at 218.8 W (14.7 kV, and 14.9 mA). The pass energy applied to the survey spectra was 150 eV, with a step size of 1 eV. A LECO CS744 CHN quantified the carbon on the catalyst surface (Table A.2).

3.2.3 Catalytic activity

A 25 mL stainless-steel hydrothermal autoclave reactor assessed the catalytic activity of the synthesized catalysts. We prepared a 10 mL lactose ($\geq$98 %, Sigma Aldrich) solution with 0.05 g g^{-1} concentration to mimic the concentrations in cheese whey [9], and we filled the reactor together with 0.4 g of the synthesized catalyst. After sealing the vessel, we placed it in an oven, operating at 190 °C for 1 h to 5 h to assess the effect of reaction time on lactose conversion, and product yield (Figure 3.1).

We selected the catalyst that produced the most LA, and evaluated the impact of temperature (150 °C to 190 °C) on lactic acid yield, and lactose conversion for an agitated autoclave placed in an oil bath. An ice bath quenched the reaction. The liquid product separated from the solid catalyst through a Büchner funnel, and a 0.22 µm polytetrafluoroethylene membrane filtered the solution prior to the analysis with high performance liquid chromatography (UHPLC 3000, equipped with UV, and RI detectors). For the agitated reaction, a 10 mL distilled water washed the spent catalyst to recover all the reacted product. These samples are denoted as wash. An Aminex HPX-87H column eluted lactose, glucose, lactic acid, formic acid, and HMF, while an Hi-Plex Ca, eluted galactose, and fructose for product quantification through comparison with standard calibration curves. The mobile phase was a 0.05 N H_2SO_4 solution, at 0.6 mL min^{-1}. The column temperature set point was 60 °C, and the RI detector operated at 40 °C. The RI detected sugars (lactose glucose, galactose, and fructose) while, the UV detected lactic acid, and formic acid at 210 nm, and HMF at 285 nm [85–87]. One mole of glucose or galactose produces 2 mol of lactic acid, 1 mol of HMF or 6 mol of formic acid. We calculated product yield, and conversion based on (3.1), and (3.2):

$$Y_{\mathrm{p}} = \left(\frac{nC_{\mathrm{p}}}{nC_{\mathrm{r}}}\right) \times \left(\frac{n_{\mathrm{p}}}{n_{\mathrm{r}}}\right) \tag{3.1}$$

$$X = \left(\frac{n_{\mathrm{i,lactose}} - n_{\mathrm{f,lactose}}}{n_{\mathrm{i,lactose}}}\right) \tag{3.2}$$

where nC_{p} is the number of carbon atoms in the product, nC_{r} is the number of carbon atoms in the reactant (for lactose, nC_{r}=12), n_{p} is the number of moles of the product, n_{r},

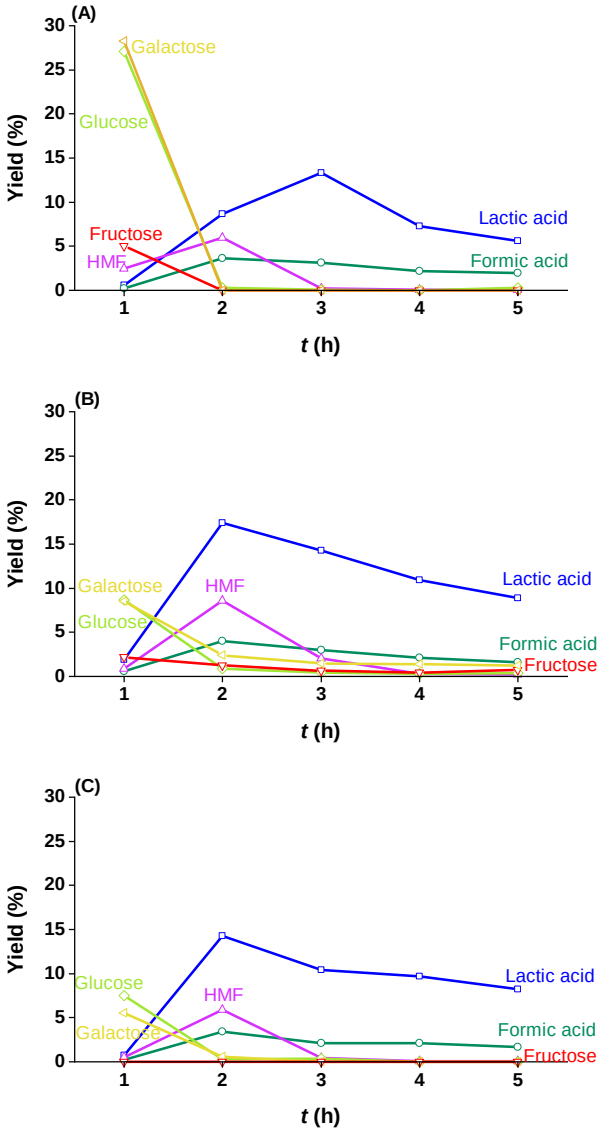

Figure 3.1 Impact of reaction time on Sn_{10}/γ-Al_2O_3 **(A)**, Er_{15}/γ-Al_2O_3 **(B)**, and $Sn_{10}Er_{15}/\gamma$-Al_2O_3 **(C)** on lactic acid, formic acid, HMF, fructose, glucose, and galactose yields. Reaction conditions: Lactose 5 %, 190 °C, 1 to 5h.

the number of moles of the reactant, $n_{\mathrm{i,lactose}}$ is the initial number of moles of lactose, and $n_{\mathrm{f,lactose}}$ is the final number of moles of lactose.

3.3 Results and discussion

3.3.1 Catalysts Characterization

XRF confirmed that tin and erbium impregnated the γ-Al_2O_3 support in their oxide form (Table 3.2). The results suggest that tin volatilizes during calcination.

Table 3.2 Metal loading of various γ-Al_2O_3 catalysts analyzed by XRF

Catalyst	Metal loading (in % mass)	
	SnO_2	Er_2O_3
Sn_{10}/Al_2O_3	5	0
Sn_{15}/Al_2O_3	8	0
$Sn_{10}Er_{10}/Al_2O_3$	5	10
$Sn_{10}Er_{15}/Al_2O_3$	4	13
Er_{10}/Al_2O_3	0	11
Er_{15}/Al_2O_3	0	15

XRD patterns (Figure 3.2) confirmed the γ-Al_2O_3 phase of the monometallic, and bimetallic catalysts [88] (PDF 00-001-1303). The supports impregnated with tin exhibited crystalline peaks specific to SnO_2 [89] (PDF-04-007-3489). For powders with erbium, the patterns did not present any Er_2O_3, which indicates that erbium is amorphous or well dispersed on the alumina support [4].

The surface area of γ-Al_2O_3 support is $200\,m^2\,g^{-1}$ with an average pore volume of $0.53\,cm^3\,g^{-1}$, and pore diameter of 8.7 nm (Table 3.3). For monometallic catalysts, the surface area decreases by $50\,m^2\,g^{-1}$ when incorporating erbium species, while a decrease of $30\,m^2\,g^{-1}$ is observed when incorporating tin. The same behaviour occurs for the bimetallic catalyst while impregnating erbium to a fixed $0.10\,g\,g^{-1}$ tin catalyst (40 $m^2\,g^{-1}$ decrease). These significant reductions indicate a possible blockage of the pores by the introduction of erbium, and tin metallic sites [57]. The higher decrease in surface area, and pore volume with erbium (0.1 $cm^3\,g^{-1}$ compared to $0.05\,cm^3\,g^{-1}$ with tin), suggests that Er mainly incorporated in the pores, while tin species deposited on the surface of the support. All catalysts exhibited type IV isotherm with H1 hysteresis loop (Figure 3.3), which is indicative of uniform distribution of narrowed range mesopores [82, 90]. It is coherent with previously reported γ-Al_2O_3 nitrogen isotherms curves [73].

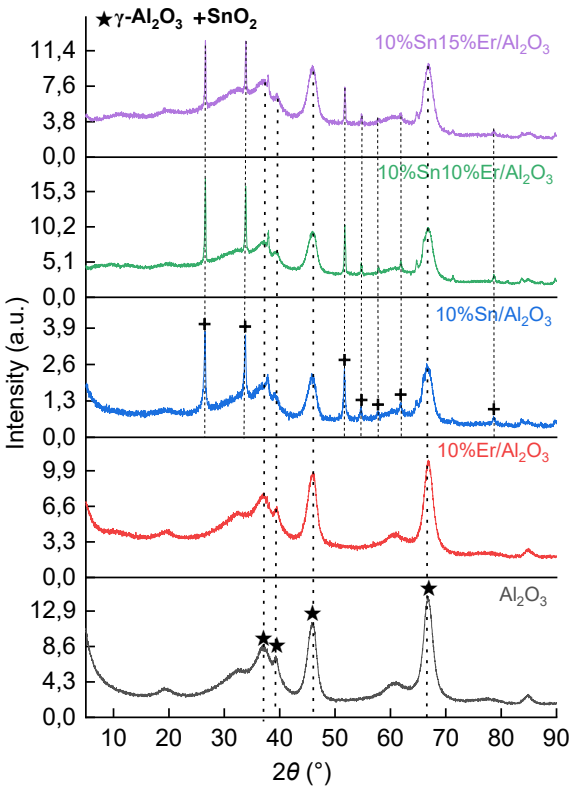

Figure 3.2 XRD patterns of monometallic, and bimetallic γ-Al_2O_3 impregnated, and air calcined during 4h, at 550 °C.

To further investigate metal disposition on alumina surface, SEM-EDS analysis identified Al, O, Sn, and Er in red, blue, green, and pink respectively for the $Sn_{10}Er_{15}/\gamma$-Al_2O_3 catalyst (Figure 3.4).

Based on the brilliance of the pictures, Al, and O remained on the surface while Sn appears as embedded inside the matrix, with some clustered particles on the support surface. The distribution of Er is more homogenous than Sn, and most likely in the core, below Al, and O. These results are consistent with XRD, which didn't detect erbium species due to their dispersion.

XPS identified the surface valence state of the samples. The survey spectra of Sn_{10}/Al_2O_3 detected Sn, Al, and O at the surface of the catalyst. In the case of bimetallic $Sn_{10}Er_{10}/Al_2O_3$, and $Sn_{10}Er_{15}/Al_2O_3$ catalysts, the aforementioned elements were present in addition to Er (Table 3.4). The atomic concentrations of Er, and Sn compared to alumina are quite constant for all the catalysts, which confirms that the distribution was invariant. The binding energy

Table 3.3 Physical properties of synthesized γ-Al_2O_3 catalysts

Catalyst	S_{BET} ($m^2\,g^{-1}$)	V_P ($cm^3\,g^{-1}$)	d_{BJH} (nm)
Al_2O_3	200	0.53	8.7
Sn_{10}/Al_2O_3	170	0.48	8.7
Er_{10}/Al_2O_3	150	0.43	8.7
$Sn_{10}Er_{10}/Al_2O_3$	160	0.42	8.7
$Sn_{10}Er_{15}/Al_2O_3$	160	0.43	8.7

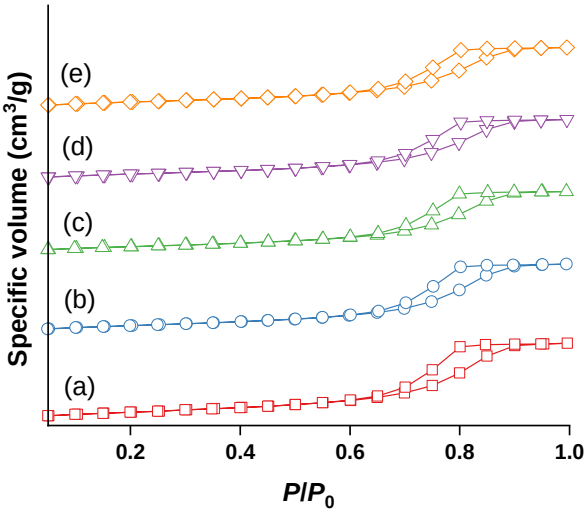

Figure 3.3 Nitrogen adsorption-desorption isotherms of (a) γ-Al_2O_3, (b) Sn_{10}/γ-Al_2O_3, (c) Er_{10}/γ-Al_2O_3, (d) $Sn_{10}Er_{10}/\gamma$-Al_2O_3, and (e) $Sn_{10}Er_{15}/\gamma$-Al_2O_3.

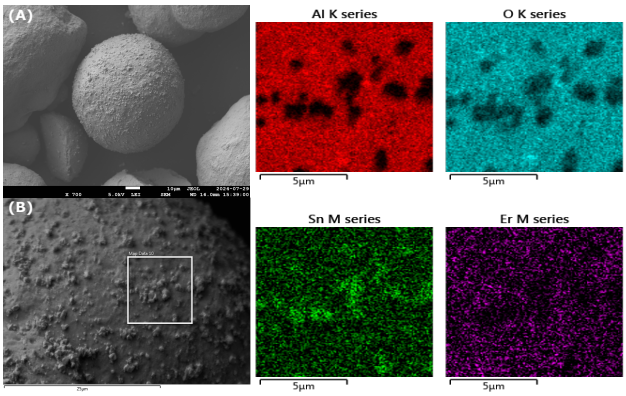

Figure 3.4 SEM-EDX images of $Sn_{10}Er_{15}/\gamma$-Al_2O_3, **(A)** x700 magnification, and 10 µm scale, **(B)** x2500 magnification, and 25 µm scale.

of Er 4d remains in the range of [168.8-169.9], and is similar to the one of $ErCl_3$. It suggests that erbium species are trivalent [57]. The binding energy of Sn 3d is characteristic of

tetrahedrally coordinated Sn species in the form of SnO_2 [91], which is in agreement with XRD results. The quantified Er content is lower than the one in the bulk catalyst, attesting that Er_2O_3 partly incorporated the pores of the support [57].

Table 3.4 XPS results from survey spectra with mass content of impregnated γ-Al_2O_3

Catalyst	Binding energy (eV)				Sn (%)	Er (%)	Atomic ratio		
	O 1s	Al 2p	Sn 3d	Er 4d			O/Al	Sn/Al	Er/Al
$ErCl_3.6H_2O$	531	0	0	169	0	48	0	0	0
Sn_{10}/Al_2O_3	530.2	73.9	486.1	0	16	0	1.76	0.09	0
$Sn_{10}Er_{10}/Al_2O_3$	532	75.1	487.4	169.8	12	2	1.85	0.09	0.03
$Sn_{10}Er_{15}/Al_2O_3$	530.5	73.7	486.1	168.8	11	1	1.79	0.07	0.03

3.3.2 Catalytic performance

Impact of metal loading

To assess the contribution of metal loading, tin, and erbium on yield we tested a 5 % lactose aqueous solution at 190 °C, during 2 h [24]. In all cases, lactose conversion was 100 %. In the absence of catalyst, HMF reached a 14 % yield. Lactic acid, and formic acid yields were 3 %, and 1 %, respectively (Figure 3.5). With pure γ-Al_2O_3, HMF yield decreased slightly to 12 %, and lactic acid yield increased to 7 %, with 2 % formic acid. Due to its Lewis acidity, alumina forms negatively charged hydroxides, when dispersed in water, that enhance the amount of H^+ protons released by the autoprotolysis of hydrothermal water. These hydrogen ions facilitate the hydrolysis of lactose to glucose, and galactose, and their subsequent conversion to lactic acid, and formic acid [92–94]. By adding Sn_{10} to the support, lactic acid, and formic acid reached respectively, 9 %, and 4 % for the Sn_{10}/γ-Al_2O_3 catalyst. Tin impregnation promote the isomerization of glucose to fructose, and its subsequent reaction to lactic acid. This correlates with the yield decrease of glucose, and galactose, with Sn_{10}/γ-Al_2O_3 compared to γ-Al_2O_3 (Figure 3.6), and the complete conversion of fructose as it was detected within 1 h of reaction, but not after 2 h (Figure 3.1).

HMF decrease agree with the studies reported by Marianou and al. [54] on the effect of Lewis acidity on glucose conversion. Increasing the Lewis acidity of a catalyst promote both the dehydration reaction to HMF, and the retro-aldol reaction to LA. Here, the decrease in HMF with the Sn catalysts may account for the formation of SnO_2 during the catalyst synthesis. Sn-OH bonds from water reacting with Sn on the surface induce a low Brønsted acidity,

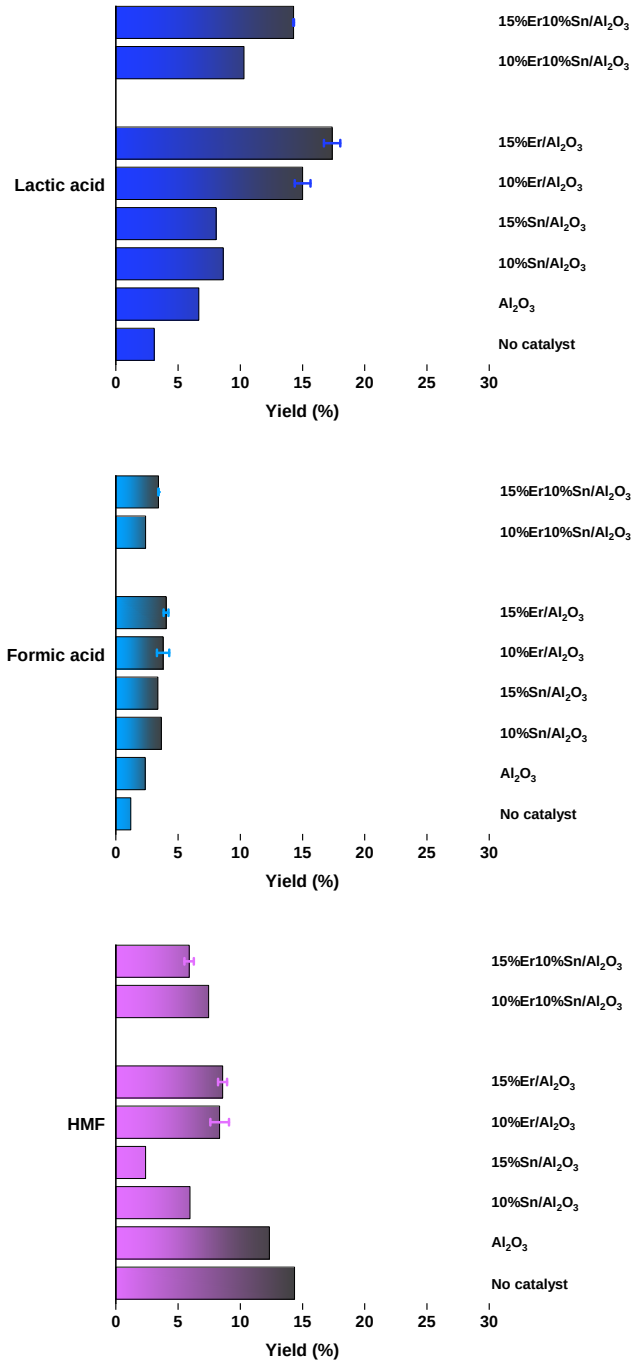

Figure 3.5 Catalytic impact of monometallic $Sn_m/\gamma\text{-}Al_2O_3$, and $Er_n/\gamma\text{-}Al_2O_3$, compared to bimetallic $Sn_mEr_n/\gamma\text{-}Al_2O_3$ on lactic acid, formic acid, and HMF yield. Reaction conditions: Lactose 5 %, 190 °C, 2h. n=2, error bars represent standard deviation.

decreasing the overall Lewis acidity of the catalyst compared to $\gamma\text{-}Al_2O_3$. With the $Er_{10}/\gamma\text{-}Al_2O_3$ catalyst, HMF yield decreased to 9 %, as opposed to the support. Xiao and al. [4], observed that Er might replace hydrogen on Al-OH surface bonds, which decreases Brønsted

acidity in the media, reducing the dehydration rates to produce HMF, and promoting lactic acid. Increasing Er content to 15 % increased lactic acid (17 %) while HMF yield remain constant (9 %). For Sn_{15}/γ-Al_2O_3 catalyst, HMF decreased to 2 %, while LA decreased slightly. SEM images show an agglomeration of Sn particles (Figure A.1), which resulted on a decreased active phase surface area. While both Lewis, and Brønsted acidity contribute to HMF production, the results show a higher performance of induced Er Lewis acidity compared to the mild Brønsted acidity originated from the SnO_2 layer on γ-Al_2O_3 in the present catalytic system. Formic acid reached a maximum of 4 % yield with the monometallic 15 % erbium catalyst. This rise is coincident with the increase in HMF yield, as formic acid forms when HMF rehydrates in water. [95, 96]. Swift and al. showed that the rate of production of HMF is equal to its rate of degradation to formic acid. Increasing the erbium content of the catalyst induces a rise in HMF production, which translates as well into an increase in formic acid yield [97].

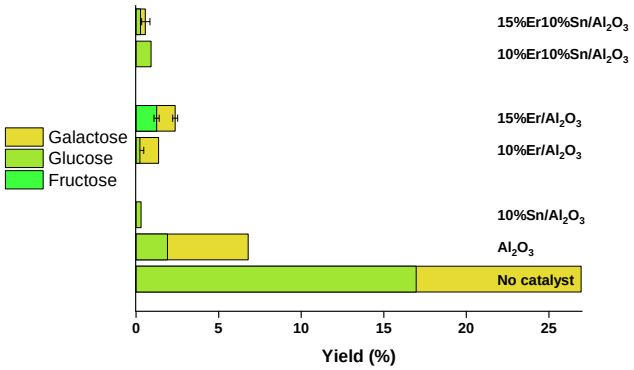

Figure 3.6 Catalytic impact of monometallic Sn_m/γ-Al_2O_3, and Er_n/γ-Al_2O_3, compared to bimetallic Sn_mEr_n/γ-Al_2O_3 on fructose, glucose, and galactose yield. Reaction conditions: Lactose 5 %, 190 °C, 2h.

We repeated the reaction with bimetallic catalysts, fixed at a mass fraction of 10 to 15 % of tin, and erbium (Figure 3.5,3.6). Increasing erbium content increases lactic acid yield, with $Sn_{10}Er_{15}/\gamma$-Al_2O_3 catalyst producing the most lactic acid (14 %) among bimetallic catalysts. Formic acid increases with fructose decrease (Figure 3.1), which is in agreement with Guo et al., who reported that formic acid production could also result from direct fructose conversion [98, 99]. HMF decrease with $Sn_{10}Er_{15}/\gamma$-Al_2O_3 may be due to its further degradation into humins. As for fructose, Er_{15}/γ-Al_2O_3 catalyst, exhibited traces of fructose (1 %). This may indicate that erbium species catalyze as well glucose, and galactose to fructose isomerization.

As the surface area of erbium oxide and tin oxide is much lower than γ-Al_2O_3, we hypothesize that their activity is low. Considering the elevated cost of Er, dispersing it on a support

minimizes loading. To compare the mentioned oxides with γ-Al_2O_3 catalysts, we tested lactose with tin oxide, erbium oxide and a mix of them at 190 °C, and 2 h. We kept the same metal loading as the supported catalysts, respectively Sn_{10}/γ-Al_2O_3, Er_{15}/γ-Al_2O_3, and $Sn_{10}Er_{15}/\gamma$-Al_2O_3 for the mix. The yields increase in the following order: Tin oxide < Erbium oxide < Tin oxide + Erbium oxide (Table A.1). Santos et al. demonstrated that tin oxide is less active because it has low water tolerant Lewis acid sites. It makes SnO_2 prone to poisoning by water [100]. Xiao et al. reacted erbium oxide with a mix of glucose and xylose, and reported that LA increased with higher erbium loading, with 15 % being the highest [4].

Overall, alumina monometallic catalysts activity was higher than bimetallic ones. As observed previously, the presence of a SnO_2 layer at the surface may hinder the catalyst activity, by inducing low Brønsted acidity.

Impact of reaction time

To assess the impact of reaction time on the catalyst performance, we selected $Sn_{10}Er_{15}/\gamma$-Al_2O_3 as the highest activity for lactic acid production, among bimetallic catalysts. We compared it to the monometallic Sn_{10}/γ-Al_2O_3, and Er_{15}/γ-Al_2O_3 catalysts as references. The bimetallic catalyst has a similar trend with Er_{15}/γ-Al_2O_3. This confirms that Er activity leads the reaction, with a maximum yield in lactic acid at 2 h, and no lactose detected in the liquid products. With the Sn_{10}/γ-Al_2O_3 catalyst, lactic acid reached its maximum (13 %) after 3 h. For all catalysts, HMF yield is the highest at 2 h (Figure 3.1). For Sn_{10}/γ-Al_2O_3, fructose maximum is at 1 h, with a 5 % yield. Lactic acid yield decreases at 4 h, which may due to side reactions, as humins form in the presence of Lewis acidic catalysts [56,75,101], and coking [102] that obstruct the catalyst active sites, and hinder subsequent conversion. Formic acid is undetected after 1 h, when glucose, and galactose are the highest for all the catalysts. However, we detect it after 2 h when fructose decreases, and HMF appear, which suggests that formic acid may originate from either or both. When increasing reaction time from 4 h to 5 h, lactic acid yield remains quite stable, which may be attributed to the complete deactivation of the catalyst. It appeared that the optimal reaction time was 2 h with Er catalysts.

Impact of agitation

Er_{15}/γ-Al_2O_3 reacted with lactose at 150, 170, and 190 °C, from 0.5 to 2 h (Figure 3.7). The behavior is similar for both 150, and 170 °C reactions: when increasing temperature, and time, lactic acid production increases with its maximum yield reached at 170 °C for 23 % of LA, including washed sample. At 190 °C, LA yield remained quite stable at 19 % from

30 min to 1 h. While, with a non-agitated vessel, LA reached its highest yield of 17 % after 2 h. Stirring increased lactic acid production, due to an increased mass transfer inside the vessel. The higher heat transfer provided by the oil bath, as opposed to hot air, also contributed to reduce the reaction residence time from 2 h to 30 min.

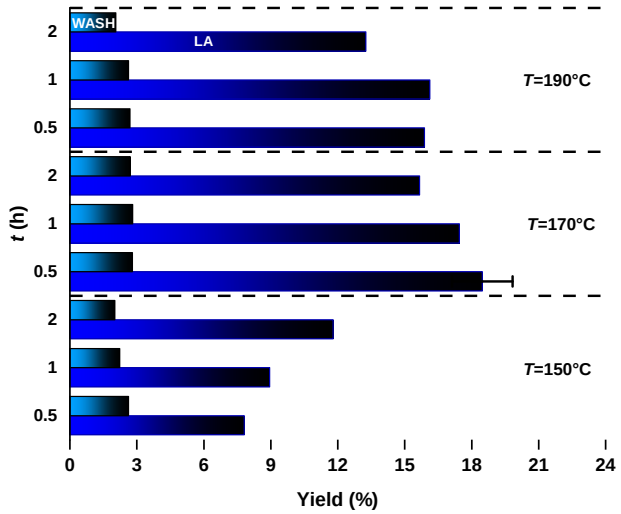

Figure 3.7 Impact of agitation on lactic acid yield, and lactose conversion, with Er_{15}/γ-Al_2O_3. Reaction conditions: Lactose 5 %. n=2, error bars represent standard deviation, 70 rpm.

Impact of reaction feedstock

We selected Er_{15}/γ-Al_2O_3, as it produced the highest yield in lactic acid to investigate the reaction scheme with the intermediates. The catalyst reacted with glucose, galactose, and fructose as feedstock, the key supposed transitional products of the reaction. Glucose, galactose, and fructose as a feedstock produced lactic acid, HMF, and formic acid. Lactic acid production follows this order: glucose, and fructose respectively yielded 23 % and 21 %. The yield decreases slightly with galactose 20 % (Figure 3.8). This is in accordance with Jeong and al., who reported that glucose conversion to lactic acid is faster than galactose one [93]. Regarding HMF, its production increases with galactose (8 %), and glucose (7 %) as feedstock compared to fructose (5 %). It suggests that glucose, and galactose may degrade directly to HMF, prior to the isomerization to fructose. Based on the previous results, we propose the following mechanism (Figure 3.9): first, lactose hydrolyzes to glucose, and galactose, which both isomerize to fructose or degrade to HMF. Fructose may dehydrate to HMF, directly convert to formic acid or produce C3 intermediates (glyceraldehyde, and dihydroxyacetone) through a retro-aldolization. A subsequent dehydration converts the mentioned intermediates to pyruvaldehyde, which yields lactic acid through an intramolecular Cannizaro reaction

in presence of hydroxide ions. Then, HMF, and lactic acid may degrade to form formic acid, and humins.

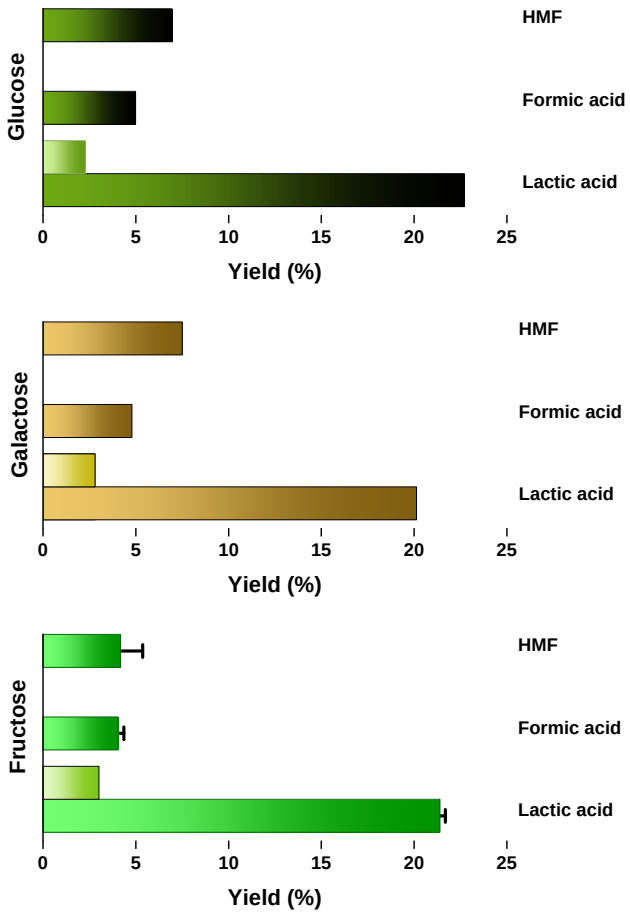

Figure 3.8 Impact of feedstock on lactic acid, formic acid, HMF, and fructose yields with Er_{15}/γ-Al_2O_3. Reaction conditions: Sugar 2.5 %, 170 °C, 0.5h. n=2, error bars represent standard deviation, 70 rpm. Wash samples (clear colours) displayed for a product yield > 1 %.

Modelling

To identify how each of the factors (temperature, time, Er and Sn concentration, and mass of catalyst) contributes to the yield, we developed a non-linear regression model [103] based on a first order series reaction (A (lactose) → B (lactic acid) → C (degradation products)) in a batch reactor:

$$C_{\mathrm{B}} = \frac{k_1 C_{\mathrm{Ao}}}{k_2 - k_1} \left(\exp k_1 t - \exp k_2 t\right) \tag{3.3}$$

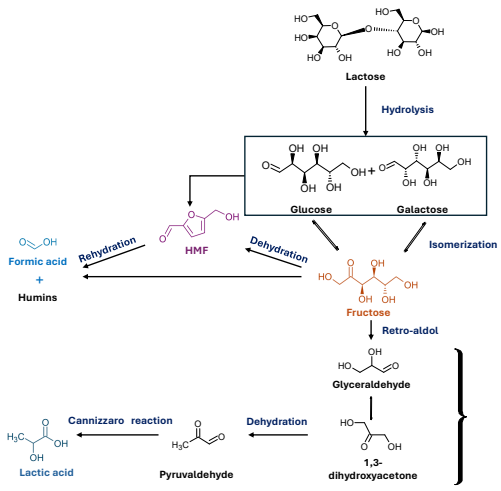

Figure 3.9 Possible reaction pathway for lactose conversion (based on the results of this study, and the reaction mechanisms proposed in ref [2–5]

.

The regression model has the essential features of this equation but the values of k_1 and k_2 in the model are not representative of a first order rate constant rather they indicate the order of magnitude contributions:

$$Y_{\mathrm{LA}} = k_1 \times \left(e^{-k_1 \times t} - e^{-k_2 \times t}\right) \tag{3.4}$$

where

$$k_1 = 0.13 \exp\left(\frac{-Ea_1}{R}\left[\frac{1}{T} - \frac{1}{463}\right]\right) \frac{(Er/Sn)^{0.1}}{m^{0.2}} \tag{3.5}$$

$$k_2 = 2.4 \exp\left(\frac{-Ea_2}{R}\left[\frac{1}{T} - \frac{1}{463}\right]\right) \frac{(Er/Sn)^{0.1}}{m^{0.2}} \tag{3.6}$$

$$t = t_0 - 1 \tag{3.7}$$

The variable t represents the time adjusted to take into account heating up of the reactor from the point we first start heating, t_0, and the value "1" is the best fit parameter suggesting it takes about 1 h to reach conditions in which the reaction begins. We have referenced one of our articles that had adopted this approach to modelling concentration [103]. The ratio of Er/Sn indicates that Er contributes to the reaction rate while Sn is in fact detrimental. Unexpectedly, more catalyst also appears to accelerate the decomposition of the lactic acid as it has a negative exponent. Finally, the pseudo-"activation" energy terms (Ea_1 and Ea_2) is much greater for the series reaction k_2 (95000) than k_1 (23000) and this limits the yield. The model accounts for 90 % of the variance in the data, which is surprisingly good considering

the data set consists of 84 independent measurements spanning a wider variable space of mass, temperature, time, and concentration (Figure 3.10). A power-law fails when one of the factors is set to zero, i.e. when we only have one active metal. To account for this deficiency, we add one to its value and so the exponent of 1, will equal 1 and thus will not contribute to the calculated yield.

$$Sn = sn(\%) + 1 \tag{3.8}$$

$$Er = er(\%) + 1 \tag{3.9}$$

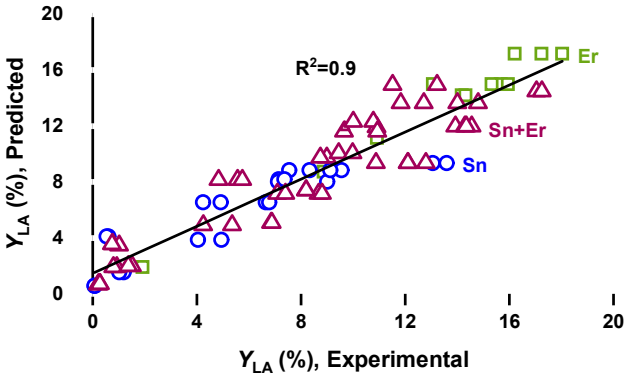

Figure 3.10 Predicted yield of lactic acid compared to experimental yield ($R^2 = 0.89$).

The model confirms that increasing the reaction time, induces a rapid decrease of LA yield compared to lactose consumption, which agrees with our data, as we observe LA decrease, starting at 2 h of reaction time Figure 3.1. However, the results show that the initial reaction time is much more lower than expected.

3.4 Conclusion

Tin, and erbium supported on γ-Al_2O_3 are both active to convert wasted lactose to lactic acid, and HMF. Erbium favours lactose hydrolysis, and is more selective towards lactic acid than Sn in the present system. The SnO_2 layer on the support, induced a mild Brønsted acidity, which had the effect of decreasing LA yield. Sn_{10}/γ-Al_2O_3, and $Sn_{10}Er_{15}/\gamma$-Al_2O_3 catalysts achieve a 100 % conversion of lactose at 190 °C in 2 h, while we observe a complete conversion at 170 °C, with Er_{15}/γ-Al_2O_3 catalyst in an agitated media within 30 min, likely due to an improved heat transfer, and mixing inside the vessel. Lactic acid reaches its maximum with Er_{15} catalyst, for a yield of 23 %, while HMF yielded the highest without catalyst at 190 °C. Galactose conversion rate to LA is slower compared to Glucose, and Fructose one, which both

yielded 25 % of LA at 170 °C, within 30 min. We fitted 84 experiments from the catalysts screening design to a non linear model, which describes the impact of time, temperature and metal ratio on LA yields. It confirms the higher energy requirement towards lactic acid formation compared to lactose consumption and its dependency on reaction time. To further evaluate the activity of Er catalyst, an analysis of the reaction kinetics is essential.

CHAPTER 4 ARTICLE 2 - ERBIUM CATALYZES LACTOSE AND WHEY PERMEATE TO LACTIC ACID AND HMF

In chapter 3, we demonstrated that $0.15\,\mathrm{g\,g^{-1}}$ of erbium oxide, supported on γ-Al_2O_3 converted all the lactose within 30 min at 170 °C. In this article, we first investigated the presence of internal and external mass transfer limitations that could hinder LA yields. Then, we assessed the effect of process parameters such as temperature, time, and pressure for multi-volume reactors, ranging from 25 to 250 mL. The reaction between fresh lactose and the spent catalyst revealed that, although the catalyst was still active, erbium leaching led to a decrease in LA yield. Finally, for different reactor's scale and time, we provided new data on the catalyst's efficiency in valorising industrial whey permeate, regarding the conversion of its lactose content, lactic acid, and HMF yield.

Maoline D. Houndedoke, Daniel Nickson, Michel Pouliot and Gregory S. Patience

Submitted in : Industrial & Engineering Chemistry Research, January 9, 2026

Abstract

Making 1 kt of cheese, produces 9 kt of cheese whey permeate, a waste with 5 % lactose, which is either discarded or dried for animal feed. One pathway to add value to this waste, is to convert it to lactic acid (LA), a monomer for polylactic acid, the largest bioplastic produced in the world. Lactose hydrolyses to glucose and galactose. While Brønsted acidity enhances lactose hydrolysis, Lewis acidity favors to lactic acid. For the first time, we tested both industrial whey permeate and purified lactose as feedstocks for LA over a heterogeneous catalyst–Er_2O_3/Al_2O_3 . LA Yield from whey permeate reached 14 %, while the maximum yield with purified lactose was 22 %. LA yield was invariant with respect to mixing speed while increasing temperature accelerates the time it takes to reach quasi-equilibrium. Yield was also independent of pressure with either air, He, N_2, or H_2 in the vapour space above the liquid phase in autoclave. LA yield over spent catalyst with fresh lactose was only 11 %, which indicates that the catalyst deactivates. Based on XRF analyses, the Er_2O_3 mass fraction dropped from 15 % to 5 %, with 6.4 % leaching into the aqueous phase after the first step but only 0.8 % after the second test.

Keywords: Scale up, Whey permeate, Lactic acid, Heterogeneous catalysis, Batch

4.1 Introduction

Lactic acid (LA) is a promising commodity as a feedstock to produce polylactic acid (PLA), a biodegradable polymer [17, 32], with applications in food packaging, textiles, medication dispensing system, and cosmetics. In 2020, it represented 19 % of the bioplastic market, and is projected to reach 4.5 billion USD by 2030 [16], which makes it the most produced biodegradable plastic. Anaerobic fermentation is the primary synthesis route for industrial LA [104]. Microorganisms such as *lactobacillus plantarum* strain, and *lactobacillus paracasei*, produce up to $0.9\,\mathrm{g\,g^{-1}}$ of lactic acid from sugar cane molasses, and $1\,\mathrm{g\,g^{-1}}$ from a mix of potato stillage waste, and sugar beet molasses [17]. A compelling feedstock for LA production is lactose derived from dairy waste streams. Lactose accounts for 5 % of cheese whey permeate (CWP), a byproduct of cheese making. In 2020, cheese production in Canada reached 540 kt, which is equivalent to almost 5 Mt of CWP [8].

The reaction pathway from lactose to LA includes lactose hydrolysis to galactose and glucose, isomerization to fructose, followed by triose formation (dihydroxyacetone, and glyceraldehyde), through retro aldol condensation, or fructose dehydration to 5-hydromethylfurfural (HMF), another green platform chemical [22,55,105]. Saavedra and al, tested various streams of carbon sources to produce LA, including lactose, galactose, sucrose, maltose, and cane molasses [106]. Yields ranged in the following order: lactose<galactose, maltose<sucrose<sugar cane. Brinques et al achieved a yield of more than $1\,\mathrm{g\,g^{-1}}$ of LA, starting from cheese whey as feedstock, with *lactobacillus plantarum*, after 48 h of reaction [107]. Although fermentation processes achieve high yields, they operate with yeast extract and dilute substrates, which results in feeble volumetric productivity [32, 107]. The process also requires reaction times up to 4 days, and nutrient supplement or bacteria growth [36, 64, 108].

An alternative is to produce LA with chemocatalysis. Wislicenus first discovered the process in 1863 [109]. Hydrogen cyanide reacts to acetaldehyde with a base catalyst to produce lactonitrile. After distillation, HCl or H_2SO_4 hydrolyses it to LA. However, the process depends on expensive petroleum material. Consequently, manufacturers of LA, such as Natureworks LLC(USA), and Musahino chemicals (Japan), shifted LA production to fermentation [36,37]. Few articles address the chemical conversion of lactose to lactic acid, through heterogeneous catalysis [24, 65].

We previously converted lactose to LA, in 30 min, at 170 °C, with a solid catalyst made of Er impregnated on γ-Al_2O_3 [6]. Here we investigated the relationship between reactor scale, agitation, temperature, time, and fresh vs spent catalyst on lactose conversion and LA yield. We report for the first time the heterogeneous catalysis of whey permeate to LA. CWP yield

was 6 % lower compared to pure lactose, potentially due to CWP ash content.

4.2 Experimental methodology

4.2.1 Catalyst synthesis

We combined 2 g of Al_2O_3 (Puralox SCCa-5/200, Sasol Chemicals USA) with 0.62 g of 99 % $ErCl_3 \cdot 6H_2O$ (Sigma Aldrich) in 1 g of water at room temperature [6]. The powder dried in an oven overnight at 60 °C then calcined for 4 h at 550 °C, with a ramp of 5 °C min^{-1}. This treatment oxidized the Er while driving off most of the Cl so that the catalyst retained a mass fraction of 0.15 g g^{-1} Er_2O_3. We adopted the following nomenclature to represent the catalyst: Er_{15}/Al_2O_3.

4.2.2 Batch experiments

Stainless steel autoclaves (SS304L) with volumes of 50 mL (R_{50}) and 250 mL (R_{250}) (Figure 4.1), were charged with 20 mL and 100 mL of a 5 % lactose solution with 0.8 g and 4 g of Er_{15}/Al_2O_3. After sealing the reactors, an electric mantle heated the solution from ambient temperature to the set-point (150–190 °C). After the autoclave reached the set-point, it was held at that temperature for 30 min to 2 h. Complementary experiments were completed at 170 °C in which we examined the solution after it reached the set-point and at 5 min, 10 min, 20 min, 30 min, 45 min, and 1 h. The results were compared to previously reported data in a 25 mL batch autoclave (R_{25} filled with 10 mL of lactose) [6]. To evaluate the effect of pressure, we blanketed R_{250} with N_2, He, or H_2, at 0.2 MPa, 2 MPa, and 2.5 MPa. He has a higher thermal conductivity than N_2, and H_2 can act as a reducing agent of coke precursors [31, 58, 110]. Spray-dried cheese whey permeate (Agropur) reacted with Er_{15}/Al_2O_3 in water in the R_{25} and R_{250} autoclaves. To assess time influence on conversion and yield, we varied the reaction time from 0–3 h, at 170 °C.

In all the experiments, we plunged the autoclave into an ice bath to quench the reaction as soon as possible. A Büchner funnel separated the liquid product from the spent catalyst. Distilled water washed the catalyst, and a 0.22 µm polytetrafluoroethylene membrane filtered the samples prior to high performance liquid chromatography (HPLC) analyses.

4.2.3 Products quantification

An HPLC (UHPLC 3000, with UV, and RI detectors) quantified reaction products, based on calibration curves for lactose, lactic acid, and HMF. The liquid product eluted in a Aminex

Figure 4.1 Multi scale lab reactors. From left to right: 250 mL (R_{250}), 3× 25 mL (R_{25}), and 2× 50 mL (R_{50}).

HPX-87H column, with 0.05 N H_2SO_4 as solvent. Conversion and carbon yield are defined with equations 4.1, 4.2, and 4.3, where n represents moles:

$$X = \left(\frac{n_{\text{i,lactose}} - n_{\text{f,lactose}}}{n_{\text{i,lactose}}} \right) \tag{4.1}$$

$$Y_{\text{LA}} = \left(\frac{3}{12} \right) \times \left(\frac{n_{\text{LA}}}{n_{\text{lactose}}} \right) \tag{4.2}$$

$$Y_{\text{HMF}} = \left(\frac{6}{12} \right) \times \left(\frac{n_{\text{HMF}}}{n_{\text{lactose}}} \right) \tag{4.3}$$

4.2.4 Characterization and statistical analysis

X-Ray fluorescence (XRF) from Malvern PANalytical (Epsilon 4) equipped with a silicon drift detector at 135 eV, measured the bulk element composition of spent catalyst [83]. An Horiba LA-950 particle size analyzer, measured the mean size of Er_{15}/Al_2O_3 [111] and a Keyence microscope captured imaging of the particles with their diameter, at 500x magnification. An analysis of variance evaluated significant differences for reactions supplemented with N_2 [112] with Statistica (Version 14.0.1.25, TIBCO Software). Analyses were performed by selecting a confidence level of 95 % on Statistica. X-ray spectroscopy (XPS) of the spent catalyst, with a Thermo Scientific ESCALAB 250Xi analyzer identified the elements chemical state and quantified them, with an Al Kα monochromatic source at 218.8 W (14.7 kV, and 14.9 mA). The pass energy applied to the survey spectra was 150 eV, with a step size of 1 eV. A JEOL JSM-7600F scanning electron microscope revealed the morphology of the spent

catalyst (resolution of 1 nm at 15 kV) and the surface element composition through EDX.

4.3 Results and discussion

4.3.1 Internal and external mass transfer limitations

The first parameter we tested was rotational speed for different reactor volumes, as we hypothesized that stirring would enhance lactose diffusion to catalyst surface, and consequently within its pores [113]. Therefore, in case of external mass transfer limitations, lactose conversion would increase with rotation speed, and consequently LA yield. Preliminary confirmed that external mass transfer limitation was negligible, as agitation speed slightly affected LA yield: for all conditions, the yield only varied from 20-<23 % although the magnetic stirrer reached 2000 rpm in R_{250} but only 200 rpm in R_{25}, and R_{50} (Figure 4.3). Mears numbers confirmed the absence of external mass transfer [114, 115] (ω) :

$$\omega = \frac{r_{\text{i,lactose}} \times \rho_{\text{p}} \times R_{\text{p}}}{k_{\text{c}} C_{\text{i, lactose}}} < \frac{0.15}{n} \tag{4.4}$$

With:

$$k_{\text{c}} = \frac{N_{\text{Sh}} \times D_{\text{m}}}{2R_{\text{p}}} \tag{4.5}$$

$$N_{\text{Sh}} = 2 + 0.55 N_{\text{Re}}^{0.5} N_{\text{Sc}}^{0.33} \tag{4.6}$$

$$N_{\text{Re}} = \frac{\rho \times N \times D^2}{\mu} \tag{4.7}$$

$$N_{\text{Sc}} = \frac{\nu}{D_{\text{m}}} \tag{4.8}$$

with, $r_{i,lactose}$ the initial rate of lactose conversion, ρ_{p}, and R_{p}, the catalyst's particle density furnished by the manufacturer (850 kg m^{-3}), and its mean radius of 82 µm (Figure 4.2). The mass transfer coefficient is k_{c}, with D_{m} (2.3×10^{-9} m^2 s^{-1}) the diffusion coefficient of lactose in water based on Wilke-Chang correlation [116]. As water is the main component of the liquid feed ($\geq$ 95 %), its viscosity at 150 °C was considered for the calculation: 181 µPa s at

150 °C [117]. N_{Sh} represents the Sherwood number, N_{Re}, the Reynolds number, N_{Sc} as the Schmidt number, and n, the reaction order, considered as 1. The fluid velocity is N (s^{-1}), D is the diameter of the stirrer (m) and ρ, water density ($1000\,\mathrm{kg\,m}^{-3}$). The kinematic density of water is ν ($\mathrm{m}^2\,\mathrm{s}^{-1}$) with $\nu = \mu/\rho$. N_{Sh} increases by a factor of 5, from 10–100 mL, and consequently Mears number decreases by a factor of 5 as well (Table 4.1).

In all cases, the Mears number confirmed the absence of external mass transfer resistance at 150 °C, as it was lower than 0.15. To evaluate internal mass transfer, we calculated the Weisz-Prater modulus (ϕ) [64, 114, 118] with:

$$\phi = \frac{r_{i,\mathrm{lactose}} \times \rho_{\mathrm{p}} \times R_{\mathrm{p}}^2}{D_{\mathrm{eff}} C_{i,\mathrm{lactose}}} < 1 \tag{4.9}$$

$$D_{\mathrm{eff}} = \frac{\phi_{\mathrm{p}} \times \sigma_{\mathrm{c}}}{\tau} \times D_{\mathrm{m}} \tag{4.10}$$

$D_{\mathbf{eff}}$ represents the effective diffusion coefficient;

$\phi_{\mathbf{p}}$ is the particle porosity (0.37, calculated as the ratio of the pore volume, and total volume [6, 119]);

$\sigma_{\mathbf{c}}$ is the constriction factor, which is function of the ratio between the maximum, and minimum pore areas, and accounts for changes in the cross sectional area of diffusion pathway; and,

τ refers to the tortuosity (σ_{c}/τ=0.123) [120].

Internal mass transfer is not limiting the reaction, as ϕ was 0.2 for R_{25} and 0.1 for R_{50} and R_{250}.

Table 4.1 Mears parameters for multiscale lactose conversion

Volume mL	N_{Sh}	k_{c} $\mathrm{m}^2\,\mathrm{s}^{-1}$	r_i, lactose $\mathrm{mol\,s}^{-1}\,\mathrm{kg}^{-1}$	Mears number
10	108	3×10^{-3}	2×10^{-3}	1×10^{-4}
20	152	4×10^{-3}	1×10^{-3}	7×10^{-5}
100	507	1×10^{-2}	1×10^{-3}	2×10^{-5}

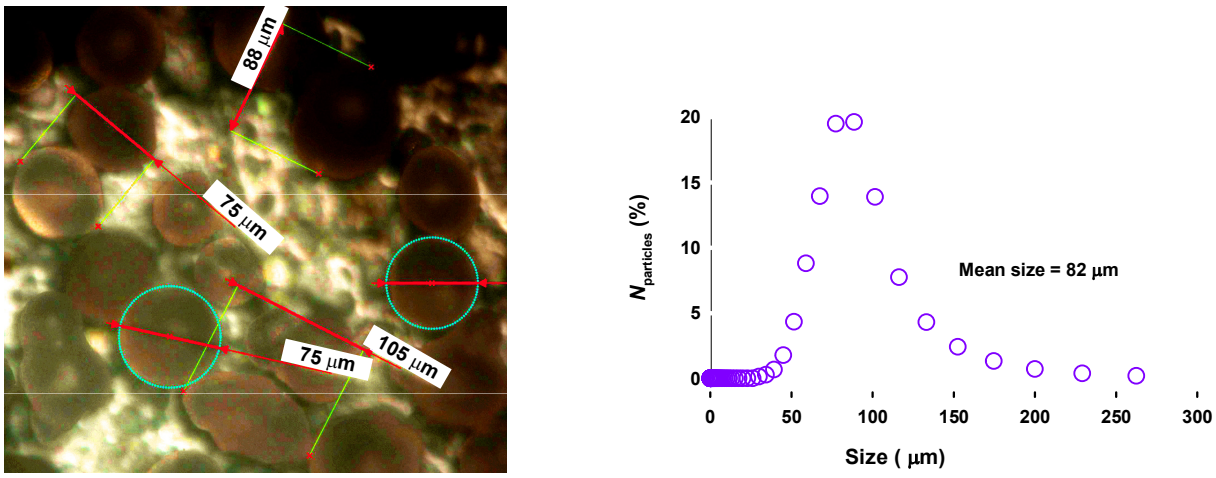

Figure 4.2 Particle size distribution of Er_{15}/γ-Al_2O_3 (right), and microscope imaging. x500 magnification (left).

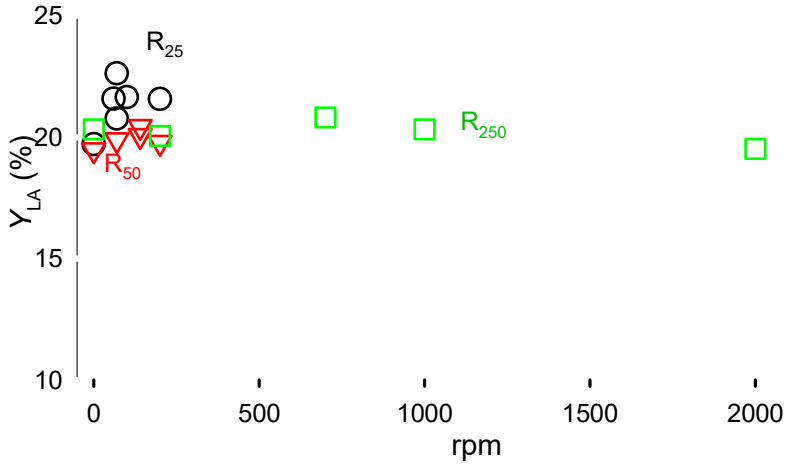

Figure 4.3 Lactic acid yield as a function of reactor volume, and magnetic stirrer rotational speed. Reaction conditions: Lactose 5 %, Er_{15}/γ-Al_2O_3, 170 °C, heating time of 1 h, 0 to 2000 rpm.

4.3.2 Temperature

Lactose reacted at 150 °C, 170 °C, and 190 °C with Er_{15}/γ-Al_2O_3, from 30 min–2 h. We compared previously reported data in R_{25} [6] with R_{50}, and R_{250}.

While the autoclave heats, lactose reacts (Figure 4.5). So, selecting a time zero is somewhat arbitrary: For R_{250}, it takes 63 min to reach 150 °C and another 10 min to reach 190 °C. To account for the reaction during the heating period, we considered the time to reach the

target temperature and the reaction time as heating time (Figure 4.4). At 190 °C the yield is initially high as the lactose reacts during the transient heating and then drops as lactic acid began to degrade. This trend is repeated at 170 °C. From 2 h of reaction time (corresponding to 2.3 h of heating time), LA yield is essentially independent of volume or temperature.

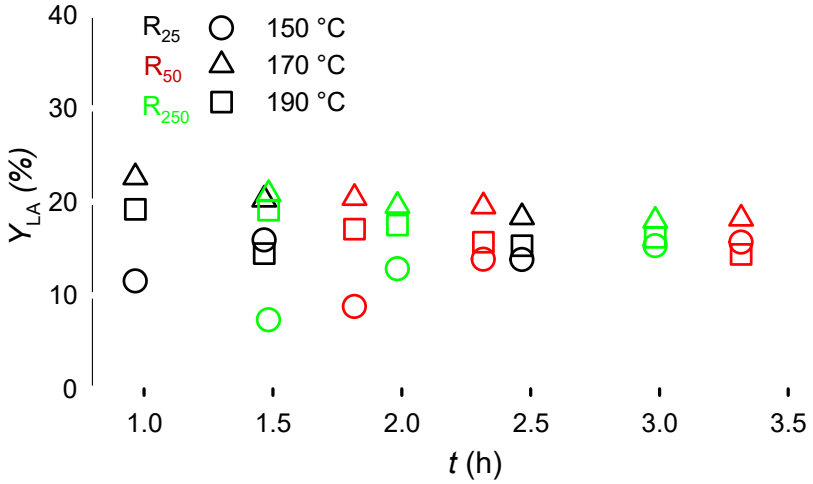

Figure 4.4 Lactic acid yield as a function of reactor volume, temperature, and heating time. Reaction conditions: Lactose 5 %, Er_{15}/γ-Al_2O_3, 70 rpm for R_{25} [6], 140 rpm for R_{50}, and 700 rpm for R_{250}. The colour represents autoclave volume, while the symbol type corresponds to temperature. It took 30 min to heat R_{25} (black symbols) from ambient to the set-point. The time on the y-axis includes the heating time and the time at the set temperature.

Here, we are the first to report that as reaction time increases, LA sourced from lactose, reaches a quasi-equilibrium independent of conditions. Bicker et al. reacted dihydroxyacetone, fructose, and glucose over $ZnSo_4$ in a continuous reactor at subcritical conditions (200–360 °C and 25 MPa) [49]. At residence times above 100 s, conversion was essentially 100 % for each of the substrates. Selectivity with glucose as a feedstock was 24 % while it reached 28 % with fructose (hexoses) and 55 % for the dihydroxyacetone (3 carbon molecule) (Figures 8-10 in their article). For each reaction, the exit concentration of the lactic acid was close to 50 % of the inlet substrate concentration. Lactic acid yield from fructose over erbium was equivalent to lactose (25 % versus 23 %), which is similar to the results of Bicker et al. but at very different conditions [6, 49].

Wang et al. converted glucose, fructose, mannose, and sucrose to ethyl lactate in ethanol. The conversion involves a retro-aldol condensation of fructose to trioses (glyceraldehyde, and

dihydroxyacetone), followed by their dehydration to methylglyoxal, and acetalization to yield ethyl lactate (EL) [114, 121]. As the retro-aldol reaction is endothermic, increasing temperature thermodynamically benefited EL production, which confirms the observed behaviour in this study.

4.3.3 Time

A complementary study evaluated the impact of volume and time on LA yield at 170 °C. The R_{50} and R_{250} curves in Figure 4.5 overlap sooner than R_{25}. After 1 h of heating, R_{25} reached a yield of 23 %, while it was only 17 % in the R_{250}.

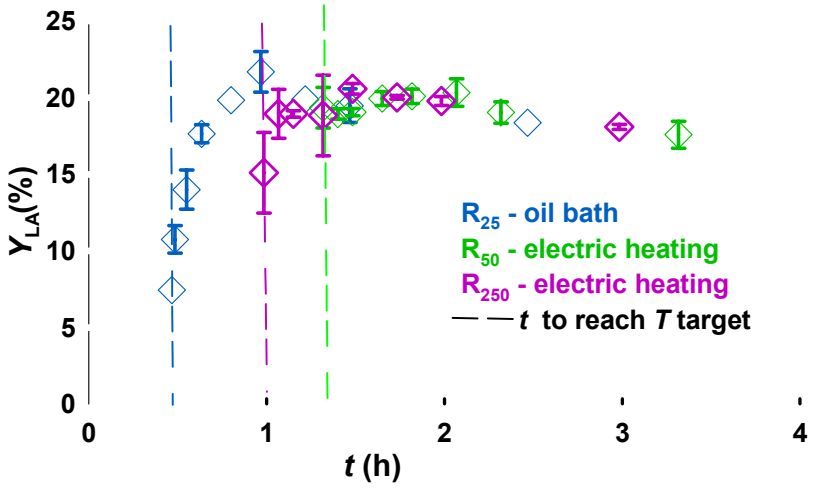

Figure 4.5 Lactic acid yield in function of reactor volume, and time. Reaction conditions: Lactose 5 %, Er_{15}/γ-Al_2O_3, 170 °C, 70 rpm for R_{25} [6], 140 rpm for R_{50}, and 700 rpm for R_{250}. Error bars represent standard deviation with $n = 2$. The vertical, coloured-dashed line represents the time it took the autoclave to reach the set-point temperature.

This trend highlights the differences in the heating rates of the reactors: An electric mantle heated R_{50} and R_{250} autoclaves, an oil bath heated the R_{25}vessel: R_{25} heated at $6\,°\,min^{-1}$ while R_{250} heated at $3\,°\,min^{-1}$ (Figure 4.6). Theses values match the heating rate range in the literature for subcritical water processes, from 2 to $7\,°\,min^{-1}$ [122, 123]. Consequently, the initial time of reaction for R1 ($t_{0,R_{25}}$) started after 29 min of heating, while $t_{0,R_{250}}$, was after 59 min. This is the first report of heating time effect on the multiscale conversion of lactose, with a heterogeneous catalyst. An analogous process of brewer's spent grain conversion to glucose, xylose, and arabinose by Alonso et al., confirmed that heating time

was a critical factor. Laboratory scale experiments with a heating time of 16 min yielded a higher arabinose content than at the pilot scale, with a heating time of 5 min. However, both were compared at 22 min, not accounting for the time delay induced by the heating time, which explains the discrepancies in their results [123]. The difference becomes insignificant after 1.5 h (Figure 4.5).

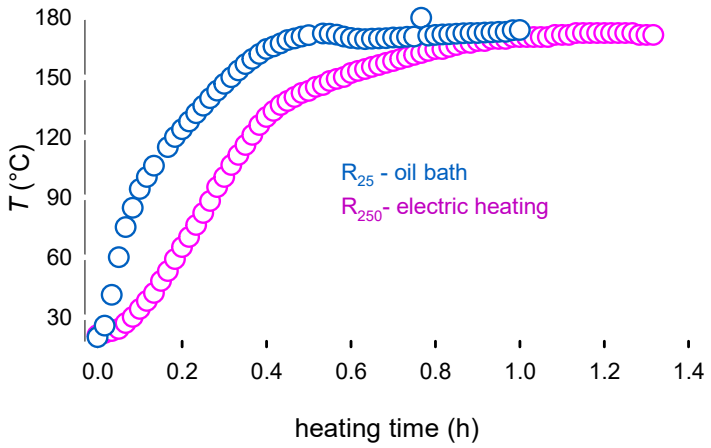

Figure 4.6 Heating curves for R_{25} and R_{250}. The target temperature was 170 °C. Reaction conditions: Lactose 5 %, Er_{15}/γ-Al_2O_3, 70 rpm for R_{25}, and 700 rpm for R_{250}.

4.3.4 Pressure

The influence of pressure on lactose conversion, LA, and HMF yield was assessed inside R_{250} (Figure 4.7) at 3 levels: ambient, 2 MPa, and 2.5 MPa. We also tested 0.2 MPa to assess the impact of H_2 on LA yield since H_2 can act as a reducing agent of carbonaceous solid precursors [124, 125]. LA reached a maximum yield of 22 % at 2.5 MPa with N_2. With He, and H_2, LA yield was essentially constant from 0.2 MPa to 2.5 MPa. Lactose conversion and HMF yield are also quite constant for both He and N_2, ranging from 95 % to 98 %, and 9 % to 10 %. With H_2, HMF reached 11 %, while lactose conversion was 95 %.

An analysis of variance (ANOVA) assessed if the yields were sensitive to pressure in the presence of N_2. The p-value>0.05, which suggests that LA yield is insensitive to P_{N_2}. Monteiro et al. performed the hydrothermal treatment of sugarcane bagasse at 2.5 MPa and 10 MPa. Their study aligns with our results as they observed that pressure was insignificant for oligosaccharides release [126].

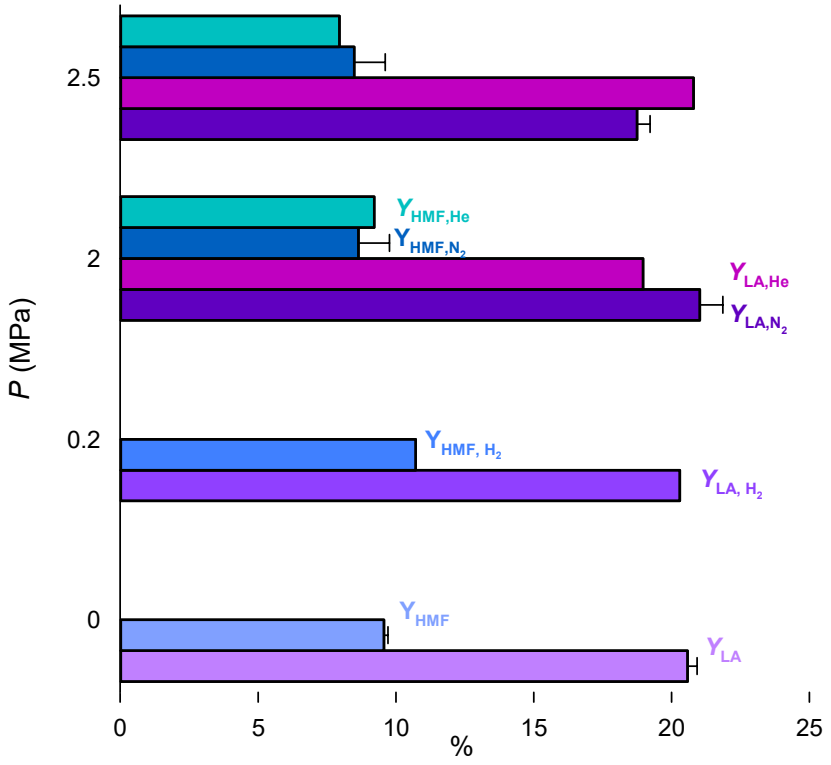

Figure 4.7 Influence of nitrogen, and helium on lactose conversion, lactic acid, and HMF yield. Reaction conditions: Lactose 5 %, Er_{15}/γ-Al_2O_3, 170 °C, R_{250} at 700 rpm. Error bars represent standard deviation with n = 2.

4.3.5 Coked catalyst activity

As previous experimentation showed that LA yield increased with temperature and time until reaching an equilibrium at a complete conversion of lactose, we hypothesized that Er_{15}/γ-Al_2O_3 was still active. To test this assumption, spent catalyst reacted with fresh lactose (Figure 4.8). Surprisingly, the lactose conversion reached 95 % with a LA yield of 11 % and 13 % HMF yield. When comparing to fresh catalyst, lactic acid yield decreases 8 % (absolute) but HMF increases 3 %. While used catalyst still hydrolyses lactose, the consecutive conversion of monosaccharides is challenging as the yield to glucose reached 22 %.

We compared the XRF analysis of the fresh catalyst with the spent one. Er leached during the reaction, as it decreased from 15 % to 5 %. The analysis of the liquid product confirmed the presence of Er in the sample (Table 4.2).

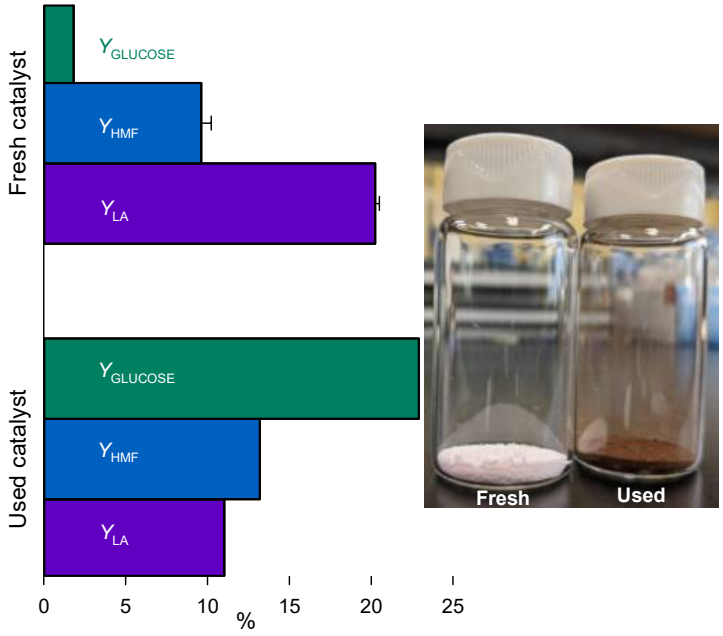

Figure 4.8 Used catalyst activity for lactose, and whey permeate conversion to lactic acid, HMF, and glucose. Reaction conditions: Lactose 5 %, 30 min. Er_{15}/γ-Al_2O_3, 170 °C, R_{50} at 140 rpm. Experiment with fresh catalyst repeated twice. Error bars represent standard deviation with $n = 2$.

Table 4.2 XRF analysis of fresh and spent catalyst

Sample	Er_2O_3 (%)	
	Fresh catalyst	Used catalyst
Powder	15	5
Liquid sample	6	0.7
Liquid sample (wash)	0.4	0.1

Er can replace hydrogen on Al-OH surface bonds, decreasing Brønsted acidity. With Er leaching, the reverse effect may increase Brønsted acidity, which favors lactose hydrolysis and fructose dehydration to HMF [4,56]. Interestingly, only 0.8 % of the erbium leached into the liquid sample compared to 6.4 % with fresh catalyst. Amorphous carbon deposited on the catalyst surface may encapsulate Er, which decreases leaching [127]. Er is strongly oxophilic and may bind preferentially with oxygenated compounds of the reaction products than the catalyst [128, 129].

An XPS analysis of the spent catalyst characterized the chemical state of C, Al and O at the surface of the catalyst (Table 4.3).

Table 4.3 XPS Analysis of spent catalyst

Element	Chemical state	Peak binding energy (eV)	Atomic %
C	C-C, C=C	284.8	17.8
C	C-O	286.3	8.3
C	C=O	287.6	3.8
C	O-C=O	289.1	2.5
C	π to π^*	291.5	0.6
Al	Al_2O_3	74.9	16.8
O	Al_2O_3	531.05	11.2
O	C=O	532.5	7.9
O	C-O, C-O-C	533.1	9.4
O	O*-C=O	534.2	2.8
O	Al-OH	531.9	18.9

C-C and C=C bonds represented 54 % of the carbon quantified by XPS. The analysis also confirmed the presence of surface AlOH. SEM revealed that the formed carbon exists mainly in the form of aggregates, not bound to the support (Figure 4.9).

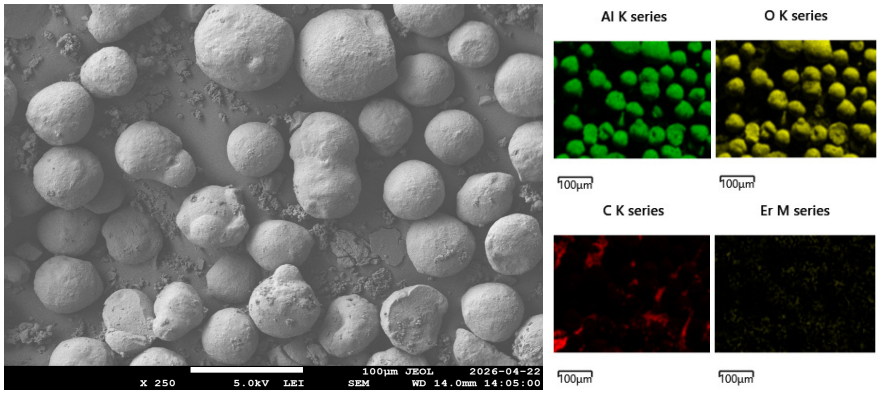

Figure 4.9 SEM-EDX of the spent catalyst. x250 magnification.

4.3.6 Towards whey permeate conversion

Wet tested industrial whey permeate with the three autoclaves and varying reaction time from 0–3 h. The LA yield was highest in R_{25} at 11 %, while the HMF yield was 10 %, and the whey permeate conversion was 71 % (Figure 4.10A). Subsequent testing consisted in varying reaction time in R_{25}. Conversion, LA, and HMF yield increased with time up to 1.5 h, with respective percentages of 93 %, 14 %, and 15 %. Longer reaction time (3 h) increased whey permeate conversion to 99 %, while LA, and HMF yield remained constant (Figure 4.10B).

This is the first record of heterogeneous conversion of whey permeate to LA, with a solid catalyst, which represents a proof of concept. These results agree with Turner et al., who performed the fermentation of lactose, and whey permeate to LA with a yeast engineered *S. cerevisiae*. With lactose, LA yield reached $0.58\,\mathrm{g\,g^{-1}}$ in 143 h, while they obtained $0.358\,\mathrm{g\,g^{-1}}$ with whey permeate in 110 h [130]. CWP furnished by Agropur contains 6.5 % of ash [131], which may decrease lactose hydrolysis.

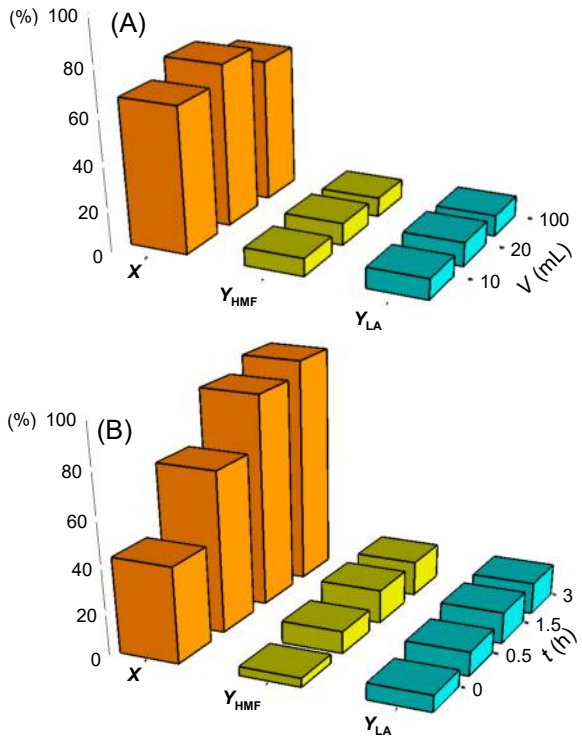

Figure 4.10 Influence of reaction volume **(A)**, and time **(B)** on whey permeate conversion, lactic acid, and HMF yield. Reaction conditions: whey permeate 4.4 %, Er_{15}/γ-Al_2O_3, 170 °C, 70 rpm for R_{25} [6], 140 rpm for R_{50}, and 700 rpm for R_{250}. The results in **B** are the main mean values of two tests, at 170 °C, and 30 min.

4.4 Conclusion

Here, we are the first to report the impact of mixing, temperature, time, and pressure on heterogeneous lactose conversion to LA, in multiscale-reactors. For the tested reaction volumes, LA yield was independent of agitation speed, and it reached an equilibrium when increasing

temperature, and heating time. Similarly to mixing, ANOVA results confirmed that yield was independent of pressure, and gas composition(H_2, N_2 or He). Lactose reaction with spent catalyst suggests that carbon deposited on spent Er_{15}/γ-Al_2O_3 may encapsulate Er, which explains the lower leaching effect at the consecutive second use of the catalyst. XPS revealed that the carbon chemical state is mainly C-C and C=C type bonds, while SEM-EDX indicate that it forms aggregates, not bound to the support of the catalyst. Testing of whey permeate resulted in a maximum yield of 14 % LA, and 15 % of HMF. These results gives valuable insights for dairy whey permeate valorization to lactic acid. Future research should focus on enhancing the strength of Er links to the support, and adequate carbon treatment to conserve the properties of the catalyst.

CHAPTER 5 ARTICLE 3 - UNVEILING THE KINETICS OF LACTOSE CATALYZED TO LACTIC ACID OVER Er/γ-Al_2O_3

The chapter 4 revealed the presence of a quasi-equilibrium: LA yield ranged between 20 and 23 %, as the temperature and heating time increased. In this chapter, we examined each step of the process through its kinetics: we derived the rate constant and the activation energy for lactose hydrolysis, glucose isomerization to fructose, and the subsequent conversion of each monosaccharide to LA, HMF and humins. Then, we built a model, that predicts the concentration of each substrate with an R^2 =0.99 and fits to experimental data combining 4 feeds: lactose, glucose, galactose, and fructose. These results aim to provide guidance to researchers for optimizing the heterogeneous process of lactose to lactic acid and reactor scaling.

Maoline D. Houndedoke, Marius Escoffier, Daria C. Boffito and Gregory S. Patience

Submitted in: Chemical Engineering Journal, March 11, 2026

Abstract

Whey permeate is an undesired by-product from making cheese that is disposed of or dried and sold as animal feed. Lactose is its primary constituent (4.4-5 % by mass) and reacts to high valued platform chemicals like galactose, lactic acid (LA), 5-hydroxymethylfurfural (HMF) but humins form in the liquid phase that compromise selectivity and productivity. Here we report a kinetic model that predicts product selectivity (lactose, glucose, galactose, fructose, LA, HMF and humins) as a function of temperature and time. The reaction pathway starts with lactose hydrolysis to glucose and galactose. Glucose isomerizes to fructose while the galactose converts to LA and HMF. Fructose is in equilibrium with glucose and also produces LA and HMF most likely through C3-intermediates (glyceraldehyde, dihydroxyacetone (DHA), and pyruvaldehyde (PVA)) adsorbed on the surface. When we fed the glyceraldehyde, it produced LA and HMF, but the DHA and PVA were absent from the HPLC peaks when fructose was the feedstock. Galactose produces more LA than glucose, while glucose isomerization and minimizing humins remain critical steps for the process. LA yield from fructose reaches 28 % at 150 °C, in 5 min over an erbium on γ-alumina catalyst.

Keywords: kinetics, lactose, lactic acid, heterogeneous catalysis, whey permeate, carbon waste

5.1 Introduction

Lactic acid (LA) is a feedstock for large volume commodities in in cosmetics, medicine, and especially, bioplastics, with biodegradable polylactic acid plastic [67]. Industrial biomass, like lactose from the cheese making process, is a potential feedstock to replace fossil fuels: LA yield from a 5 % solution of lactose over erbium catalyst reaches 23 % at 170 °C [6]. While multiple articles mention the kinetics of monosaccharides to value added products [132–136], there's a lack in the literature regarding kinetics of lactose to LA. The challenges are mainly due to the multiple steps of consecutive and parallel reactions in the process, and the formation of humins during sugars' degradation. The mechanism towards LA, with dissacharides implies hydrolysis to hexoses (glucose, fructose, xylose etc.) and their subsequent conversion to C3-intermediates (glyceraldehyde, dihydroxyacetone (DHA) and pyruvaldehyde (PVA) [2,64,70, 72,77,78,137].

Bicker et al. studied the kinetics of pyruvaldehyde, fructose and glucose degradation in supercritical water (300 °C) with Zn salts [49]. They reported a similar activation energy for glucose and fructose, while pyruvaldehyde was 4 orders of magnitude lower. However, the study neglects the kinetics of forming humins or the series reaction of PVA to LA. Lourvanij et al. reacted glucose with acidic Y-Zeolite from 110 °C to 160 °C: there was a step change in how much carbon formed at 130 °C [71]. All the glucose converted at 160 °C, within 8 h. The hydrolysis kinetics' of cellobiose were slower than for either sucrose, maltose between 50 °C and 80 °C over acidic solid catalysts (amberlite, mixed oxides and functionalized niobium solids) [138]. The maximum conversion was 20 % after 50 h, at 80 °C. Similarly to lactose, the 1,4-glycosidic bonds of cellobiose are more stable than the 1,2-glycosidic bonds of sucrose, requiring more energy to split and therefore higher reaction temperatures.

Swesi et al. reported the conversion of more than 50 % of cellulose, within 6 h, at 190 °C, without catalyst [139]. With ZrW as a solid Lewis acidic catalyst, the main product was LA within 5 h, while 5-(hydroxymethyl)furfural (HMF) and glucose predominated without catalyst. The pseudo-first-order kinetic constant for cellulose with ZrW was twice as high compared to no catalyst. Lindsay et al. investigated the kinetics of lactose conversion to glucose and galactose, with sulphuric acid, zirconium phosphate, and acidic resin Amberlyst 70, at 160 °C [43]. Among 12 lactose models catalyzed by H_2SO_4, the simplest and most accurate appeared to be the one with acid-catalyzed lactose conversion, coupled with thermal hydrolysis. Acid-catalyzed degradation of glucose and galactose were neglected as it had no impact on the model predictions. The model lacks any mention to by-products.

Here we are the first to propose a model characterizing the kinetics of lactose hydrolysis,

isomerization, retro-aldol condensation, hydrolysis, dehydration, and hydration to LA over a heterogeneous catalyst. The model accounts solid humins. Supplementary reactions starting from glucose, galactose, and fructose further refined the model. We conducted all the experiments in a stirred batch autoclave, with $0.15\,\mathrm{g\,g^{-1}}$ of Er solid catalyst on γ-Al_2O_3. The most critical challenge in the process is to isomerize glucose to fructose.

5.2 Materials and methods

5.2.1 Materials

Lactose ($\geq$98 %), glucose($\geq$99.5 %), fructose($\geq$99 %), galactose($\geq$99 %), HMF($\geq$99 %), lactic acid(DL,85 %), and erbium (III) chloride hexahydrate (99.9 %) were purchased from Sigma Aldrich. In all the experiments, distilled water was the solvent. Puralox SCCa-5/200 γ-Al_2O_3 was the catalyst support (Sasol Chemicals, USA).

5.2.2 Catalyst synthesis and characterization

$ErCl_3 \cdot 6H_2O$ (0.62 g) dissolved in 1 mL of water at room temperature. We added the solution dropwise to 2 g of γ-Al_2O_3, which then dried overnight at 60 °C. It then calcined at 550 °C, with a heating ramp of $5\,^\circ\,\mathrm{min^{-1}}$. The catalyst was identified as Er_{15}/Al_2O_3, as it contains a mass fraction of $0.15\,\mathrm{g\,g^{-1}}$ Er_2O_3. A LECO CS744 carbon and sulfur analyzer quantified the carbonaceous species responsible of the browning for the spent catalyst [140]. Each sample was analyzed twice and we associated the quantified mass of carbon to solid humins production.

5.2.3 Experimental methodology and product quantification

We conducted all the experiments in a 25 mL batch autoclave [6]. An oil bath, mounted on a hot plate, heated the sealed reactor from ambient to the set temperature (130, 150, 170, and 190 °C). A 0.4 g sample of the catalyst reacted with 0.5 g of lactose or 0.25 g of either glucose, galactose or fructose dissolved in 10 mL of distilled water. Reaction time ranged from 0 min (time at which the reactor reaches the set temperature) to 1 h, for a total of 90 experiments. An ice bath quickly quenched the reaction, and we filtered the products with a Büchner funnel. We washed the spent catalyst with 10 mL of distilled water and it dried in an oven overnight to quantify carbon content. We further filtered the liquid product with a 0.22 µm polytetrafluoroethylene membrane before HPLC analysis. Humins yield is the ratio of the mass of carbon on the catalyst to the number of moles of lactose (n_{lactose}) divided by

12, where the mass of carbon is product of the mass fraction of carbon (x_{C}) and mass of catalyst (m_{catalyst}):

$$Y_{\mathrm{humins}} = \left(\frac{1}{12}\right) \times \left(\frac{x_{\mathrm{C}} \times m_{\mathrm{catalyst}}}{n_{\mathrm{lactose}}}\right) \tag{5.1}$$

5.2.4 Kinetic modelling

We based the simplified kinetic modelling of lactose to lactic acid and HMF on the following assumptions:

1. Lactose hydrolysis and subsequent conversion to LA and HMF follows a pseudo homogeneous first-order approach (equations 5.2 to 5.8) [25]. Only thermal and acid catalyzed hydrolysis of lactose are considered [43].

2. The reverse reaction of fructose to glucose is non-negligible (equations 5.3 and 5.4) [26]. Lactose hydrolysis, fructose and galactose conversion to LA and HMF, glucose, galactose conversion, and degradation routes are all irreversible reactions.

3. Humins are either solids or soluble oligomers. Here, we explore the kinetics of the formation of solid humins, whose concentration corresponds to the carbon content of species deposited on the catalyst surface [27]. The model assumes that they originate from HMF, fructose, and galactose [28–31].

4. LA, HMF, and solid humins are the main products of dissacharides and monosaccharides conversion. All other by-products are negligible.

Following a first order kinetic approach, mass balance relates to the reactions rate as:

$$\frac{\mathrm{d}C_{\mathrm{lactose}}}{\mathrm{d}t} = -k_1 \cdot C_{\mathrm{lactose}} \tag{5.2}$$

$$\frac{\mathrm{d}C_{\mathrm{Gluc}}}{\mathrm{d}t} = k_1 \cdot C_{\mathrm{lactose}} - (k_2 + k_{dec-gluc}) \cdot C_{\mathrm{Gluc}} + k_3 \cdot C_{\mathrm{Fruc}} \tag{5.3}$$

$$\frac{\mathrm{d}C_{\mathrm{Fruc}}}{\mathrm{d}t} = k_2 \cdot C_{\mathrm{Gluc}} - (k_3 + k_4 + k_5 + k_{dec-fruc}) \cdot C_{\mathrm{Fruc}} \tag{5.4}$$

$$\frac{\mathrm{d}C_{\mathrm{Gal}}}{\mathrm{d}t} = k_1 \cdot C_{\mathrm{Lactose}} - (k_6 + k_7 + k_{dec-gal}) \cdot C_{\mathrm{Gal}} \tag{5.5}$$

$$\frac{\mathrm{d}C_{\mathrm{LA}}}{\mathrm{d}t} = 2k_4 \cdot C_{\mathrm{Fruc}} + 2k_6 \cdot C_{\mathrm{Gal}} - k_{dec-LA} \cdot C_{\mathrm{LA}} \tag{5.6}$$

$$\frac{\mathrm{d}C_{\mathrm{HMF}}}{\mathrm{d}t} = k_5 \cdot C_{\mathrm{Fruc}} + k_7 \cdot C_{\mathrm{Gal}} - k_{dec-HMF} \cdot C_{\mathrm{HMF}} \tag{5.7}$$

$$\frac{\mathrm{d}C_{\mathrm{Humins}}}{\mathrm{d}t} = 6k_{dec-gal} \cdot C_{\mathrm{Gal}} + 6k_{dec-HMF} \cdot C_{\mathrm{HMF}} + 6k_{dec-fruc} \cdot C_{\mathrm{Fruc}} \tag{5.8}$$

$k_{dec-gluc}, k_{dec-gal}, k_{dec-LA}, k_{dec-HMF}$ corresponds to the degradation kinetic rates of glucose, galactose, LA, and HMF to humins; and, $k_1, k_2, k_3, k_4, k_5, k_6, k_7$ are the kinetic constants of lactose hydrolysis (thermal and acid catalyzed), glucose to fructose isomerization, reverse isomerization of fructose to glucose, reaction 4, reaction 5, reaction 6, and reaction 7 respectively.

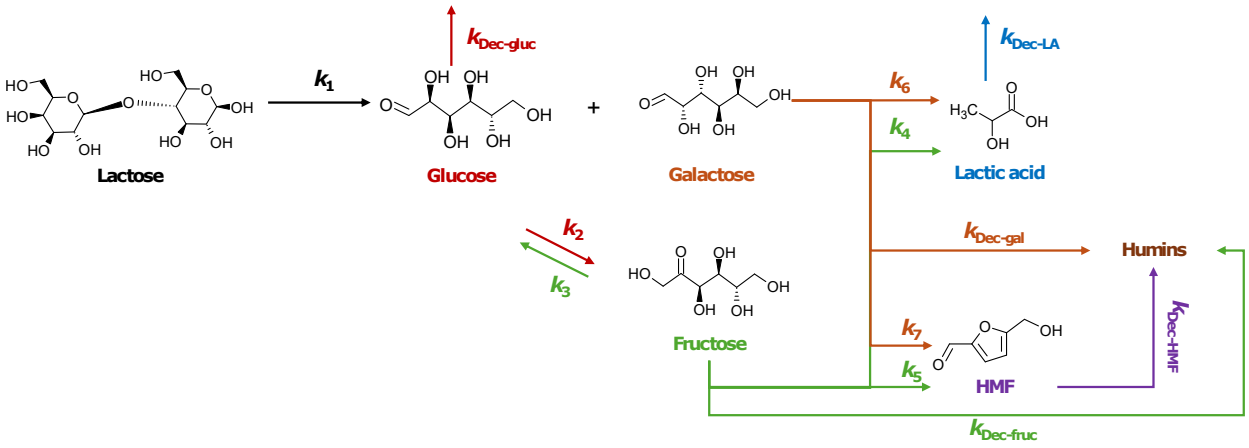

Figure 5.1 Lactose to LA, HMF, and humins reaction scheme.

Computation of reactions rate constants was as followed:

1. Lactose hydrolysis rate based on equations:

$$\frac{\mathrm{d}C_{\mathrm{Lactose}}}{\mathrm{d}t} = C_{\mathrm{Lactose,i}} \times \exp\left[-k \times \left(t + t_0 \times \left(\frac{T}{443}\right)^{\beta_0}\right)\right] \tag{5.9}$$

$$k = k_0 \times \exp\left[\frac{-Ea}{8.314} \times \left(\frac{1}{T} - 0.002257\right)\right] \tag{5.10}$$

With:

k lactose hydrolysis rate constant;

t reaction time once the reactor reached the target T;

t_0 time to heat the reactor to the target T;

T reaction T;

$\beta_\mathbf{0}$ T impact factor on t_0. If β is negative, with T above 170 °C, the effect of initialization time on lactose consumption decreases;

k_0 pre-exponential Arrhenius factor;

Ea activation energy;

Experimental data of lactose conversion fitted to the model, through the regression wizard of Sigma Plot 12.5., with reactions at 110, 130, 150, and 190 °C.

2. The ODE15s solver in MATLAB R2025b integrated the subsequent differential equations, and we optimized the model with the nonlinear least-squares tool, to minimize errors between the experimental data and predicted values [141,142]. We implemented the modified Arrhenius plot and experimental time as defined in equations 5.9 and 5.10 to account for the reactors heating time. The solver derived the kinetic rate constants and associated activation energy for each reaction step. A bootstrap loop of 1000 iterations [143] measured the incertitude on rates, for a CI of 95 % and a total of 475 experimental data points. In the loop, the model generates a noise based on the standard deviation of residuals from the original data multiplied by a randomized number. Then, the noise is multiplied by the mean of current observations to account for the magnitude of experimental data. The nonlinear least-squares tool integrates the new set of pseudo data points to display the effect on the rates and activation energies, and construct the CI.

5.3 Results and discussion

5.3.1 Lactose conversion

Lactose reacted with Er_{15}/γ-Al_2O_3 at 110, 130, 150, 170, and 190 °C, from 0 min (time at which the reactor reaches the target temperature) to 60 min (Figure 5.2).

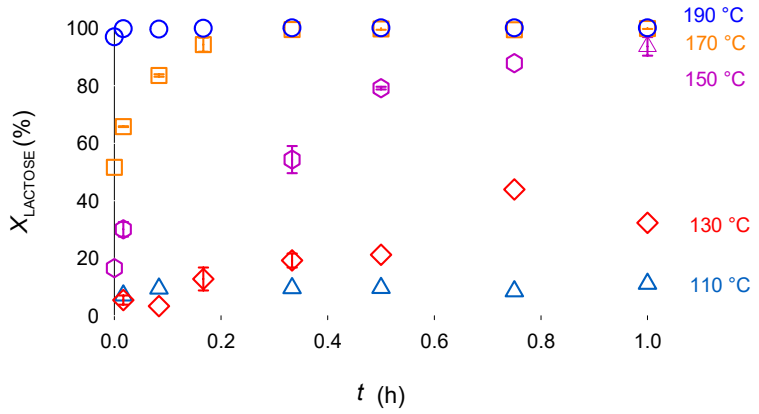

Figure 5.2 Lactose conversion with time, from 110 to 190 °C. Reaction conditions: Lactose 0.14 mmol, 0.4 g of Er_{15}/γ-Al_2O_3, n=2, error bars represent standard deviation, 70 rpm.

At 110 °C, lactose is essentially inactive: the highest conversion was 11 % after 1 h. Increasing temperature accelerates lactose conversion [19]. At 130 °C and 150 °C, conversion ranges from 3 % to 44 % and 17 % to 96 % respectively. Lactose completely converts at 170 °C within 30 min as previously reported [6]. Thus, we selected 130, 150, and 170 as the reference temperatures to conduct kinetics studies of lactose conversion to LA and HMF. To evaluate the catalyst effect on the kinetics, we performed blank experiments at 170 °C (Figure 5.3).

Lactose conversion at 0 min, goes from 7 % without catalyst to 52 % with Er_{15}/γ-Al_2O_3 (Figure 5.3A): the H^+ ions provided by the autoprotolysis of water combined to the catalyst Lewis acidity increases lactose hydrolysis by an initial factor of 7 [139]. Similarly to what was observed with H_2PtCl_6 and cellulose conversion, $ErCl_3$ on γ-Al_2O_3 could shift the dissociation equilibrium of water and therefore increase the release of protons in the media [92, 93, 144].

The difference between the two conditions decreases with time, with lactose reaching more than 90 % conversion after 45 min in both cases. The presence of Er_{15}/γ-Al_2O_3 clearly catalyzes the production of lactic acid, reaching 23 % compared to a maximum yield of 1 % for blank experiments (Figure 5.3B). In the case of HMF, yields are similar in both situations (Figure 5.3C), which suggests that the autoprotolysis of water mainly catalyzes HMF and lactose degradation, while erbium catalyzes lactic acid production. A high initial concentration of substrate leads to reduced energy consumption and reactor scale.

Therefore, we did complementary reactions to investigate the impact of varying lactose concentration on the reaction efficiency. A 20 mL solution of 0.025 to 1 g g^{-1} of lactose reacted with 0.8 g of Er_{15}/γ-Al_2O_3 (Figure 5.4A) at 170 °C. The time axis includes the time to heat

the reactor and the reaction time. Lactose solutions of 2.5 % and 5 % both had a similar degree of conversion with time, which suggests the reaction is first order. However, at 10 % conversion was lower, which may be due to deactivation due to humins. In all cases, lactose conversion was complete within 2 h. The yield of lactic acid was quite stable when increasing lactose concentration: it ranged from 18 to 21 %, which may suggest the presence of an equilibrium (Figure 5.4B). For HMF yield, it decreased when increasing lactose concentration to $0.1\,\mathrm{g\,g^{-1}}$, which is similar to what Liu and al. reported when reacting a 10 % maltose solution with nobium phosphate [145] (Figure 5.4C).

We also assessed the impact of catalyst loading, from 0.2 to 0.8 g in 10 mL of a fixed 5 % lactose solution (Figure B.1). All the samples resulted in a complete conversion of lactose at 170 °C and 30 min. LA yield was the highest for a catalyst loading of 0.4 g, while HMF decreased with increased loading. Surprisingly, solid humins yield was the lowest for 0.8 g of catalyst: Brønsted acidity catalyzes oligomers conversion to insoluble humins. A higher loading of $Er_{15}/\gamma\text{-}Al_2O_3$ may increase Lewis acidity and therefore decrease humins formation [27].

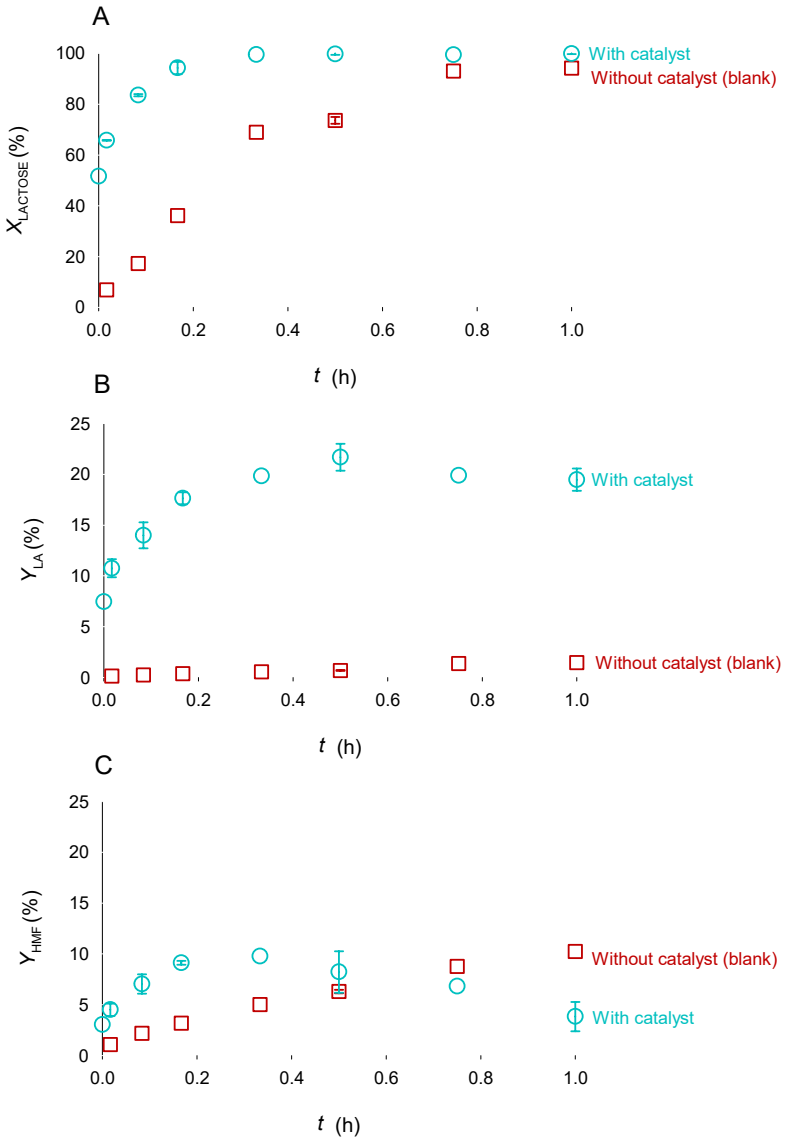

Figure 5.3 Comparison of lactose conversion (A), lactic acid(B), and HMF (C) yield time profile with Er_{15}/γ-Al_2O_3 and without catalyst. Reaction conditions: Lactose 0.14 mmol, n=2, error bars represent standard deviation, 70 rpm. 170 °C.

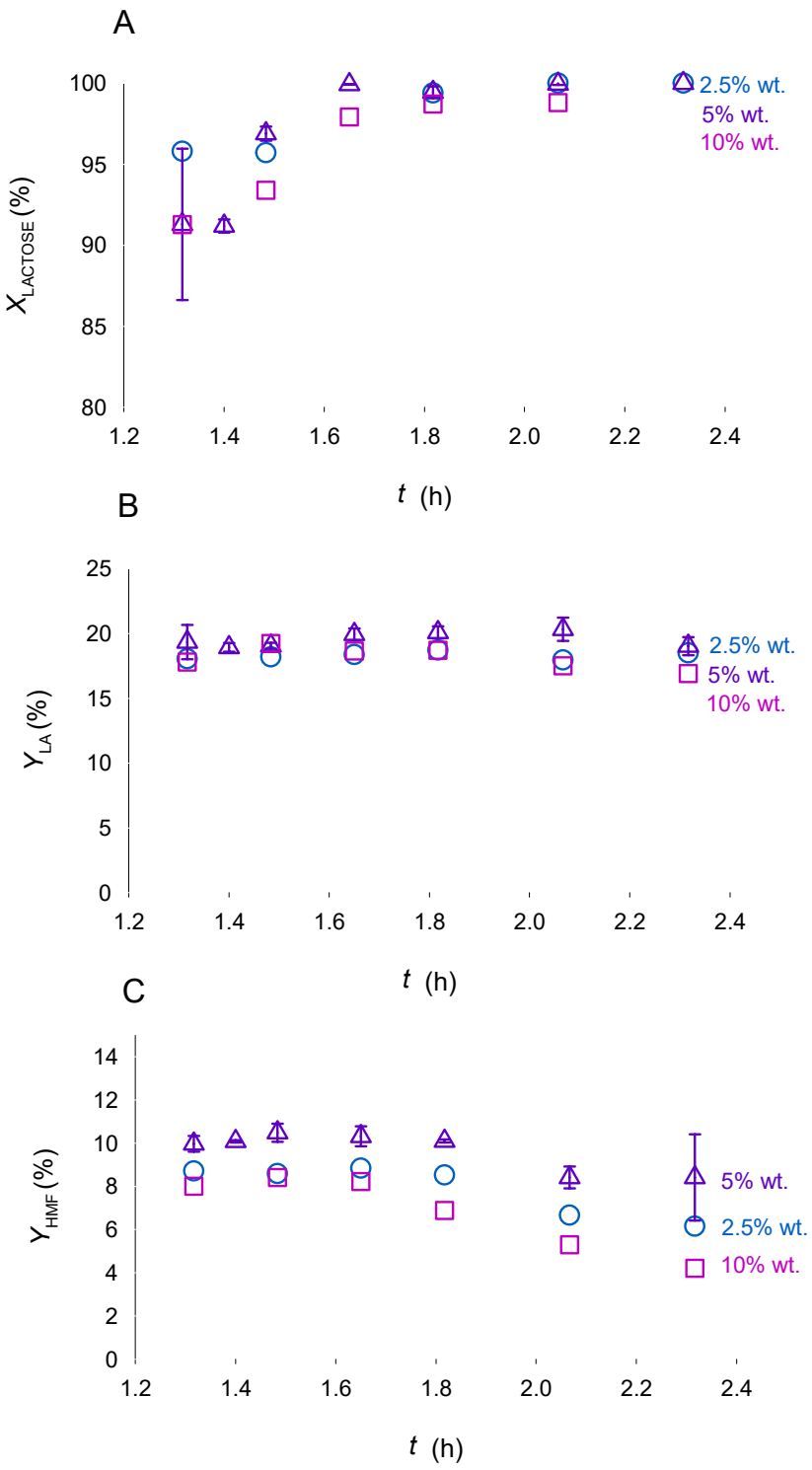

Figure 5.4 Time trajectory of lactose conversion, lactic acid, and HMF yield for different concentrations (0.025, 0.05 and 0.1 g g^{-1}). Reaction conditions: Lactose, 0.14 (2.5 %), 0.28 (5 %) and 0.56 mmol (10 %), 0.8 g of Er_{15}/γ-Al_2O_3, 20 mL, 170 °C, n=2, error bars represent standard deviation, 140 rpm.

5.3.2 Monosaccharides conversion

To identify the impact of lactose intermediates on conversion, glucose, galactose, and fructose reacted at 130, 150, and 190 °C in water (Figure 5.5). At 130 °C, fructose exhibits the highest conversion with a maximum of 89 % reached at 1 h. These are in accordance with Wang et al.: they tested fructose with acid catalysts, such as glucose/p-toluenesulfonic acid (Glu-TsOH), Amberlyst-15, and H-beta zeolites in DMSO and water. With Glu-TsOH, the conversion reached 100 % at 130 °C with DMSO, while the maximum was only 67 % in water, within 1.5 h [146]. This may suggest that $Er_{15}/\gamma\text{-}Al_2O_3$ is less prone to water poisoning than Glu-TsOH for fructose conversion [100]. For galactose, up to 75 % reacted within 1 h, compared to 63 % with glucose. It may indicate that galactose degradation requires a lower activation energy than for glucose one [99, 147]. Similarly, Catrinck et al. reported that glucose conversion at 135 °C ranges from 5 to 35 % with phosphate catalysts modified by titanium, aluminium, nobium, and zirconium for a reaction time of 200 min [148, 149]. Comparing these results to this study confirm that $Er_{15}/\gamma\text{-}Al_2O_3$ is a good candidate for glucose conversion. The conversion gap decreases for increased temperatures: at 150 °C and 45 min, the conversion was higher than 90 % for all the monomers.

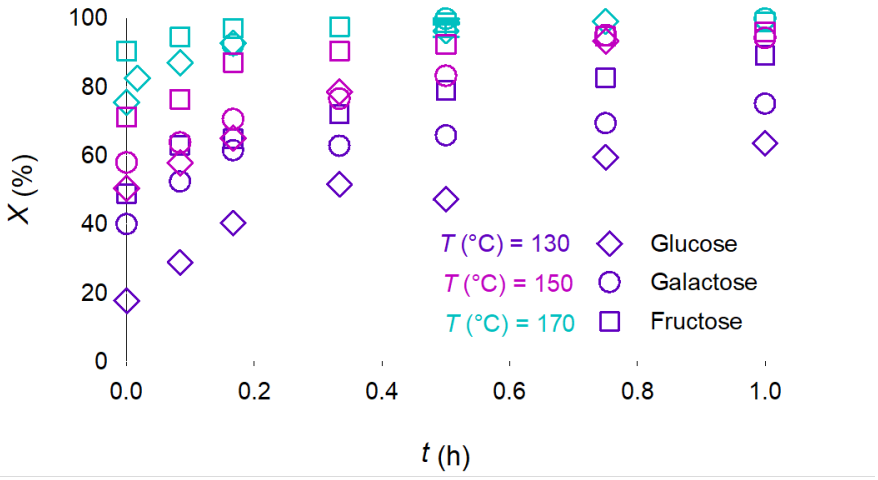

Figure 5.5 Lactose conversion with time, at 130, 150, and 170 °C. Reaction conditions: Glucose, galactose, and fructose 0.14 mmol, 0.4 g of $Er_{15}/\gamma\text{-}Al_2O_3$, n=2, error bars represent standard deviation, 70 rpm.

5.3.3 Lactic acid production

We assessed feedstock contribution on lactic acid yield: fructose shows the highest yield at 130 °C, with a yield of 26 % (Figure 5.6). While galactose and glucose exhibit a LA yield of 18 and 15 % respectively, lactose one is the lowest with a yield of 4 %. At this temperature, the corresponding conversion of lactose does not exceed 44 %, which may explain this discrepancy. These results also confirm that LA originate from glucose and galactose produced by lactose hydrolysis, and the subsequent isomerization of glucose to fructose. Results from fructose and glucose are similar to the ones reported by De clippel et al. with bifunctional carbon-silica catalysts in methanol. They obtained respectively 32 and 17 % of methyl lactate from fructose and glucose, although under harsher conditions (155 °C, 20 h) [137]. The yield difference between glucose and fructose is due to the isomerization of glucose to fructose which is a critical step for producing LA, and requires high temperatures [56, 63]. At 150 °C, LA from fructose reaches 28 % within 5 min, then starts degrading. It is in agreement with the thermogravimetry analysis of LA performed by Komesu and al., which indicates more than 70 % loss at 200 °C ([150], Figure 2a). Meanwhile, for the same conditions, LA from glucose and galactose reached a maximum of 21 % and 22 % respectively, and lactose, 16 %. Holm et al. reported an equilibrium, between glyceraldehyde (GLY) and dihydroxyacetone which may hinder LA production. GLY originates from the retro-aldol cleavage of fructose and was detected via HPLC but not DHA [151]. A further increase of temperature to 170 celsius, displaced the quasi-equilibrium to higher yields at reduced reaction time, but also degraded LA faster. These results highlight the competition between monosaccharides being produced and converted to LA, and LA degradation at high temperatures (Figure 5.6 C).

5.3.4 Humins and HMF production

From 130 to 170 °C, humins appear to be the highest with hexoses (fructose, galactose, and glucose) compared to lactose (Figure 5.7). Humins from fructose and galactose exhibited similar yields with a maximum of 22 and 26 % at 130 and 170 °C respectively from fructose, and 26 % at 150 °C from galactose. These results suggest that humins don't originate from the direct degradation of lactose but instead from the consecutive degradation of its hydrolysis product. It was reported that humins form through soluble oligomers produced by hexoses and HMF [27, 28].

We also plotted HMF against time, for 130, 150, and 170 °C. Flannely and al. reported a higher initial yield of HMF with fructose and glucose at 150 °C, than with galactose with 2.5 g g^{-1} of H_2SO_4 [99]. In this catalytic system, galactose gave the highest yield when reacting with Er_{15}/γ-Al_2O_3: 8 and 10 % of HMF yield for 130 °C and 150 °C respectively.

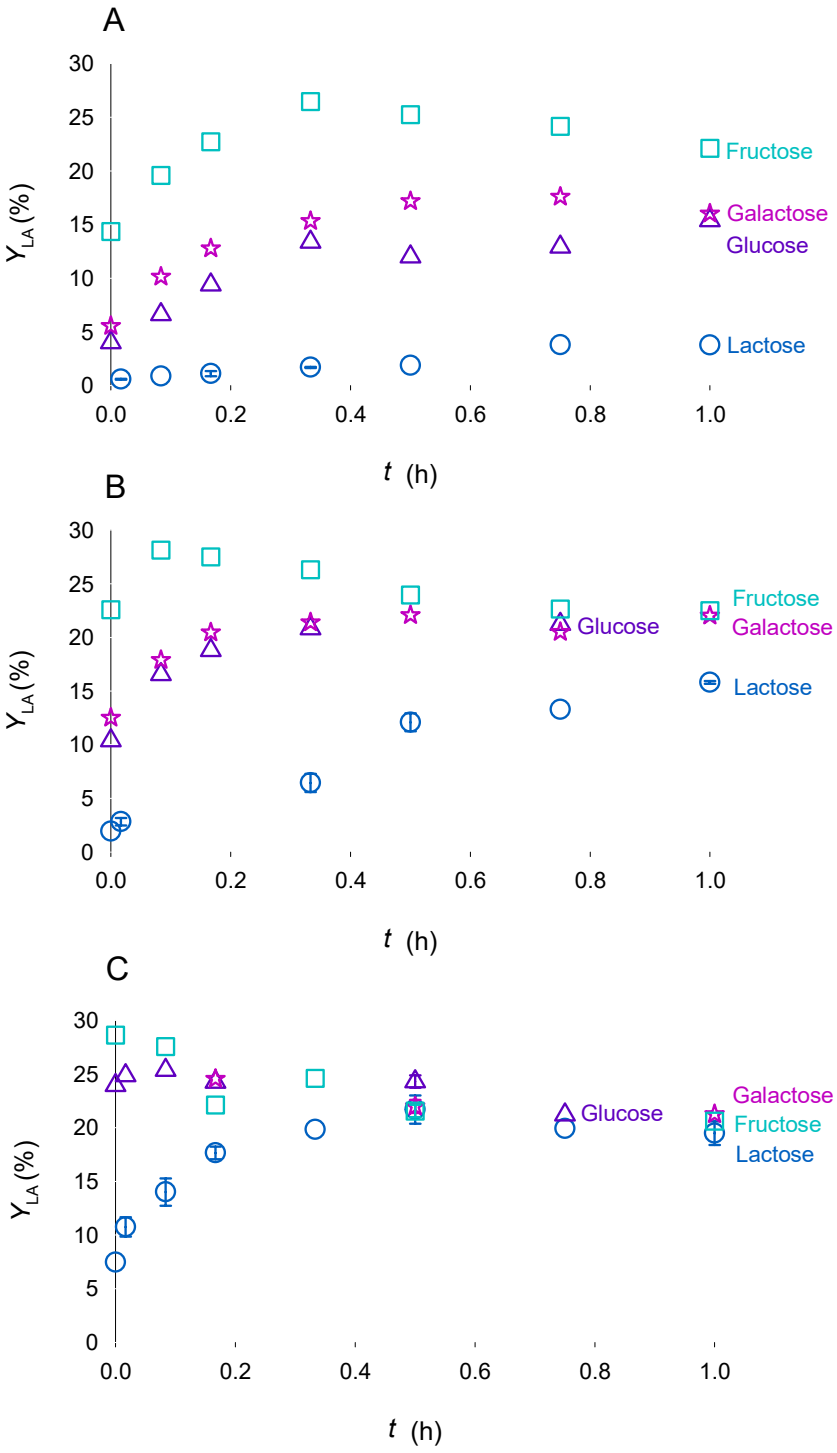

Figure 5.6 Lactic acid production with lactose, glucose, galactose, or fructose as feedstock, at 130 (A), 150(B), and 170 °C(C). Reaction conditions: Lactose, glucose, galactose, or fructose 0.14 mmol, 0.4 g of Er_{15}/γ-Al_2O_3, n=2, error bars represent standard deviation, 70 rpm.

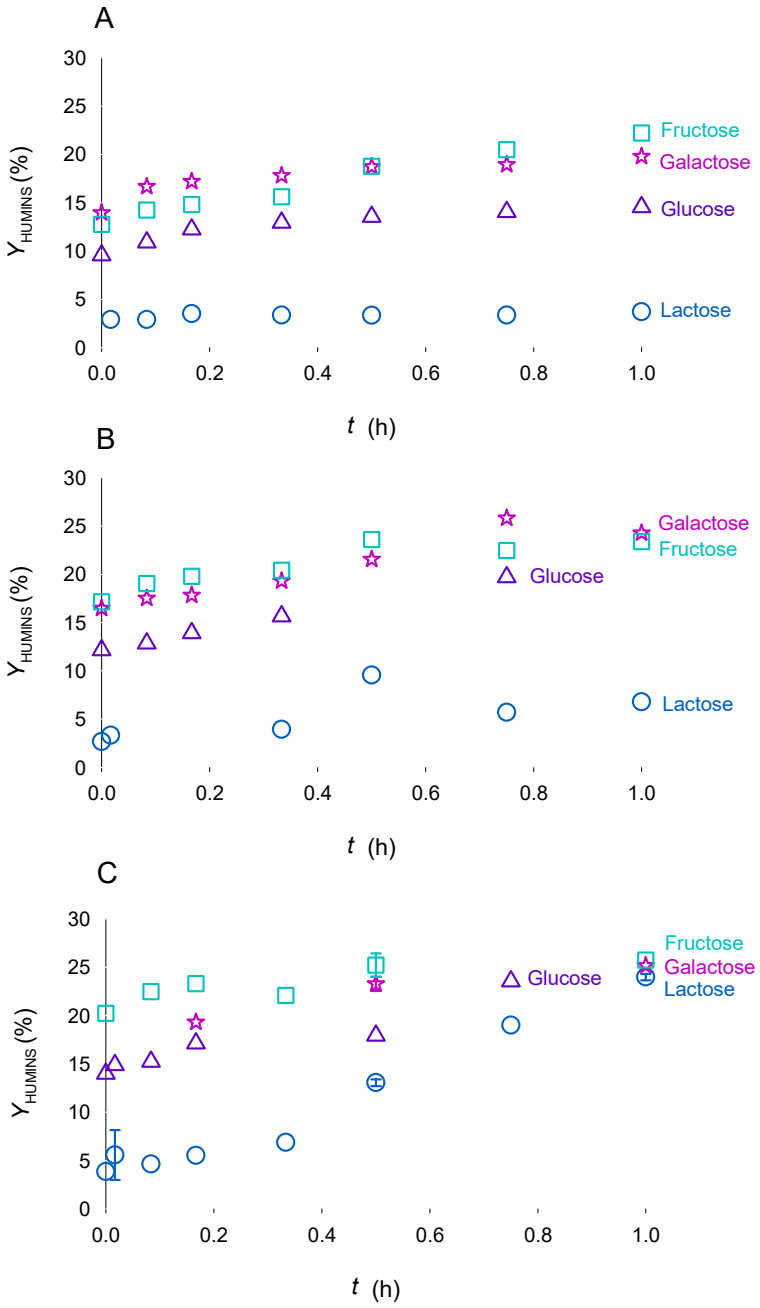

Figure 5.7 Humins production with lactose, glucose, galactose, or fructose as feedstock, at 130 (A), 150(B), and 170 °C(C). Reaction conditions: Lactose, glucose, galactose, or fructose 0.14 mmol, 0.4 g of Er_{15}/γ-Al_2O_3, n=2, error bars represent standard deviation, 70 rpm.

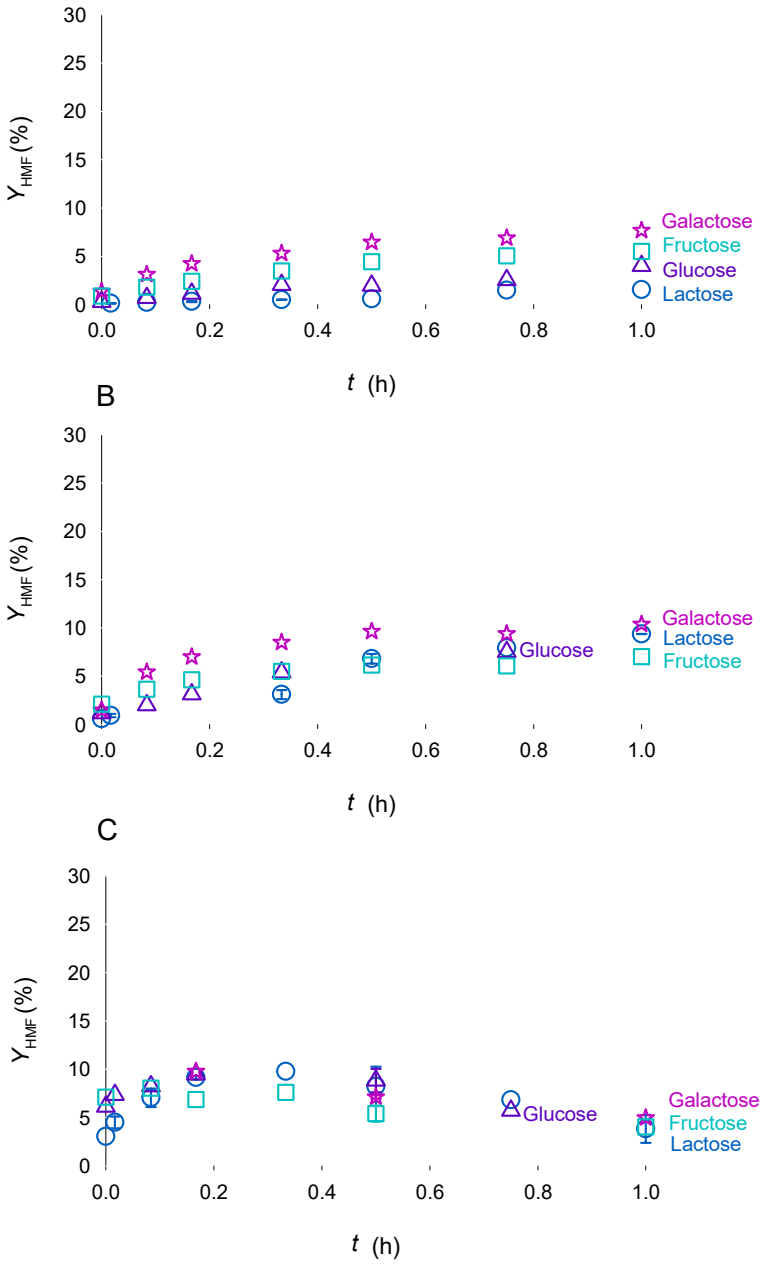

Figure 5.8 HMF production with lactose, glucose, galactose, or fructose as feedstock, at 130 (A), 150(B), and 170 °C(C). Reaction conditions: Lactose, glucose, galactose, or fructose 0.14 mmol, 0.4 g of Er_{15}/γ-Al_2O_3, n=2, error bars represent standard deviation, 70 rpm.

5.3.5 Kinetic analysis

The modelized lactose hydrolysis fits for a first order reaction as reported by Lindsay et al., when converting lactose to a syrup of glucose and galactose with Amberlyst 70 and zirconium phosphate at 150 °C. Our data shows a linear correlation, with an R^2 of 0.99 for predicted values compared to experimental ones (Figure 5.9). This confirms the hypothesis that lactose hydrolysis is the predominant reaction in this system. The resulting activation energy of 126 kJ mol^{-1} is in agreement with the one reported, which was 135.5 kJ mol^{-1} [43]. t_0 was equal to 0.07 h, and β_0 to -1.8: for temperatures higher than 190 °C, the heating time is nearly not affecting the reaction time, while for up to 170 °C, the delayed time corresponds to an additional 4 min. The model estimates well lactose initial concentration: the simulated value was 0.13 mol L^{-1}, while the experimental value was 0.14 mol L^{-1}. The measured k_0, which corresponds to the pre-exponential Arrhenius factor, was equal to 12 h^{-1}.

.

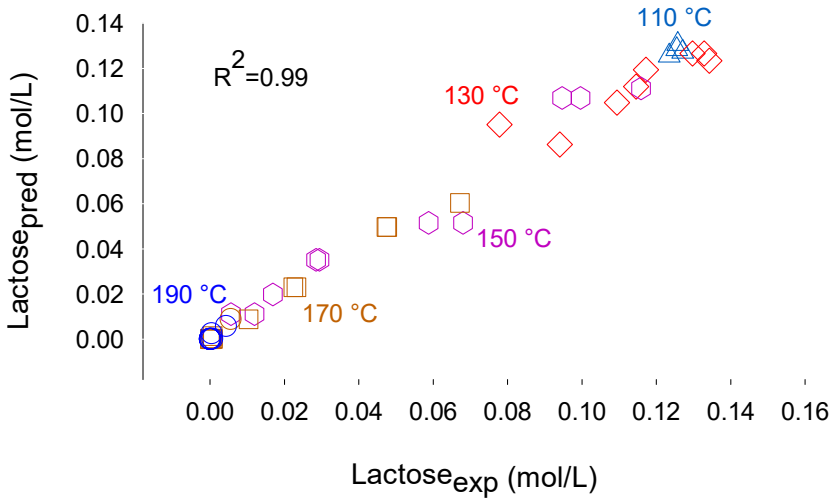

Figure 5.9 Predicted values of lactose conversion in function of experimental data, at 130, 150, 170, and 190 °C. Reaction conditions: Lactose, 0.14 mmol, 0.4 g of Er_{15}/γ-Al_2O_3, n=2, error bars represent standard deviation, 70 rpm.

In order to assess the kinetic parameters of consecutive reactions leading to lactic acid, we modeled each step on MATLAB R2025b, based on equations 5.2-5.8, and compared these values to previously reported ones (Table 5.1). While galactose to LA, is absent of the literature, values for HMF to humins agree well with Ramli et al. and Chen et al. [25, 152]. For lactose hydrolysis, parameters from Sigma Plot simulation amd MATLAB are of the same order of magnitude, although Ea calculated by Sigma Plot is lower: the data set

included additional data at 110 °C and 190 °C compared to MATLAB one. Results confirm that the most challenging part of the reaction is glucose to fructose isomerization, and its reverse reaction as they exhibit a high activation energy requirement of 175 kJ mol^{-1}. This step is key to further conversion to LA and the results confirm, that there's a limitation in LA production due to this equilibrium. Fructose and galactose conversion to LA competes with their degradation to humins with similar activation energies and order of magnitude for k_0. Therefore, decreasing reaction selectivity to solid humins is another critical challenge to favor LA formation. For this purpose, Niobium phosphate (PNb) catalyst appears to be a good candidate as it limits humins formation, with a high activation energy requirement, while promoting HMF production [133]. Here, LA degradation requires the lowest activation energy, which agrees with reported TGA results [150]. Regarding fructose to lactic acid kinetics, experimental Ea is analogous to PVA conversion one, which indicate that the retro-aldol condensation with Er_{15}/γ-Al_2O_3 is not a rate limiting step. Fructose and galactose conversion to HMF exhibit lower Ea than the ones reported with homogeneous catalysts, respectively HCl and H_2SO_4. The discrepancy between reported Ea for glucose degradation and our study could originate from a difference in reaction matrix: Zhao et al. operated at higher temperatures than the ones studied here, while Lindsay et al. measured the kinetics with an homogeneous catalyst [43,135]. However, our Ea value is in agreement with Kumar et al., when reacting glucose with ionic liquid [153]. Regarding galactose to humins, Ringgani et al. and Martina et al. included HMF production, however, solid humins and other by-products were not quantified, which explains the difference observed compared to this study [30, 154].

A pareto plot confirms the accuracy of the model, as predicted values match with experimental data for all species, independently of the feedstock, with a global R^2 of 0.99 (Figure 5.10, B.2, B.3, and B.4). The predicted t_0 was equal to 0.5 h, and β_0 to 3.4: this disparity with the previous results obtained in Sigma Plot for lactose hydrolysis (Figure 5.9), sheds lights on the effect of intermediates and by-products on the kinetic parameters. The optimized model shows that up to 170 °C, the delayed time correspond to an additional 30 min.

5.4 Conclusion

The pseudo-homogeneous first order model characterizes the kinetics of lactose conversion to lactic acid with a solid acidic catalyst: Glucose to fructose isomerization was the critical energy barrier, with 175 kJ mol^{-1}, while humins formation from galactose, fructose and HMF was only 62, 52, and 62 kJ mol^{-1}. A parity plot demonstrated that the model fit the data over the full range of temperature from 130 °C to 170 °C, for 7 species—lactose, glucose, galactose,

.

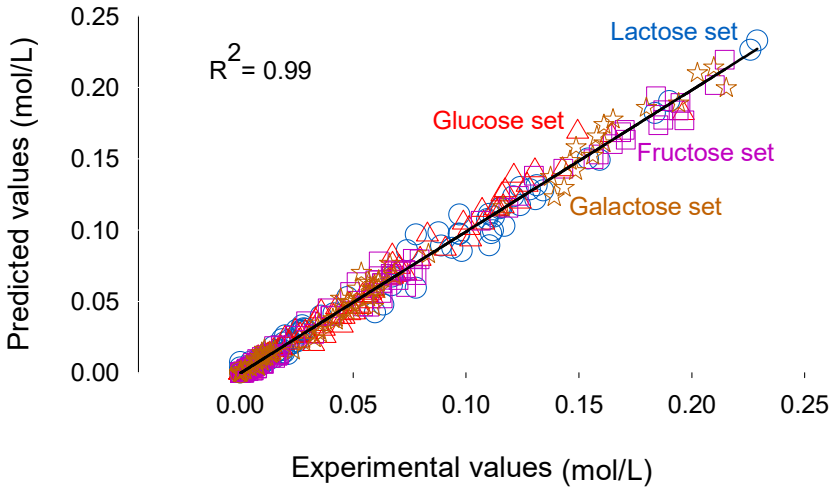

Figure 5.10 Parito plot of predicted concentrations in function of experimental data, from lactose, glucose, galactose, and fructose set. Reaction conditions: Lactose, glucose, galactose or fructose, 0.14 mmol, 0.4 g of Er_{15}/γ-Al_2O_3, 70 rpm.

fructose, lactic acid, HMF, and humins—with 4 feedstocks. While galactose is more prone to convert to LA than glucose, yield was highest for fructose reaching 28 % within 5 min at 150 °C. These results confirm the need to develop novel technologies to overcome the isomerization barrier of glucose to fructose. Shan et al., for example, reported that Al-loaded lignin could reach up to 58.5 % yield of fructose from glucose in ethanol, at 140 °C. The corresponding activation energy was 65 kJ mol^{-1}, which makes it a good potential material for further functionalized catalysts, to maximize LA yields [158]. PNb is another promising option, due to its strong protonic acidity and its water-tolerant properties [138].

Table 5.1 Reported kinetic parameters for chemical hydrolysis of lactose and its intermediates to lactic acid. (†fructose intermediate,‡ [IL-SO3H][Cl])

k_x	Reaction	This study		Literature	Reaction conditions
		$k_{0,x}$ h^{-1}	95 %CI Ea kJ mol^{-1}	Ea kJ mol^{-1}	
1	Lactose hydrolysis	14	[130–133]	136	120–160 °C, H_2SO_4 [43]
2	Glucose → Fructose	21	[166–187]	86 106	125–145 °C, PNb [133] 125–145 °C, ZrPO [134]
3	Fructose → Glucose	24	[165–186]	66	80–120 °C, TEA [155]
4	Fructose → Lactic acid	3	[53–55]	Fructose to DHA: 80 DHA to PVA: 68 PVA to LA: 67	150–220 °C, Cr-Sn-β-zeolite [156]
5	Fructose → HMF	2	[100–107]	25 126†	125–145 °C, PNb [133] 74–147 °C, HCl [97]
6	Galactose → Lactic acid	3	[66–69]	–	–
7	Galactose → HMF	2	[65–69]	125 140	150–190 °C, H_2SO_4 [154] 140–200 °C, H_2SO_4 [157]
8	Lactic acid → Degradation	0.7	10	51–Arrhenius 48–Kissinger	Heating rate: 10 K min^{-1} [150]
9	HMF → Humins	0.7	[55–69]	55 70 133	140–200 °C, $CrCl_3$ [152] 120–200 °C, Fe/HY zeolite [25] 125–145 °C, PNb [133]
10	Glucose → Degradation	7	[75–80]	69 106 102	145–175 °C, $NiSO_4.6H_2O$‡ [153] 180–240 °C, Ru/Ac [135] 200–300 °C, $ZnSO_4$ [49]
11	Galactose → Humins	0.9	[59–65]	123 131 182	140–200 °C, H_2SO_4 [157] 150–190 °C, H_2SO_4 [154] 112–153 °C, H_2O/MIBK [30]
12	Fructose → Humins	1	[49–54]	71 134	140–200 °C, $CrCl_3$ [152] 125–145 °C, PNb [133]

CHAPTER 6 CONCLUSION

6.1 Summary of Works

Cheese whey permeate is an abundant resource, that is unfortunately poorly valorized. Its lactose content makes it suitable as a raw material for biobase green products such as lactic acid, the monomer for the polylactic acid bioplastic. Through this doctoral project, we bridged the gap of knowledge by demonstrating that it was possible to convert cheese whey permeate to lactic acid with an heterogeneous catalyst, as opposed to traditional fermentation techniques.

We first identified solid catalyst that could potentially completely convert lactose, while being selective to lactic acid production. We selected tin and erbium based on their Lewis acidic property and their performance in converting monosaccharides and cellulose to LA. Erbium contributed both to lactose hydrolysis and lactic acid production, while being more selective than tin. We reported a maximum LA yield of 23 % from lactose, with Er_{15} catalyst, at 170 °C within a relatively fast time of 30 min. Based on this experimentation, we fitted 84 experiments from the catalysts screening design to a non linear model, which predicts the impact of reaction time, temperature and metal ratio on LA yield.

Then, we tested different configurations to assess the impact of mixing, temperature, time, and pressure on the reaction efficiency in multiscale vessels. Our results indicated that lactic acid production was invariant regarding agitation speed, pressure, and gas composition, while it reached an equilibrium when increasing temperature, and heating time. The XRF analysis of the spent catalyst and the liquid product revealed that erbium leached from the support. Therefore, the successive run of spent catalyst with fresh lactose yielded about the half of LA with fresh catalyst. Then, we compared lactose results to cheese whey permeate: LA yield with CWP reached 14 % LA, and 15 % of HMF. The discrepancy for LA yield between lactose yield and CWP may originate from the presence of ashes in the former.

To investigate on the previously mentioned quasi-equilibrium, we studied the kinetic modelling of lactose to lactic acid. The experimental fitted with a pseudo pseudo-homogeneous first order model. Results indicate that glucose to fructose isomerization was the critical activation energy barrier, while humins formation were facilitated, with a low Ea. A parity plot demonstrated that the model fitted with 475 data points from 130 °C to 170 °C, for all products and 4 feedstocks—lactose, glucose, galactose and fructose, with an $R^2 = 0.99$. These results provided reference kinetic parameters for the heterogeneous conversion of lactose to

LA.

6.2 Limitations and future research

We demonstrated that erbium could effectively catalyze lactose to LA. However, the synergistic effect of tin and erbium was hindered by the layer of SnO_2 clusters covering erbium species. Another approach would be to synthesize the catalyst via a non-hydrolytic sol-gel (NHSG) methodology. Eran and al. reported the synthesis of iron supported on SASOL alumina catalysts (catalox and dispal), with potassium and copper as promoters [159].

The NHSG method preserved the shape of the support, while K and Cu were distributed evenly. This catalyst preparation could favor the dispersion of tin and erbium in this catalytic system, and therefore, promote the combined conversion of lactose to lactic acid, with tin enhancing the isomerization of glucose to fructose and erbium the selectivity to lactic acid.

LA yield from whey permeate reached 14 %, compared to up to 22 % with lactose. Further research should focus on the design of catalytic systems that would perform efficiently in presence of the minerals contained in CWP. Kohler and al. reported up to 68 % of LA from glucose, with an Sn-βzeolite and $CaSO_4$ salts, at 200 °C. The report mentioned that sulfate ions increased Brønted while calcium contributed to the Lewis acidity. Complementary reactions with other minerals such as $MgSO_4$ and $CaCO_3$ exhibited LA yields of 64 % and 58 % respectively [160]. Erbium leaching is an additional limitation, as it reduces the ability of the catalyst to be recycled.

The kinetic study revealed that the main limitation was the activation energy barrier for the isomerization of glucose to fructose. Solid catalysts that effectively overcome this barrier are compelling candidates for lactose valorization to LA. Shan and al. reported that Al-loaded lignin reached 58.5 % yield of fructose from glucose in ethanol, at 140 °C. The corresponding activation energy was 65 $kJ\,mol^{-1}$, which makes it a good potential material for further functionalized materials [158]. Another promising option is nobium phosphate, which features a strong protonic acidity with water-tolerant properties [138].

Kinetic results provided in this study could contribute to the simulation of the process on Aspen HYSYS, and thus, the scale-up of the reactors. Softwares like COMSOL Multiphysics, will help merging information about kinetics and heat and mass transfer areas. A technico-economic analysis can then establish the profitability of the process based on the aforementioned information.

REFERENCES

[1] L. Jánovová and K. Hroboňová, "Stationary phase type and temperature effect on hplc separation of lactic acid enantiomers," *Acta Chimica Slovaca*, vol. 14, no. 1, pp. 60–65, 2021.

[2] M. Xia *et al.*, "Synergetic effects of bimetals in modified beta zeolite for lactic acid synthesis from biomass-derived carbohydrates," *RSC Adv*, vol. 8, no. 16, pp. 8965–8975, 2018. [Online]. Available: https://www.ncbi.nlm.nih.gov/pubmed/35539821

[3] Y. Zhao *et al.*, "Comparative study on the dehydration of biomass-derived disaccharides and polysaccharides to 5-hydroxymethylfurfural," *Energy & Fuels*, vol. 33, no. 10, pp. 9985–9995, 2019. [Online]. Available: https://doi.org/10.1021/acs.energyfuels.9b02863

[4] Y. Xiao *et al.*, "Selective transformation of typical sugars to lactic acid catalyzed by dealuminated zsm-5 supported erbium," *Renewable Energy*, vol. 187, pp. 551–560, 2022.

[5] L. Yang *et al.*, "Direct conversion of cellulose into ethyl lactate in supercritical ethanol-water solutions," *ChemSusChem*, vol. 9, no. 1, pp. 36–41, 2016. [Online]. Available: https://www.ncbi.nlm.nih.gov/pubmed/26685114

[6] M. D. Houndedoke *et al.*, "Unraveling one pot lactose conversion to lactic acid and hmf over sn-er/γ-Al_2O_3," *Catalysis Today*, 2025.

[7] OCDE, *Études économiques de l'OCDE : Canada 2023*, ser. Études économiques de l'OCDE : Canada, 2023.

[8] M. Lupescu, "Dairy and products annual," Tech. Rep., 2023.

[9] A. F. Pires *et al.*, "Dairy by-products: A review on the valorization of whey and second cheese whey," *Foods*, vol. 10, no. 5, 2021. [Online]. Available: https://www.ncbi.nlm.nih.gov/pubmed/34066033

[10] F. C. Sampaio *et al.*, "Cheese whey permeate fermentation by kluyveromyces lactis: a combined approach to wastewater treatment and bioethanol production," *Environ Technol*, vol. 41, no. 24, pp. 3210–3218, 2020. [Online]. Available: https://www.ncbi.nlm.nih.gov/pubmed/30955482

[11] M. J. Lindsay *et al.*, "Catalytic production of glucose-galactose syrup from greek yogurt acid whey in a continuous-flow reactor," *ChemSusChem*, vol. 13, no. 4, pp. 791–802, 2020. [Online]. Available: https://www.ncbi.nlm.nih.gov/pubmed/31872524

[12] E. De Jong *et al.*, "Bio based chemicals a 2020 update," Report, 2020.

[13] F. A. Castillo Martinez *et al.*, "Lactic acid properties, applications and production: A review," *Trends in Food Science & Technology*, vol. 30, no. 1, pp. 70–83, 2013.

[14] D. Garlotta, "A literature review of poly(lactic acid)," *Journal of Polymers and the Environment*, vol. 9, p. 22, 2001.

[15] S. Xu *et al.*, "Directing the simultaneous conversion of hemicellulose and cellulose in raw biomass to lactic acid," *ACS Sustainable Chemistry & Engineering*, vol. 8, no. 10, pp. 4244–4255, 2020.

[16] 2025. [Online]. Available: https://www.marketsandmarkets.com/Market-Reports/polylactic-acid-pla-market-29418964.html

[17] N. I. N. Haris *et al.*, "A review on lactic acid production via microbial fermentation from biowaste: insights on scaling up to industrial process," *Biofuels, Bioproducts and Biorefining*, vol. 19, no. 2, pp. 437–452, 2024.

[18] V. Luongo *et al.*, "Repeated-batch fermentation of cheese whey for semi-continuous lactic acid production using mixed cultures at uncontrolled ph," *Sustainability*, vol. 11, no. 12, 2019.

[19] H. C. Chen and R. R. Zall, "Continuous lactose hydrolysis in fixed-bed and expanded-bed reactors containing catalytic resins," *Journal of Food Science*, vol. 48, no. 6, pp. 1741–1744, 2006.

[20] R. Lai *et al.*, "Review on synthesis of lactic acid and lactates from biomass derived carbohydrates via chemocatalysis routes," *Bioresource Technology*, vol. 419, p. 132031, 2025. [Online]. Available: https://www.ncbi.nlm.nih.gov/pubmed/39746382

[21] X. Lyu *et al.*, "Enhancement of catalytic activity by γ-niooh for the production of methyl lactate from sugars in near-critical methanol solutions," *Industrial & Engineering Chemistry Research*, vol. 58, no. 9, pp. 3659–3665, 2019.

[22] M.-A. P., A. Aho, and D. Y. Murzin, "Heterogeneous catalytic synthesis of methyl lactate and lactic acid from sugars and their derivatives," *ChemSusChem*, vol. 13,

no. 18, pp. 4833–4855, 2020. [Online]. Available: https://www.ncbi.nlm.nih.gov/pubmed/32667135

[23] X. Lu, L. Wang, and X. Lu, "Catalytic conversion of sugars to methyl lactate over mg-mof-74 in near-critical methanol solutions," *Catalysis Communications*, vol. 110, pp. 23–27, 2018.

[24] W. Dong *et al.*, "Selective chemical conversion of sugars in aqueous solutions without alkali to lactic acid over a zn-sn-beta lewis acid-base catalyst," *Sci Rep*, vol. 6, p. 26713, 2016. [Online]. Available: https://www.ncbi.nlm.nih.gov/pubmed/27222322

[25] N. A. S. Ramli and N. A. S. Amin, "Kinetic study of glucose conversion to levulinic acid over fe/hy zeolite catalyst," *Chemical Engineering Journal*, vol. 283, pp. 150–159, 2016.

[26] F. S. Asghari and H. Yoshida, "Acid-catalyzed production of 5-hydroxymethyl furfural from d-fructose in subcritical water>," *Industrial & Engineering Chemistry Research*, vol. 45, no. 7, pp. 2163–2173, 2006.

[27] S. Liu *et al.*, "Advances in understanding the humins: Formation , prevention and application," *Applications in Energy and Combustion Science*, vol. 10, 2022.

[28] J. C. Velasco Calderon, J. S. Arora, and S. H. Mushrif, "Mechanistic investigation into the formation of humins in acid-catalyzed biomass reactions," *ACS Omega*, vol. 7, no. 49, pp. 44 786–44 795, 2022. [Online]. Available: https://www.ncbi.nlm.nih.gov/pubmed/36530267

[29] C. Sanpitakseree *et al.*, "Unveiling kinetics post rate-determining step in brønsted acid-catalyzed reactions of fructose: A strategy for 5-hydroxymethylfurfural production from concentrated feedstock," *Chemical Engineering Journal*, vol. 492, 2024.

[30] A. Martina *et al.*, "Biobased chemicals from d-galactose: An efficient route to 5-hydroxymethylfurfural using a water/mibk system in combination with an hcl/alcl(3) catalyst," *ACS Omega*, vol. 9, no. 39, pp. 40 378–40 393, 2024. [Online]. Available: https://www.ncbi.nlm.nih.gov/pubmed/39372015

[31] W. Wang *et al.*, "The kinetics of aqueous lactose hydrolysis with sulfuric acid," *Reaction Chemistry & Engineering*, vol. 10, no. 7, pp. 1676–1691, 2025.

[32] J. Iglesias *et al.*, "Advances in catalytic routes for the production of carboxylic acids from biomass: a step forward for sustainable polymers," *Chemical Society Reviews*, vol. 49, no. 16, 2020.

[33] 2026. [Online]. Available: https://www.marketsandmarkets.com/Market-Reports/polylacticacid-387.html

[34] 2026. [Online]. Available: https://www.statista.com/statistics/1310499/lactic-acid-market-value-worldwide/

[35] A. S. Rathore and A. Singh, "Biomass to fuels and chemicals: A review of enabling processes and technologies," *Journal of Chemical Technology & Biotechnology*, vol. 97, no. 3, pp. 597–607, 2021.

[36] R. Datta and M. Henry, "Lactic acid: recent advances in products, processes and technologies — a review," *Journal of Chemical Technology & Biotechnology*, vol. 81, no. 7, pp. 1119–1129, 2006.

[37] P. Pal *et al.*, "Process intensification in lactic acid production: A review of membrane based processes," *Chemical Engineering and Processing: Process Intensification*, vol. 48, no. 11-12, pp. 1549–1559, 2009.

[38] M. Alvarado-Morales *et al.*, "Municipal biopulp as substrate for lactic acid production focusing on downstream processing," *Journal of Environmental Chemical Engineering*, vol. 9, no. 2, 2021.

[39] A. Karnaouri *et al.*, "Efficient production of nutraceuticals and lactic acid from lignocellulosic biomass by combining organosolv fractionation with enzymatic/fermentative routes," *Bioresour Technol*, vol. 341, p. 125846, 2021. [Online]. Available: https://www.ncbi.nlm.nih.gov/pubmed/34474235

[40] D. Mladenović *et al.*, "Lactic acid production on molasses enriched potato stillage by lactobacillus paracasei immobilized onto agro-industrial waste supports," *Industrial Crops and Products*, vol. 124, pp. 142–148, 2018.

[41] A. R. Prazeres, F. Carvalho, and J. Rivas, "Cheese whey management: a review," *J Environ Manage*, vol. 110, pp. 48–68, 2012. [Online]. Available: https://www.ncbi.nlm.nih.gov/pubmed/22721610

[42] L. T. O'Donoghue and E. G. Murphy, "Nondairy food applications of whey and milk permeates: Direct and indirect uses," *Compr Rev Food Sci Food Saf*, vol. 22, no. 4, pp. 2652–2677, 2023. [Online]. Available: https://www.ncbi.nlm.nih.gov/pubmed/37070222

[43] M. J. Lindsay *et al.*, "Production of monosaccharides and whey protein from acid whey waste streams in the dairy industry," *Green Chemistry*, vol. 20, no. 8, pp. 1824–1834, 2018.

[44] U. D. E. Council, "Permeate: An in-demand ingredient," 2021. [Online]. Available: https://usdairyexcellence.org/wp-content/uploads/2023/12/2021-Permeate-New-Product-Introduction-Snapshot.pdf

[45] P. Yang *et al.*, "Biohydrogen production from cheese processing wastewater by anaerobic fermentation using mixed microbial communities," *International Journal of Hydrogen Energy*, vol. 32, no. 18, pp. 4761–4771, 2007.

[46] A. Vasala, J. Panula, and P. Neubauer, "Efficient lactic acid production from high salt containing dairy by-products by lactobacillus salivarius ssp. salicinius with pre-treatment by proteolytic microorganisms," *J Biotechnol*, vol. 117, no. 4, pp. 421–31, 2005. [Online]. Available: https://www.ncbi.nlm.nih.gov/pubmed/15876466

[47] B. Delmoitie *et al.*, "Tailoring non-axenic lactic acid fermentation from cheese whey permeate targeting a flexible lactic acid platform," *J Environ Manage*, vol. 373, p. 123529, 2025. [Online]. Available: https://www.ncbi.nlm.nih.gov/pubmed/39632307

[48] L. Kong *et al.*, "Hydrothermal catalytic conversion of biomass for lactic acid production," *Journal of Chemical Technology & Biotechnology*, vol. 83, no. 3, pp. 383–388, 2008.

[49] M. Bicker *et al.*, "Catalytical conversion of carbohydrates in subcritical water: A new chemical process for lactic acid production," *Journal of Molecular Catalysis A: Chemical*, vol. 239, no. 1-2, pp. 151–157, 2005.

[50] X. Yan *et al.*, "Hydrothermal conversion of carbohydrate biomass to lactic acid," *AIChE Journal*, vol. 56, no. 10, pp. 2727–2733, 2010.

[51] Y. Wang *et al.*, "Chemical synthesis of lactic acid from cellulose catalysed by lead(ii) ions in water," *Nature Communications*, vol. 4, p. 2141, 2013. [Online]. Available: https://www.ncbi.nlm.nih.gov/pubmed/23846730

[52] N. Kutrakul *et al.*, "Highly selective catalytic conversion of raw sugar and sugarcane bagasse to lactic acid over ybcl3, ercl3, and cecl3 lewis acid catalysts without alkaline in a hot-compressed water reaction system," *Chemical Engineering Research and Design*, vol. 187, pp. 549–569, 2022.

[53] X. Lei *et al.*, "One-pot catalytic conversion of carbohydrate biomass to lactic acid using an ercl3 catalyst," *Applied Catalysis A: General*, vol. 482, pp. 78–83, 2014.

[54] A. A. Marianou *et al.*, "Effect of lewis and brønsted acidity on glucose conversion to 5-hmf and lactic acid in aqueous and organic media," *Applied Catalysis A: General*, vol. 555, pp. 75–87, 2018.

[55] P. Wattanapaphawong, P. Reubroycharoen, and A. Yamaguchi, "Conversion of cellulose into lactic acid using zirconium oxide catalysts," *RSC Advances*, vol. 7, no. 30, pp. 18 561–18 568, 2017.

[56] A. A. Marianou *et al.*, "Cellulose conversion into lactic acid over supported hpa catalysts," *Green Chemistry*, vol. 21, no. 22, pp. 6161–6178, 2019.

[57] H. Li *et al.*, "Production of lactic acid from cellulose catalyzed by alumina-supported er2o3 catalysts," *Research on Chemical Intermediates*, vol. 42, no. 9, pp. 7199–7211, 2016.

[58] F.-F. Wang *et al.*, "Er/β-zeolite-catalyzed one-pot conversion of cellulose to lactic acid," *Journal of Porous Materials*, vol. 24, no. 3, pp. 697–706, 2016.

[59] M. S. Holm, S. Saravanamurugan, and E. Taarning, "Conversion of sugars to lactic acid derivatives using heterogeneous zeotype catalysts," *Science*, vol. 328, no. 5978, pp. 602–605, 2010. [Online]. Available: https://doi.org/10.1126/science.1183990

[60] M. G. Gänzle, G. Haase, and P. Jelen, "Lactose: Crystallization, hydrolysis and value-added derivatives," *International Dairy Journal*, vol. 18, no. 7, pp. 685–694, 2008.

[61] a. a. Sadaki Asakuma, H.K. Biesalski, *ADVANCED DAIRY CHEMISTRY, Lactose, Water, Salts and Minor Constituents, THIRD EDITION*, 2009, vol. 3.

[62] Y. Roman-Leshkov *et al.*, "Mechanism of glucose isomerization using a solid lewis acid catalyst in water," *Angew Chem Int Ed Engl*, vol. 49, no. 47, pp. 8954–7, 2010. [Online]. Available: https://www.ncbi.nlm.nih.gov/pubmed/20963742

[63] T. Saulnier-Bellemare and G. S. Patience, "Homogeneous and heterogeneous catalysis of glucose to lactic acid and lactates: A review," *ACS Omega*, vol. 9, no. 22, pp. 23 121–23 137, 2024. [Online]. Available: https://www.ncbi.nlm.nih.gov/pubmed/38854556

[64] R. M. West *et al.*, "Zeolite h-usy for the production of lactic acid and methyl lactate from c3-sugars," *Journal of Catalysis*, vol. 269, no. 1, pp. 122–130, 2010.

[65] P. A. Rivera-Quintero *et al.*, "Sn-silica catalyzes cheese whey to lactic acid in a fluidized bed reactor," *Catalysis Today*, vol. 454, 2025.

[66] F. Kähler, O. Porc, and M. Carus, "RCI carbon flows report: Compilation of supply and demand of fossil and renewable carbon on a global and european level," nova-institut, Tech. Rep., 2023. [Online]. Available: www.renewable-carbon-initiative.com

[67] P. Maki-Arvela *et al.*, "Production of lactic acid/lactates from biomass and their catalytic transformations to commodities," *Chem Rev*, vol. 114, no. 3, pp. 1909–71, 2014. [Online]. Available: https://www.ncbi.nlm.nih.gov/pubmed/24344682

[68] T. T. Thuy Vu *et al.*, "Sustainable one-pot synthesis of 5-(hydroxymethyl)furfural from c6-sugars by enhanced h+ exchange heterogeneous catalysis," *ACS Sustainable Chemistry & Engineering*, vol. 11, no. 48, pp. 17 130–17 141, 2023.

[69] H. Shirai, S. Ikeda, and E. W. Qian, "One-pot production of 5-hydroxymethylfurfural from cellulose using solid acid catalysts," *Fuel Processing Technology*, vol. 159, pp. 280–286, 2017.

[70] A. Modak *et al.*, "One-pot conversion of glucose to 5-hydroxymethylfurfural under aqueous conditions using acid/base bifunctional mesoporous silica catalyst," *Renewable Energy*, vol. 212, pp. 97–110, 2023.

[71] K. Lourvanij and G. L. Rorrer, "Reactions of aqueous glucose solutions over solid-acid y-zeolite catalyst at 110-160 °c," p. 9, 1993.

[72] J. Guan *et al.*, "The mechanism of glucose conversion to 5-hydroxymethylfurfural catalyzed by metal chlorides in ionic liquid: A theoretical study," *Computational and Theoretical Chemistry*, vol. 963, no. 2-3, pp. 453–462, 2011.

[73] C. Kosri *et al.*, "Selective conversion of xylose to lactic acid over metal-based lewis acid supported on γ-al2o3 catalysts," *Catalysis Today*, vol. 367, pp. 205–212, 2021.

[74] R. De Clercq, M. Dusselier, and B. F. Sels, "Heterogeneous catalysis for bio-based polyester monomers from cellulosic biomass: advances, challenges and prospects," *Green Chem.*, vol. 19, no. 21, pp. 5012–5040, 2017.

[75] J. He *et al.*, "Catalytic upgrading of biomass-derived sugars with acidic nanoporous materials: Structural role in carbon-chain length variation," *ChemSusChem*, vol. 12, no. 2, pp. 347–378, 2019. [Online]. Available: https://www.ncbi.nlm.nih.gov/pubmed/30407741

[76] Z. Shen *et al.*, "Efficient catalytic conversion of glucose into lactic acid over y-beta and yb-beta zeolites," *ACS Omega*, vol. 7, no. 29, pp. 25 200–25 209, 2022. [Online]. Available: https://www.ncbi.nlm.nih.gov/pubmed/35910139

[77] P. Bhaumik and P. L. Dhepe, *Conversion of Biomass into Sugars*. The Royal Society of Chemistry, 2015, p. 0. [Online]. Available: https://doi.org/10.1039/9781782622079-00001

[78] Y. Sun *et al.*, "Efficient production of lactic acid from sugars over sn-beta zeolite in water: catalytic performance and mechanistic insights," *Sustainable Energy & Fuels*, vol. 3, no. 5, pp. 1163–1171, 2019.

[79] Z. Nekoukar *et al.*, "Methanol poisoning as a new world challenge: A review," *Ann Med Surg (Lond)*, vol. 66, p. 102445, 2021. [Online]. Available: https://www.ncbi.nlm.nih.gov/pubmed/34141419

[80] A. Kaviraj, F. Bhunia, and N. C. Saha, "Toxicity of methanol to fish, crustacean, oligochaete worm, and aquatic ecosystem," *Int J Toxicol*, vol. 23, no. 1, pp. 55–63, 2004. [Online]. Available: https://www.ncbi.nlm.nih.gov/pubmed/15162848

[81] W. Dong *et al.*, "Rare-earth metal yttrium-modified composite metal oxide catalysts for high selectivity synthesis of biomass-derived lactic acid from cellulose," *ChemCatChem*, vol. 14, no. 12, 2022.

[82] R. Bardestani, G. S. P. Patience, and S. Kaliaguine, "Experimental methods in chemical engineering: specific surface area and pore size distribution measurements—bet, bjh, and dft," *The Canadian Journal of Chemical Engineering*, vol. 97, no. 11, pp. 2781–2791, 2019.

[83] M. Ferreiro-Gonzalez, N. Saadatkhah, and G. S. Patience, "Experimental methods in chemical engineering: X-ray fluorescence—xrf," *The Canadian Journal of Chemical Engineering*, vol. 102, no. 6, pp. 2004–2018, 2024.

[84] H. Khan *et al.*, "Experimental methods in chemical engineering: X-ray diffraction spectroscopy—xrd," *The Canadian Journal of Chemical Engineering*, vol. 98, no. 6, pp. 1255–1266, 2020.

[85] K. Enomoto, T. Hosoya, and H. Miyafuji, "High-yield production of 5-hydroxymethylfurfural from d-fructose, d-glucose, and cellulose by its in situ removal from the reaction system," *Cellulose*, vol. 25, no. 4, pp. 2249–2257, 2018.

[86] N. Shi *et al.*, "Production of lactic acid from cellulose catalyzed by easily prepared solid al2(wo4)3," *Bioresource Technology Reports*, vol. 5, pp. 66–73, 2019.

[87] J. A. Serafim, R. F. Silveira, and E. F. Vicente, "Fast determination of short-chain fatty acids and glucose simultaneously by ultraviolet/visible and refraction index detectors via high-performance liquid chromatography," *Food Analytical Methods*, vol. 14, no. 7, pp. 1387–1393, 2021.

[88] M. Haneda *et al.*, "Preparation, characterization, and activity of sno2 nanoparticles supported on al2o3 as a catalyst for the selective reduction of no with c3h6," *Journal of Materials Science*, vol. 51, no. 24, pp. 10 949–10 959, 2016.

[89] E. Peeters *et al.*, "Tandem reduction–reoxidation augments the catalytic activity of sn-beta zeolites by redispersion and respeciation of sno2 clusters," *Chemistry of Materials*, vol. 33, no. 23, pp. 9366–9381, 2021.

[90] M. Thommes *et al.*, "Physisorption of gases, with special reference to the evaluation of surface area and pore size distribution (iupac technical report)," *Pure and Applied Chemistry*, vol. 87, no. 9-10, pp. 1051–1069, 2015.

[91] B. Tang *et al.*, "Improved postsynthesis strategy to sn-beta zeolites as lewis acid catalysts for the ring-opening hydration of epoxides," *ACS Catalysis*, vol. 4, no. 8, pp. 2801–2810, 2014.

[92] F. Chambon *et al.*, "Cellulose conversion with tungstated-alumina-based catalysts: influence of the presence of platinum and mechanistic studies," *ChemSusChem*, vol. 6, no. 3, pp. 500–7, 2013. [Online]. Available: https://www.ncbi.nlm.nih.gov/pubmed/23427047

[93] G.-T. Jeong, "Valorization of dairy by-products: Optimized synthesis of 5-hydroxymethylfurfural and levulinic acid from lactose and whey," *Journal of Environmental Chemical Engineering*, vol. 10, no. 5, 2022.

[94] S. Kiatphuengporn *et al.*, "Roles of acidic sites in alumina catalysts for efficient d-xylose conversion to lactic acid," *Green Chemistry*, vol. 22, no. 24, pp. 8572–8583, 2020.

[95] F. Chambon *et al.*, "Cellulose hydrothermal conversion promoted by heterogeneous brønsted and lewis acids: Remarkable efficiency of solid lewis acids to produce lactic acid," *Applied Catalysis B: Environmental*, vol. 105, no. 1-2, pp. 171–181, 2011.

[96] R. Weingarten, W. C. Conner, and G. W. Huber, "Production of levulinic acid from cellulose by hydrothermal decomposition combined with aqueous phase dehydration with a solid acid catalyst," *Energy & Environmental Science*, vol. 5, no. 6, 2012.

[97] T. D. Swift *et al.*, "Kinetics of homogeneous brønsted acid catalyzed fructose dehydration and 5-hydroxymethyl furfural rehydration: A combined experimental and computational study," *ACS Catalysis*, vol. 4, no. 1, pp. 259–267, 2013.

[98] W. Guo *et al.*, "Selective fructose dehydration to 5-hydroxymethylfurfural from a fructose-glucose mixture over a sulfuric acid catalyst in a biphasic system: Experimental study and kinetic modelling," *Chemical Engineering Journal*, vol. 409, 2021.

[99] T. Flannelly *et al.*, "Non-stoichiometric formation of formic and levulinic acids from the hydrolysis of biomass derived hexose carbohydrates," *RSC Advances*, vol. 6, no. 7, pp. 5797–5804, 2016.

[100] K. M. A. Santos *et al.*, "The role of brønsted and water-tolerant lewis acid sites in the cascade aqueous-phase reaction of triose to lactic acid," *ChemCatChem*, vol. 11, no. 13, pp. 3054–3063, 2019.

[101] W. N. P. van der Graaff *et al.*, "Deactivation of sn-beta during carbohydrate conversion," *Applied Catalysis A: General*, vol. 564, pp. 113–122, 2018.

[102] M. S. Rahaman *et al.*, "Aluminum-based metal-organic framework as water-tolerant lewis acid catalyst for selective dihydroxyacetone isomerization to lactic acid," *ChemCatChem*, vol. 14, no. 4, 2022.

[103] M. Ferreiro González, F. Cabañas Gac, and G. S. Patience, "Alkaline solvothermal debromination of commercial brominated polystyrene," *Recycling*, vol. 10, no. 3, 2025.

[104] E. Balla *et al.*, "Poly(lactic acid): A versatile biobased polymer for the future with multifunctional properties-from monomer synthesis, polymerization techniques and molecular weight increase to pla applications," *Polymers (Basel)*, vol. 13, no. 11, 2021. [Online]. Available: https://www.ncbi.nlm.nih.gov/pubmed/34072917

[105] J. C. Overton, A. S. Engelberth, and N. S. Mosier, "Single-vessel synthesis of 5-hydroxymethylfurfural (hmf) from milled corn," *ACS Sustainable Chemistry & Engineering*, vol. 8, no. 1, pp. 18–21, 2019.

[106] S. Saavedra *et al.*, "Optimization of lactic acid production by lactobacillus plantarum strain hui1 in a medium containing sugar cane molasses," *Agronomía Colombiana*, vol. 39, no. 1, pp. 98–107, 2021.

[107] G. B. Brinques, M. do Carmo Peralba, and M. A. Ayub, "Optimization of probiotic and lactic acid production by lactobacillus plantarum in submerged bioreactor systems," *J Ind Microbiol Biotechnol*, vol. 37, no. 2, pp. 205–12, 2010. [Online]. Available: https://www.ncbi.nlm.nih.gov/pubmed/19936814

[108] J. Fitzpatrick and U. O'Keeffe, "Influence of whey protein hydrolysate addition to whey permeate batch fermentations for producing lactic acid," *Process Biochemistry*, vol. 37, pp. 183–186, 2001.

[109] J. Kim *et al.*, "Lactic acid for green chemical industry: Recent advances in and future prospects for production technology, recovery, and applications," *Fermentation*, vol. 8, no. 11, 2022.

[110] L. A. Guildner, "Thermal conductivity of gases. iii. some values of the thermal conductivities of argon, helium, and nitrogen from 0 °c to 75 °c at pressures of 1 × 105 to 2.5 × 107 pascals," *Journal of research of the National Bureau of Standards*, no. 79A(2), p. 407–413, 1975.

[111] H. Li *et al.*, "Experimental methods in chemical engineering: Particle size distribution by laser diffraction—psd," *The Canadian Journal of Chemical Engineering*, vol. 97, no. 7, pp. 1974–1981, 2019.

[112] K. Lobeda *et al.*, "Lactic acid production from food waste hydrolysate by lactobacillus pentosus: Focus on nitrogen supplementation, initial sugar concentration, ph, and fed-batch fermentation," *Journal of Food Science*, vol. 87, no. 7, pp. 3071–3083, 2022. [Online]. Available: https://www.ncbi.nlm.nih.gov/pubmed/35669993

[113] P. Kopelman and R. Argyrakis, "Stirring-in-chemical-reactions," *American Chemical Society*, 1988.

[114] E. Pighin, V. K. Díez, and J. I. Di Cosimo, "Synthesis of ethyl lactate from triose sugars on Sn/Al_2O_3 catalysts," *Applied Catalysis A: General*, vol. 517, pp. 151–160, 2016.

[115] H. S. Fogler, *Elements of Chemical Reaction Engineering*, fifth edition ed., ser. Prentice Hall International Series in the Physical and Chemical Engineering Sciences, 2016.

[116] C. R. Wilke and P. Chang, "Correlation of diffusion coefficients in dilute solutions," *AIChE Journal*, vol. 1, no. 2, pp. 264–270, 2004.

[117] J. Kestin, M. Sokolov, and W. A. Wakeham, "Viscosity of liquid water in the range −8 °C to 150 °C," *Journal of Physical and Chemical Reference Data*, vol. 7, no. 3, pp. 941–948, 1978.

[118] P. B. Weisz and C. D. Prater, *Interpretation of Measurements in Experimental Catalysis*. Academic Press, 1954, vol. 6, pp. 143–196. [Online]. Available: https://www.sciencedirect.com/science/article/pii/S0360056408603909

[119] P. Kaur, G. Verma, and S. S. Sekhon, "Biomass derived hierarchical porous carbon materials as oxygen reduction reaction electrocatalysts in fuel cells," *Progress in Materials Science*, vol. 102, pp. 1–71, 2019.

[120] J.-T. Guo *et al.*, "Measurement of pore diffusion factor of porous solid materials," *Petroleum Science*, vol. 19, no. 4, pp. 1897–1904, 2022.

[121] J. Wang *et al.*, "Temperature-responsive zn-based catalysts for efficient catalytic conversion of biomass-derived carbohydrates to ethyl lactate," *Green Chemistry*, vol. 25, no. 14, pp. 5613–5625, 2023.

[122] F. Rodriguez *et al.*, "Polysaccharides release in a laboratory-scale batch hydrothermal pretreatment of wheat straw under rigorous isothermal operation," *Molecules*, vol. 27, no. 1, 2021. [Online]. Available: https://www.ncbi.nlm.nih.gov/pubmed/35011258

[123] P. Alonso-Riaño *et al.*, "Study of subcritical water scale-up from laboratory to pilot system for brewer's spent grain valorization," *Industrial Crops and Products*, vol. 191, 2023.

[124] Y. Wang *et al.*, "Catalytic hydrotreatment of humins in mixtures of formic acid/2-propanol with supported ruthenium catalysts," *ChemSusChem*, vol. 9, no. 9, pp. 951–61, 2016. [Online]. Available: https://www.ncbi.nlm.nih.gov/pubmed/26836970

[125] ——, "Advances in humins formation mechanism, inhibition strategies, and value-added applications," *Chinese Journal of Catalysis*, vol. 71, pp. 25–53, 2025.

[126] C. R. M. Monteiro *et al.*, "Evaluation of hydrothermal sugarcane bagasse treatment for the production of xylooligosaccharides in different pressures," *Journal of Food Process Engineering*, vol. 45, no. 2, 2022.

[127] R. M. Mironenko, D. B. Eremin, and V. P. Ananikov, "The phenomenon of "dead" metal in heterogeneous catalysis: Opportunities for increasing the efficiency of carbon-supported metal catalysts," *Chemical Science*, vol. 14, no. 48, pp. 14 062–14 073, 2023.

[128] M. Oliverio *et al.*, "Erbium salts as non-toxic catalysts compatible with alternative reaction media," *Sustainability*, vol. 10, no. 3, 2018.

[129] S. Tallarico *et al.*, "Combined ultrasound/microwave chemocatalytic method for selective conversion of cellulose into lactic acid," *Sci Rep*, vol. 9, no. 1, p. 18858, 2019. [Online]. Available: https://www.ncbi.nlm.nih.gov/pubmed/31827219

[130] T. L. Turner *et al.*, "Short communication: Conversion of lactose and whey into lactic acid by engineered yeast," *Journal of Dairy Science*, vol. 100, no. 1, pp. 124–128, 2017. [Online]. Available: https://www.ncbi.nlm.nih.gov/pubmed/27837988

[131] Agropur, "Tds - 0018049 - crino permeate whey powder," Report, 2017.

[132] T. Dallas Swift *et al.*, "Tandem lewis/brønsted homogeneous acid catalysis: conversion of glucose to 5-hydoxymethylfurfural in an aqueous chromium(iii) chloride and hydrochloric acid solution," *Green Chemistry*, vol. 17, no. 10, pp. 4725–4735, 2015.

[133] M. M. d. J. Junior *et al.*, "Kinetic study of the conversion of glucose to 5-hydroxymethylfurfural using niobium phosphate," *Molecular Catalysis*, vol. 518, 2022.

[134] N. I. Villanueva and T. G. Marzialetti, "Mechanism and kinetic parameters of glucose and fructose dehydration to 5-hydroxymethylfurfural over solid phosphate catalysts in water," *Catalysis Today*, vol. 302, pp. 100–107, 2018.

[135] G. Zhao *et al.*, "Ethylene glycol production from glucose over w-ru catalysts: Maximizing yield by kinetic modeling and simulation," *AIChE Journal*, vol. 63, no. 6, pp. 2072–2080, 2016.

[136] P. Carniti *et al.*, "Niobic acid and niobium phosphate as highly acidic viable catalysts in aqueous medium: Fructose dehydration reaction," *Catalysis Today*, vol. 118, no. 3-4, pp. 373–378, 2006.

[137] F. de Clippel *et al.*, "Fast and selective sugar conversion to alkyl lactate and lactic acid with bifunctional carbon-silica catalysts," *J Am Chem Soc*, vol. 134, no. 24, pp. 10 089–101, 2012. [Online]. Available: https://www.ncbi.nlm.nih.gov/pubmed/22550936

[138] M. Marzo, A. Gervasini, and P. Carniti, "Hydrolysis of disaccharides over solid acid catalysts under green conditions," *Carbohydr Res*, vol. 347, no. 1, pp. 23–31, 2012. [Online]. Available: https://www.ncbi.nlm.nih.gov/pubmed/22127325

[139] Y. Swesi *et al.*, "Direct solid lewis acid catalyzed wood liquefaction into lactic acid: Kinetic evidences that wood pretreatment might not be a prerequisite," *ChemCatChem*, vol. 9, no. 12, pp. 2377–2382, 2017.

[140] Z. Khani *et al.*, "Coke evolution study in a liquid atomization into gas-solid fluidized bed to convert fructose to value-added chemicals," *Catalysis Today*, vol. 444, 2025.

[141] D. Jung, P. Körner, and A. Kruse, "Kinetic study on the impact of acidity and acid concentration on the formation of 5-hydroxymethylfurfural (hmf), humins, and levulinic acid in the hydrothermal conversion of fructose," *Biomass Conversion and Biorefinery*, vol. 11, no. 4, pp. 1155–1170, 2019.

[142] S. Pandey, M.-J. Dumont, and V. Orsat, "Catalytic conversion of whey permeate into 5-hydroxymethylfurfural: Optimization and kinetic modeling approach," *Food and Bioproducts Processing*, vol. 129, pp. 134–143, 2021.

[143] B. Jia *et al.*, "Catalytic, computational, and evolutionary analysis of the d-lactate dehydrogenases responsible for d-lactic acid production in lactic acid bacteria," *J Agric Food Chem*, vol. 66, no. 31, pp. 8371–8381, 2018. [Online]. Available: https://www.ncbi.nlm.nih.gov/pubmed/30008205

[144] R. M. Ravenelle *et al.*, "Effects of metal precursors on the stability and observed reactivity of pt/γ-Al_2O_3 catalysts in aqueous phase reactions," *ChemCatChem*, vol. 4, no. 4, pp. 492–494, 2012.

[145] Q. Liu, H. Liu, and D.-M. Gao, "Establishing a kinetic model of biomass-derived disaccharide hydrolysis over solid acid: A case study on hierarchically porous niobium phosphate," *Chemical Engineering Journal*, vol. 430, 2022.

[146] J. Wang *et al.*, "Efficient catalytic conversion of fructose into hydroxymethylfurfural by a novel carbon-based solid acid," *Green Chemistry*, vol. 13, no. 10, 2011.

[147] K. D. Baugh and P. L. McCarty, "Thermochemical pretreatment of lignocellulose to enhance methane fermentation: I. monosaccharide and furfurals hydrothermal decomposition and product formation rates," *Biotechnol Bioeng*, vol. 31, no. 1, pp. 50–61, 1988. [Online]. Available: https://www.ncbi.nlm.nih.gov/pubmed/18581563

[148] M. N. Catrinck *et al.*, "Direct conversion of glucose to 5-hydroxymethylfurfural using a mixture of niobic acid and niobium phosphate as a solid acid catalyst," *Fuel*, vol. 210, pp. 67–74, 2017.

[149] V. V. Ordomsky *et al.*, "Glucose dehydration to 5-hydroxymethylfurfural over phosphate catalysts," *Journal of Catalysis*, vol. 300, pp. 37–46, 2013.

[150] A. Komesu *et al.*, "Study of lactic acid thermal behavior using thermoanalytical techniques," *Journal of Chemistry*, vol. 2017, pp. 1–7, 2017.

[151] J. M. Jimenez-Martin *et al.*, "Kinetics of the valorization of hexoses with sn-usy catalysts in methanolic media: glycosidation vs. retroaldol cleavage," *Reaction Chemistry & Engineering*, vol. 10, no. 1, pp. 90–105, 2025.

[152] T.-Y. Chen *et al.*, "Fast microflow kinetics and acid catalyst deactivation in glucose conversion to 5-hydroxymethylfurfural," *Reaction Chemistry & Engineering*, vol. 6, no. 1, pp. 152–164, 2021.

[153] K. Kumar, S. Pathak, and S. Upadhyayula, "2nd generation biomass derived glucose conversion to 5-hydroxymethylfurfural and levulinic acid catalyzed by ionic liquid and transition metal sulfate: Elucidation of kinetics and mechanism," *Journal of Cleaner Production*, vol. 256, 2020.

[154] R. Ringgani *et al.*, "Experimental and kinetic modeling of galactose valorization to levulinic acid," *Bulletin of Chemical Reaction Engineering & Catalysis*, vol. 17, no. 2, pp. 451–465, 2022.

[155] J. M. Carraher, C. N. Fleitman, and J.-P. Tessonnier, "Kinetic and mechanistic study of glucose isomerization using homogeneous organic brønsted base catalysts in water," *ACS Catalysis*, vol. 5, no. 6, pp. 3162–3173, 2015.

[156] M. Xia *et al.*, "Synergistic effects and kinetic evidence of a transition metal-tin modified beta zeolite on conversion of miscanthus to lactic acid," *Applied Catalysis A: General*, vol. 583, 2019.

[157] A. Martina *et al.*, "Kinetic study on the sulfuric acid-catalyzed conversion of d-galactose to levulinic acid in water," *Industrial & Engineering Chemistry Research*, vol. 61, no. 26, pp. 9178–9191, 2022.

[158] J. Shan *et al.*, "Efficient isomerization of glucose to fructose over al-loaded functional lignin biopolymer," *Applied Catalysis B: Environment and Energy*, vol. 353, 2024.

[159] T. N. Eran *et al.*, "Copper, potassium promoted iron on metallosilicate and aluminum oxide supports synthesized via a non-hydrolytic sol-gel for fischer-tropsch," *Catalysis Today*, vol. 433, 2024.

[160] A. Kohler *et al.*, "Catalytic formation of lactic and levulinic acids from biomass derived monosaccarides through sn-beta formed by impregnation," *Catalysts*, vol. 10, no. 10, 2020.

APPENDIX A SUPPLEMENTARY INFORMATION - ARTICLE 1

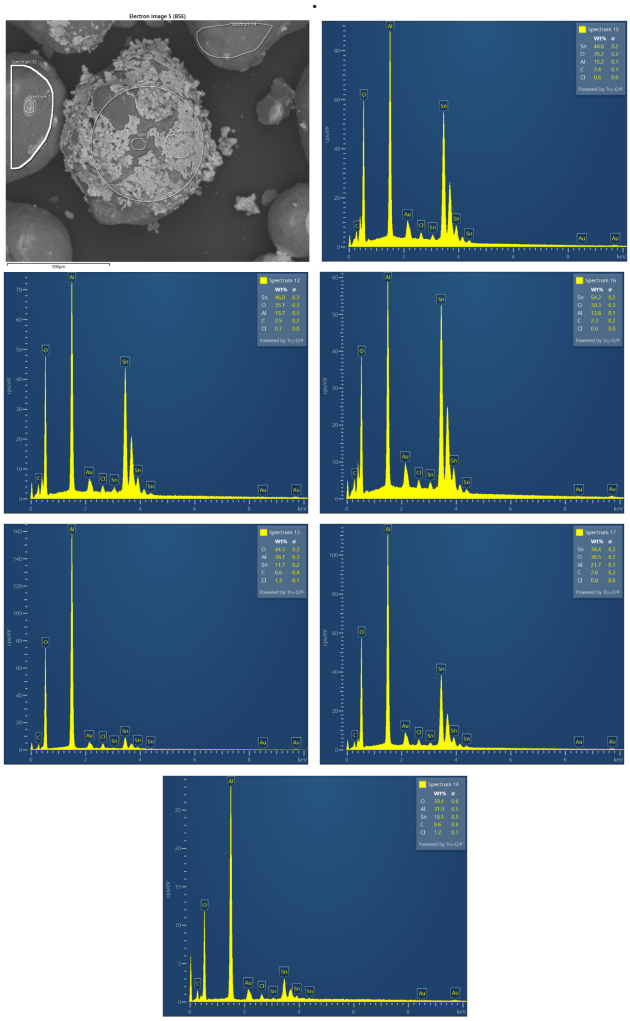

Figure A.1 SEM-EDX images of Sn_{15}/γ-Al_2O_3, x500 magnification and 100 µm scale

Table A.1 Product yield of non-supported metal oxides

Metal oxide	$Y_{\mathbf{LA}}$ (%)	$Y_{\mathbf{FA}}$ (%)	$Y_{\mathbf{HMF}}$ (%)	$Y_{\mathbf{GLUCOSE}}$ (%)	$Y_{\mathbf{GALACTOSE}}$ (%)	$Y_{\mathbf{FRUCTOSE}}$ (%)
SnO_2	1	0	9	35	36	0
Er_2O_3	7	1	11	27	30	10
SnO_2:Er_2O_3- 1:1.5	16	2	12	15	18	0

Table A.2 Product yield of non-supported metal oxides

T(°C)	t(h)	Y_{CARBON}
150	0.5	12
150	1	17.3
170	0.5	33.3
170	1	35
190	0.5	38.5
190	1	58

APPENDIX B SUPPLEMENTARY INFORMATION - ARTICLE 3

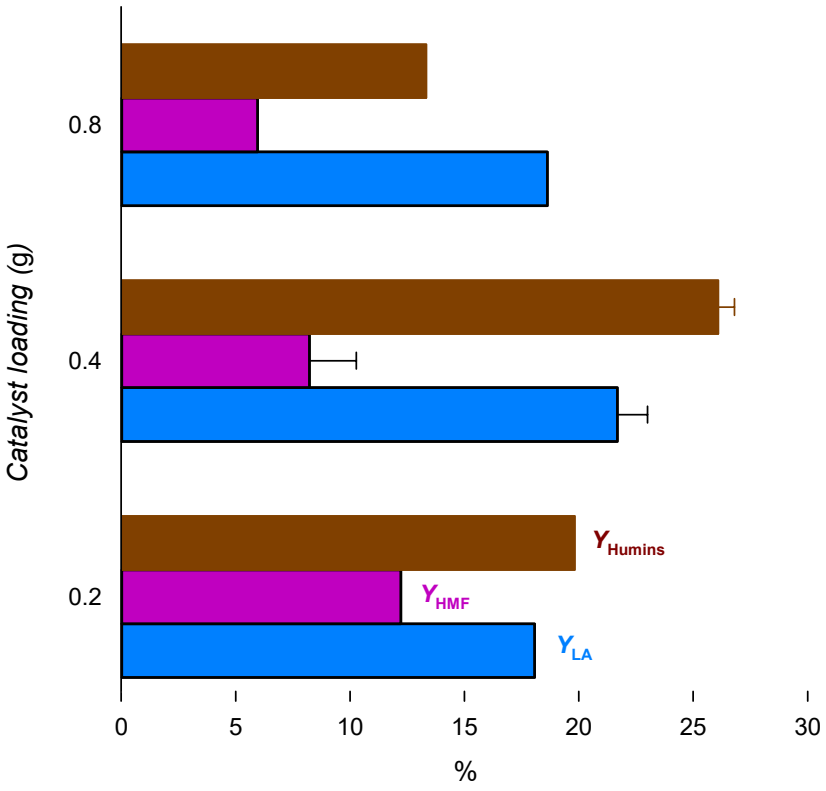

Figure B.1 Impact of catalyst loading on LA and HMF yields. Reaction conditions: Lactose, 0.14 mmol, 0.2 g , 0.4 g or 0.8 g of Er_{15}/γ-Al_2O_3, 170 °C, n=2, error bars represent standard deviation, 140 rpm.

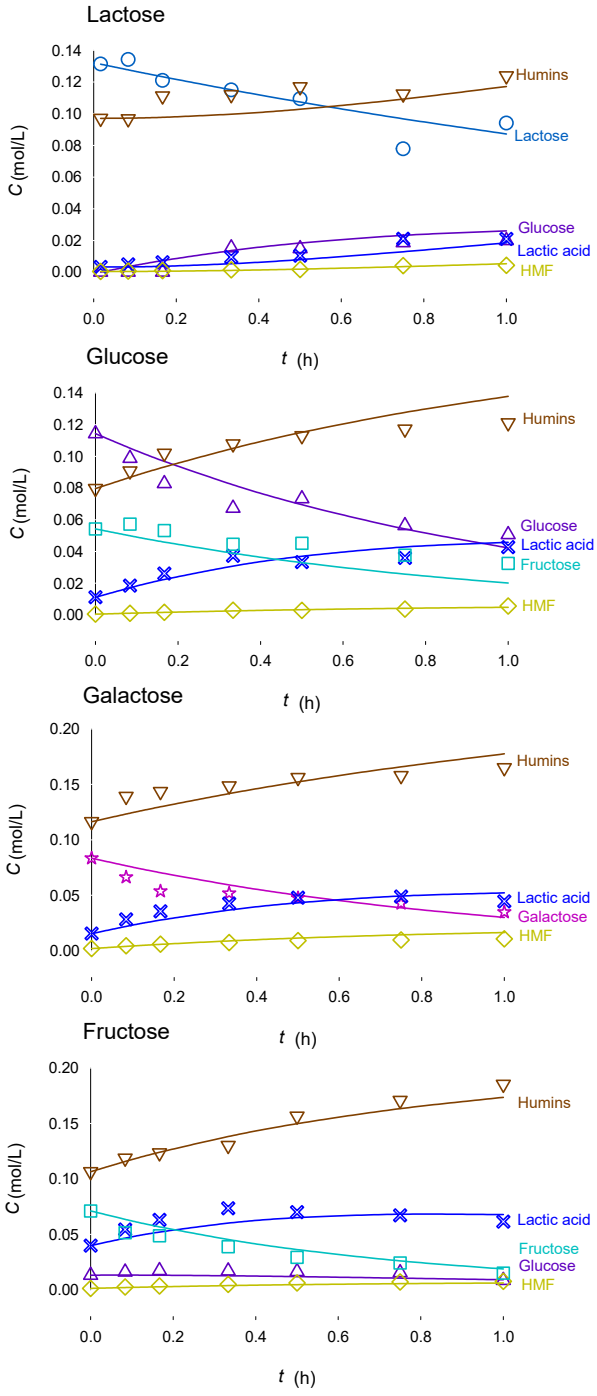

Figure B.2 Product concentration as a function of time with various feedstocks (lactose at the top, fructose at the bottom). Open symbols are experimental data, while lines corresponds to model predictions. Reaction conditions: Inlet concentration 0.14 mmol, 0.4 g of Er_{15}/γ-Al_2O_3, 130 °C, 70 rpm.

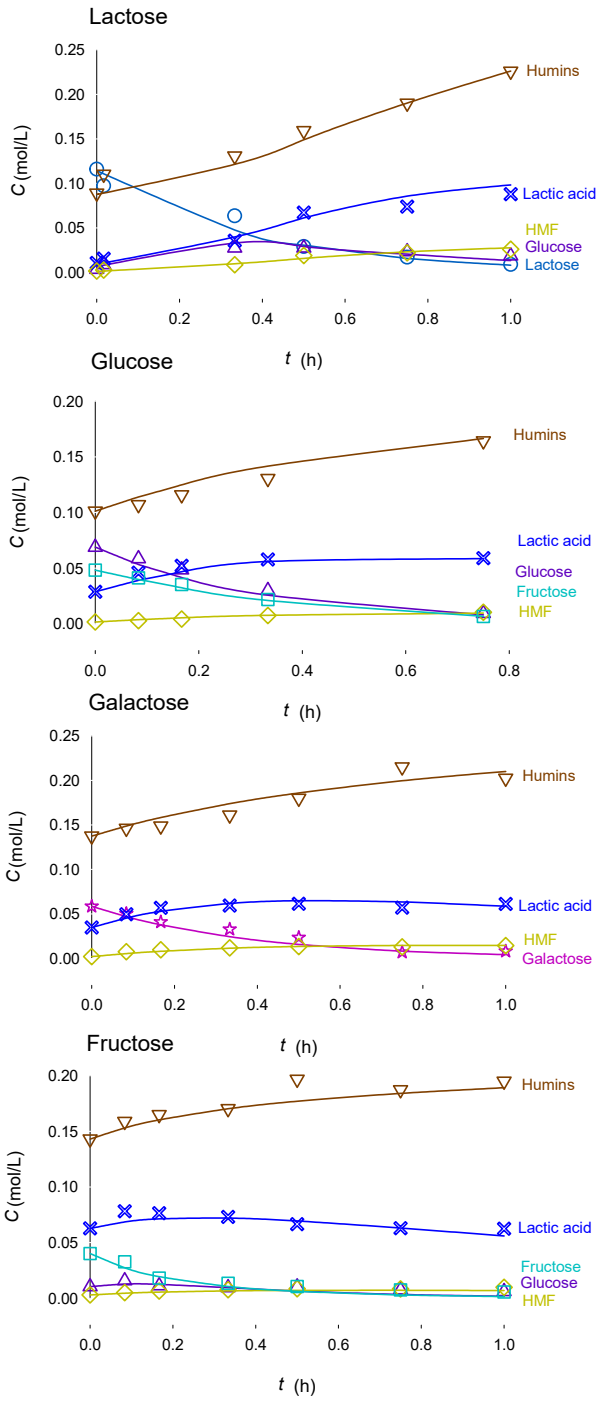

Figure B.3 Product concentration as a function of time with various feedstocks (lactose at the top, fructose at the bottom). Open symbols are experimental data, while lines corresponds to model predictions. Reaction conditions: Inlet concentration 0.14 mmol, 0.4 g of Er_{15}/γ-Al_2O_3, 150 °C, 70 rpm.

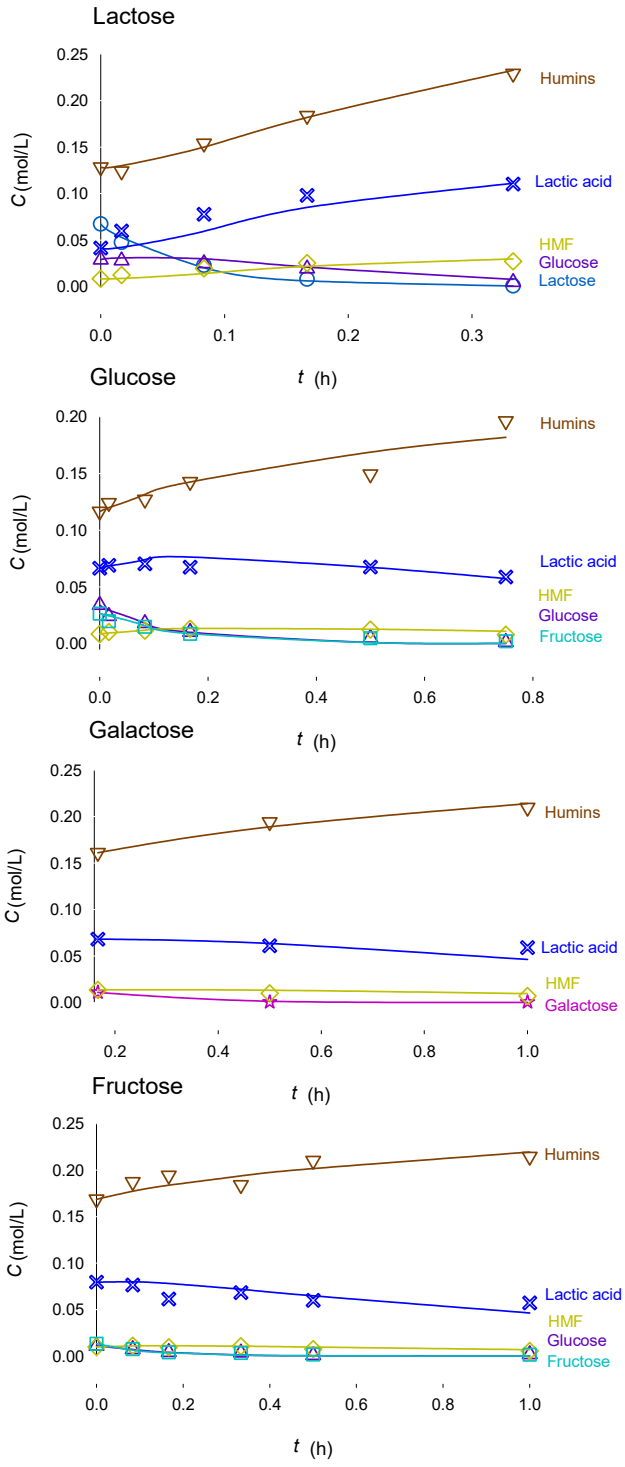

Figure B.4 Product concentration as a function of time with various feedstocks (lactose at the top, fructose at the bottom). Open symbols are experimental data, while lines corresponds to model predictions. All the lactose reacted within 20 min and so the graph only extends to 20 min. Reaction conditions: Inlet concentration 0.14 mmol, 0.4 g of Er_{15}/γ-Al_2O_3, 170 °C, 70 rpm.